Investigation of the CtrA cell cycle master regulator in *Bartonella quintana*

by

Kae Watanabe

A thesis submitted to the Victoria University of Wellington in fulfilment for the
degree of Master of Biomedical Science

Te Herenga Waka — Victoria University of Wellington
2024

Abstract

This research project aimed to address the gaps in knowledge surrounding *Bartonella quintana*, with a specific focus on understanding its cell cycle dynamics and the mechanisms underlying its virulence. *B. quintana* is an intriguing pathogen due to its ability to persist for long periods within the human vascular and intraerythrocytic environment. Specifically, for *B. quintana* to reside inside erythrocytes without causing lysis, tight regulation of the cell cycle is required to limit its replication within this niche.

CtrA is known as a master regulatory protein controlling the cell cycle in multiple alpha-proteobacteria, including *C. crescentus*. This study aimed to shed light on how this protein influences the cell cycle or morphology of *B. quintana*. The primary objective was to investigate the role of CtrA as a transcription factor within *B. quintana* and to evaluate the impact of CtrA overexpression on the bacterium.

I first used a bioinformatics approach to identify *B. quintana* promoters that contained putative CtrA binding motifs. I then used a beta-galactosidase assay to investigate the impact of heterologous CtrA protein expression on the activity of two identified promoters, *ftsH* and *ftsK*. The *ftsH* homologue gene in *C. crescentus* encodes a zinc metalloprotease that is required for the stress response and that plays a role in cell division. The *ftsK* homologue encodes an essential protein that coordinates cell division and chromosomal segregation. The results suggested a potential repressive role of CtrA on the *ftsH* gene within *B. quintana*. Expression from the *ftsK* promoter, however, was not detected, either with or without CtrA.

Because CtrA is an essential protein in most alpha-proteobacteria, I attempted to construct a conditional mutant. Although this strain could not be achieved in this project, the strain carrying the complementation plasmid was used to study the effects of CtrA overexpression in *B. quintana*. Distinct outcomes were noted in terms of viability and chromosome content between the wildtype *B. quintana* and those carrying the inducible *ctrA* plasmid. Differences in morphology were not noted, but this could be due to the lack of time available to optimise microscopy protocols.

The alteration in viability and chromosomal contents observed, when *ctrA* expression was induced on a plasmid, suggests a potential role for CtrA in the cell cycle of *B. quintana*. Further investigation is warranted to explore the functions of CtrA in *B. quintana*, not only in the context of the cell cycle but also in other aspects of *B. quintana* morphology and pathogenesis.

Acknowledgement

I would like to express my heartfelt gratitude to all those who have supported me throughout my journey as a Master's student, enabling me to complete this thesis. This endeavour would not have been possible without your encouragement, guidance, and assistance.

First and foremost, I extend my deepest thanks to my supervisor, Dr. Joanna Mackichan, for her exceptional mentorship and invaluable insights throughout this project. Her lectures were very fascinating and interesting, igniting my initial interest in the field of microbiology. Her guidance and support, throughout the project, have been instrumental in ensuring that my research stayed on the right track. Dr. Joanna not only provided regular weekly guidance but also welcomed me for further discussions in her office whenever needed. She always demonstrated positivity and provided unwavering encouragement, particularly during times when my experiments faced challenges. I am truly fortunate to have had such a fantastic supervisor.

I also would like to acknowledge the members of the Mackichan lab. Enormous thanks to Zoë, Isabelle, Brianna, and Fran, for helping me uncountable time, and for creating warm and welcoming environment in this lab. I will never forget our dinosaur trip. I wish each of you the very best in your future endeavours. I really appreciate to those from LAF lab and MMC lab for helping me out using the flow cytometry and analysing the flow cytometry profiles. A special thanks goes out to my dear friends Alex and Kirby. Your enormous moral support and the shared moments over tea/ coffee or dinner have been a source of great comfort and inspiration. All of these memories are something I will cherish for a lifetime.

Additionally, I want to express my deep gratitude to my family and my partner. I could not complete this project without their constant supports and encouragements. Thank you for always being positive and for my safe place.

Finally, great appreciation goes to Victoria University of Wellington for the financially supports with a Master’s by Thesis Scholarship.

Table of Contents

List of Figures

List of Tables

Abbreviations

BLAST – Basic Local Alignment Search Tool
bp – Base pairs
CO_2 – Carbon dioxide
CSD – Cat Scratch Disease
CTAB – Hexadecyltrimethylammonium Bromide
DAPI – 4′,6-diamidino-2-phenylindole
DMSO – Dimethyl sulfoxide
DNA – Deoxyribonucleic acid
FACS – Fluorescence-Activated Cell Sorting
FCS – Foetal Calf Serum
h – hour
HIB – Heart Infusion Broth
IPTG – Isopropyl β-D-1-thiogalactopyranoside
kb - kilobase
LB – Lysogeny Broth
LPS – Lipopolysaccharide
min – minutes
OD – Optical Density
ONPG – o-nitrophenyl-β-D-Galactoside
PBS – Phosphate Buffer Saline
PCR – Polymerase Chain Reaction
ROS – Reactive Oxygen Species
rpm – revolutions per minute
TAA – Trimeric Autotransporter Adhesins
TAE – Tris/ acetic acid/ EDTA
TLR – Toll-like receptor
T4SS – Type 4 Secretion System
UV – Ultraviolet

1. Introduction

1.1 *Bartonella* genus

Bartonella species are Gram-negative, facultative intracellular bacteria that belong to the α-2 subgroup of proteobacteria[1]. With over 40 known species, many of them are able to infect mammalian hosts, including bats and humans, and are typically transmitted through various blood-feeding arthropod vectors such as body lice, cat fleas and sandflies or through animal bites or scratches[1–3]. Interestingly, *Bartonella* infections also occur in some aquatic animals such as belugas and sea turtles[4,5]. Many diverse mammals serve as reservoirs for *Bartonella* infections; however, *Bartonella bacilliformis* and *Bartonella quintana* are only *Bartonella* spp. known that have human beings as their mammalian reservoir[1]. In addition to these two *Bartonella* species, many zoonotic *Bartonella* spp. can cause disease in humans via incidental infections (Table 1-1).

Table 1-1 :Summary of *Bartonella* species reported to cause disease in humans. Mammalian reservoir and arthropod hosts are listed (where known), along with reported disease pathology[6].

***Bartonella* spp.**	**Reservoir/vector hosts**	**Human disease pathology**
B. alsatica	Rabbit	Endocarditis, lymphadenopathy
B. bacilliformis	Human/sandfly	Oroya fever and verruga peruana
B. clarridgeiae	Cat/cat flea	Lymphadenitis
B. elizabethae	Rat	Endocarditis, neuroretinitis
B. grahamii,	Rat	Neuroretinitis
B. henselae	Cat/cat flea	Cat scratch disease, lymphadenitis, endocarditis, etc
B. koehlerae	Cat	Endocarditis, lymphadenitis
B. quintana	human/body louse	Trench fever, endocarditis, bacillary angiomatosis, etc
B. rochalimae	Canid(fox and dog)[7]	Bacteraemia, fever, splenomegaly
B. tamiae	Unknown	Febrile illness
B. vinsonii subsp. *Arupensis*	Dog, rodent/ticks	Bacteraemia, fever, endocarditis
B. vinsonii subsp. *Berkhoffii*	Dog/ticks	Endocarditis
B. washoensis	Fleas	Myocarditis, meningitis
B. melophagi	Sheep / Sheep ked	Bacteraemia
B. ancashi	Unknown	Verruga peruana
B. mayotimonensis[8]	Bat	Endocarditis

The *Bartonella* spp. that currently cause human disease most frequently are *B. henselae, B. bacilliformis* and *B. quintana.* All of these are fastidious bacteria; *B. henselae* and *B. quintana* are rod-shaped bacteria, while *B. bacilliformis* is a flagellated coccobacillus.

1.1.1 Disease Prevalence and Transmission

Most *Bartonella* species are transmitted between mammalian hosts by blood-feeding arthropod vectors. In most cases, the geographic distribution and prevalence of the arthropod vector, or in some cases the reservoir host, determines the prevalence of human infection.

1.1.1.1 *Bartonella bacilliformis*

B. bacilliformis infection causes Carrión disease, which can either present in an acute form, known as Oroya fever, or a chronic form, known as verruga peruana (Peruvian warts). The vector for *B. bacilliformis* is the female sandfly genus *Lutzomyia*, and the reservoir host is humans. The prevalence of Carrión disease correlates with the geographical distribution of *Lutzomyia* sandflies, its main transmission vector. The disease is usually limited to high-altitude locations around the Andes mountains in South America, including Colombia and Ecuador, with most cases reported in Peru[9]. Sporadic cases have also been reported in Bolivia and Chile[10]. Carrión disease was first reported in 1870 in Peru when a new railway line was constructed from Lima to Oroya[11]. This first major outbreak of Oroya fever, mainly in workmen building the railway, resulted in several thousand deaths[11].

1.1.1.2 *Bartonella henselae*

Cat scratch disease (CSD) was first described in the 1930s, with the association with cats established in the 1950s[12,13]. Years later, *B. henselae* was isolated and shown to be the agent of the infection. Humans are incidental, not reservoir, hosts for *B. henselae*. CSD occurs worldwide, including in the United States, Europe and Asia, but is most prevalent in warm and humid areas, in accordance with the geographical distribution of its cat flea vector[17]. *Ctenocephalides felis*, the cat flea, is an ectoparasite of both domestic and feral cats, usually kittens. *B. henselae* replicates in the flea gut and is inoculated on cat fur or skin when the flea excretes contaminated faeces, which cats are exposed to via grooming of their fur or

claws. Incidental infection in humans occurs with bites or scratches from infected cats that are frequently asymptomatic[13–15].Young cats are more associated with this infection and more likely to be bacteraemic compared to older cats. This may be due to older cats' previous exposure to *B. henselae,* resulting in effective antibodies that prevent infection. CSD occurs most frequently in children, with an incidence of 6.4 cases per 100,000 population in adults, versus 9.4 cases in the same population for children globally[11,13,16].

1.1.1.3 *Bartonella quintana*

The main vector for *B. quintana* transmission is the human body louse, *Pediculus humanus,* but several studies have suggested that other blood-feeding arthropods, such as bed bugs and head lice, can contribute to transmission of *B. quintana*[17,18]. DNA from *B. quintana* has been detected from ticks and cat fleas, but their ability to transmit *B. quintana* has not been established[19,20]. The reservoir host for *B. quintana* is humans, though incidental infections have occasionally been reported in companion animals, such as cats[20,21].

Serological and molecular evidence reveals that *B. quintana* and trench fever occur worldwide[22–24]. Since its discovery in 1915, trench fever epidemics have occurred periodically. More recently, major outbreaks have occurred among homeless populations in the United States and Europe[25–27]. Because the outbreaks occur in homeless populations and urban areas, a modern term for this disease is "urban trench fever". Several paediatric patients with *B. quintana* endocarditis were reported in Ethiopia the late 2010s; in 2020, a small outbreak of trench fever was reported among the homeless population in Denver, Colorado[28,29]. Poor hygiene, crowded living conditions, malnutrition and exposure to cold temperatures over prolonged periods are risk factors for trench fever. These conditions frequently arise within the modern homeless population; in the past, military troops also often experienced these risk factors[30]. Interestingly, alcoholism is also considered a risk factor[31]. Most of these risk factors are the result of increased risk of body louse infestation. Immunocompromised hosts are also more susceptible to trench fever, compared to immunocompetent hosts, and often experience worse prognoses due to critical complications such as bacillary angiomatosis and endocarditis[22]. Since the 1990s, several sporadic outbreaks have been reported among homeless populations, as well as immunocompromised populations, including patients with HIV or those who have undergone organ transplantation[22,32,33].

Overall, exposure to arthropod vectors or reservoir hosts is a critical factor in the prevalence or epidemiology of *Bartonella* infections.

1.1.1.3.1 Historical aspects of *B. quintana*

Trench fever was first recognised in 1915, early after the onset of trench warfare during World War I[34,35]. After it was determined that trench fever was distinct from typhoid and dengue fevers, Hunt and Rankin named this disease after the Trench Troop which was affected by this disease in 1915[36,37]. During World War 1, over 1 million soldiers were estimated to be affected[38]. The War Office Trench Fever Investigation Commission first attempted to determine if the disease was caused by bacteria or protozoa, though they did not reach a conclusion[39]. Soon after, in 1916, Topfer reported that trench fever patients were often infested by lice and that the lice contain a large number of what they identified as "Rickettsia bodies" in their gut[40]. Furthermore, Arkwright and others identified the transmission vector and also found that trench fever occurs when human body lice feed and excrete faeces on the patient's skin. This enables the bacteria to enter the body following scratching of the contaminated faeces into the bite wound[41]. They also found that people do not suffer from trench fever when lice only feed, confirming that scratching of the contaminated faeces into the bite wound is the main transmission route for this disease. Later, trench fever re-emerged in World War II on a larger scale around the world, with German soldiers carrying the disease to Northern Europe, including Norway and Finland[35,42]. Trench fever patients were also reported during the war in some Asian countries, including Japan and China[35]. After the war, there were several outbreaks of trench fever around the world, mostly in homeless populations and among immunocompromised patients. The outbreaks after the war occurred in Poland[42], Mexico[43], Tunisia, Ethiopia[44], Burundi[45] and Japan[46] in the 20th century, and some small-scale outbreaks have been reported in the 21st century as well[47,48].

Recent discoveries revealed that *B. quintana* caused trench fever outbreaks even before its discovery in World War I. For example, the DNA of *B. quintana* was identified in dental pulp from Napoleon's soldiers, suggesting *B. quintana* infections occurred in the early 19th century[49]. This is consistent with the fact that many of Napoleon's soldiers died because of infectious disease and that soldiers living in close, unhygienic environments were susceptible to trench fever. Real-time PCR of ancient dental pulps has also revealed *B. quintana*

bacteraemia in remains from 4,000 years ago, the earliest evidence of arthropod-borne infections in humans[50].

1.1.2 Clinical manifestations

Bartonella infections can cause a wide range of manifestations, from common mild symptoms, such as fever, to more serious complications, such as bacteraemia and severe inflammation in internal organs. The pathophysiology differs depending on which species is causing the infection, but many *Bartonella* infections can occur in acute or chronic phases. Immune compromised individuals tend to have more severe manifestations of the infection compared to immune competent individuals. There is no single treatment for *Bartonella* infection, with the optimal treatment determined based on the clinical manifestations and pathogenicity[6].

B. bacilliformis infection is clearly distinguishable from other types of *Bartonella* infections. *B. bacilliformis* causes Carrión disease. The acute form, Oroya fever, typically occurs first, and may be followed by the chronic form, verruga peruana. Carrión disease is by far the most severe form of bartonellosis, compared to *B. quintana* or *B. henselae* infections. Oroya fever is characterised by headache, fever, malaise, and most importantly, a potentially highly fatal haemolytic anaemia[11,51]. As a result of this anaemia, Oroya fever results in nearly 90% mortality if left untreated, though this may vary between different *B. bacilliformis* genetic variants[52,53]. In the chronic phase, verruga peruana, patients get eruptive cutaneous lesions on the skin that appear up to 8 weeks after the acute phase and persist for months or even years[51]. This is a type of vasoproliferative lesion and is caused by bacterial colonisation of the endothelium.

B. henselae causes CSD as an acute infection when the bacteria are transmitted into the human host via a cat scratch or bite. CSD causes regional lymphadenopathy, along with fever, which commonly develops over one to three weeks[13]. Although the swelling occurs in lymph nodes in healthy individuals, immunocompromised patients may have inflammation in different organs, including the brain, bones, heart valves, central nervous system, and eyes[54]. Infection frequently occurs in the liver and spleen, causing cysts known as bacillary peliosis as a chronic infection. In immune competent hosts, lymphadenopathy usually resolves spontaneously at around four weeks, and is self-limiting in almost 90% of children[13]. *B.*

henselae is less likely to cause a chronic infection in humans, thus bacteraemia is not a common manifestation, as it is with *B. quintana*.

B. quintana causes trench fever, also known as five-day fever, in its acute phase of infection. Trench fever is characterised by a relapsing fever that occurs at five-day intervals, along with non-specific symptoms such as headache, dizziness and shin pain[55]. The disease occurs after a long period of incubation, usually up to a month[15,22,38,56]. Trench fever is usually self-limiting in healthy patients, however, immunocompromised, organ transplant, and alcoholic patients are at risk for severe manifestations[22]. The severity and prognosis varies among patients, depending on immune status, with severe cases leading to critical complications or even death[22]. *B. quintana* is reported to reside in endothelial cells, which results in a vasoproliferative lesion called bacillary angiomatosis, particularly in immune compromised individuals[57]. The most common location for these lesions is the skin, but other parts of the body, such as bone marrow and the liver, can also be affected (Figure 1-1)[35]. Bacteraemia, recovery of viable bacteria in the host bloodstream, is a common chronic manifestation of *B. quintana* infection and often occurs in immunocompromised hosts [58]. Surprisingly, there is evidence that some patients can be chronically infected with *B. quintana* for months or even years[1]. Culture-negative endocarditis, an inflammation in heart chambers and valves, is also a common chronic manifestation of this infection.

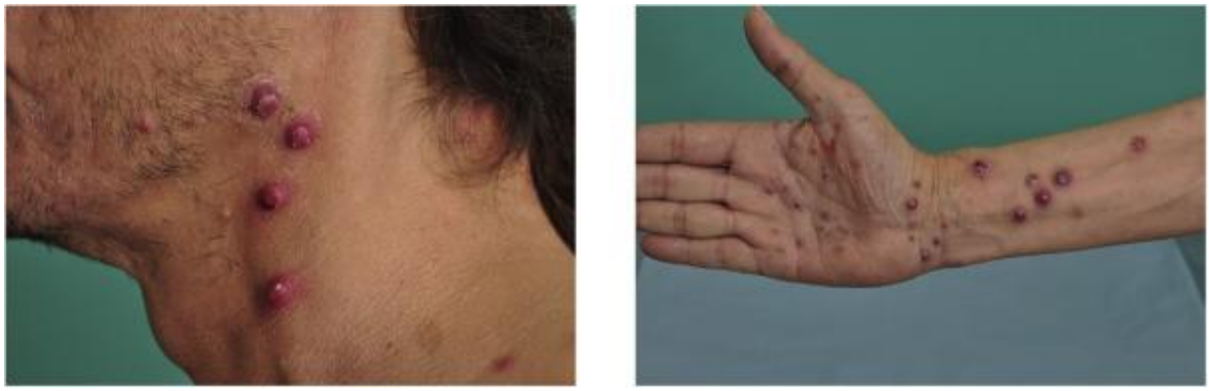

Figure 1-1: Characteristics of bacillary angiomatosis in an organ transplant patient. This picture was reproduced from Ferløv Schwensen et al.[59] under a Creative Commons license.

1.1.2 Interaction between *Bartonella* and erythrocytes

Bartonella bacteria usually reside in the vectors' gut prior to inoculation of the mammalian host, via faeces, saliva or direct inoculation by biting the host. *Bartonella*, after

inoculation and invasion of the dermal tissues, colonises the primary niche. This niche is thought to be migratory cells such as macrophages, dendritic cells, or erythroblasts, where the bacteria reside until the cells migrate to the next niche[60,61]. *Bartonella* then colonises vasculature endothelium tissues where they may persist intracellularly. The bacteria then emerge into the bloodstream from those endothelial cells after 2 to 5 days and invade erythrocytes. After limited replication inside the erythrocytes, typically reaching up to eight bacteria per erythrocyte, the bacteria persist in the intraerythrocytic niche for the duration of the erythrocyte's lifespan [62]. This period in the erythrocyte enables *Bartonella* to evade host immune surveillance. Intraerythrocytic bacteria are subsequently taken up by blood-feeding arthropods, completing the transmission cycle (Figure 1-2)[15,60,63].

B. bacilliformis also have an alternative route of entry, by entering into the capillary lumen directly through the open bite wound, without residing in the primary niche[60]. Although humans are only an incidental host of *B. henselae,* inoculation of the bacteria can cause illness. *B. henselae* invades a primary niche to circulate in the body and cause inflammation and proliferation in other parts of the body. This is consistent with the clinical manifestations of *B. henselae* which involves proliferation in lymph nodes. *B. henselae* does not invade human erythrocytes, therefore this bacterium is not transmitted further from humans.

The main difference between *B. bacilliformis* and other two *Bartonella* is that *B. bacilliformis* infects, and potentially lyses, up to 100% of erythrocytes, causing severe haemolytic anaemia. *B. henselae* and *B. quintana*, by contrast, only affect 1-5% of erythrocytes, which remain intact and functional, enabling the bacteria to persist and be transmitted[62,63]. This is consistent with the high fatality rate of *B. bacilliformis* haemolytic anaemia, but the low mortality of *B. henselae* and *B. quintana* in immune competent hosts.

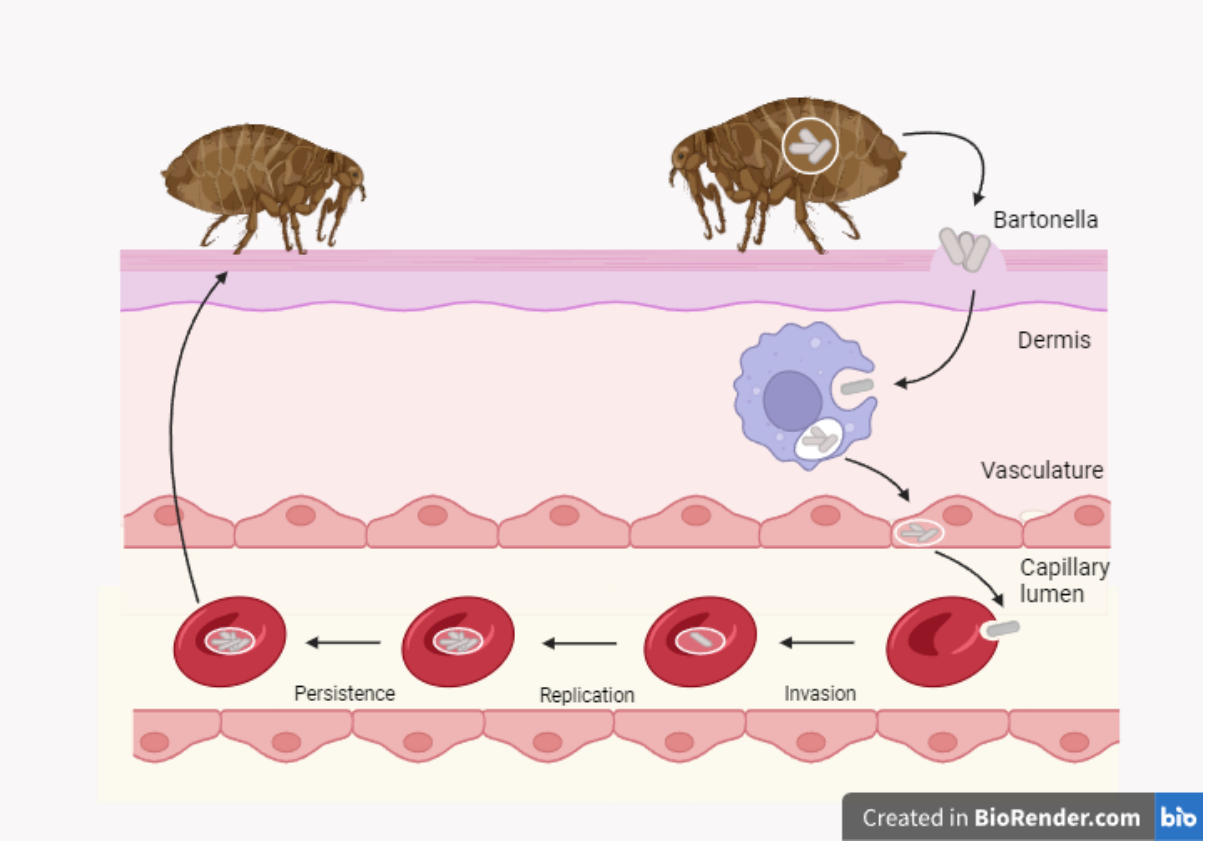

Figure 1-2: A diagram of the basic transmission route of *Bartonella*. Haematogenous, or blood-feeding, arthropod vectors that carry *Bartonella* in their gut excrete on the host skin during a blood meal. The bacteria then invade the dermis through the open wound. The bacteria then colonise migratory and epithelial cells. *Bartonella* resides for a few days and is released into the capillary lumen. *Bartonella* in the bloodstream invade erythrocytes and replicate a limited number of rounds. Intraerythrocytic *Bartonella* persists long-term until the end of the erythrocyte life. This persistence facilitates the next transmission via other blood-sucking vectors. This diagram is adapted from Harms and Dehio[15] with permission from American Society for Microbiology. This figure was created by BioRender.com.

1.1.3 *Bartonella* Virulence factors

During the course of infection, *Bartonella* utilise different mechanisms to enable host colonisation, evasion of host immunity, and persistence until transmission can occur. One important virulence and host adaptation mechanism is the type 4 secretion system (T4SS). The T4SS is absent from *B. bacilliformis,* but *B. henselae,* and *B. quintana* share some common T4SS functions. The T4SS is composed of multiple structural proteins that mediate the translocation of effector molecules across both bacterial membranes and the host cell cytoplasmic membrane[64]. There are two types of T4SS in *B. henselae* and *B. quintana*: VirB-D4 and Trw.

The VirB-D4 T4SS is expressed on endothelial cells and allows the translocation of *Bartonella* effector proteins (Beps) into host cells. Beps contribute to bacterial virulence by altering multiple signalling pathways in endothelial and immune cells. The effects of the Beps include inhibition of apoptosis, induction of proinflammatory signalling through the NF-κB pathway, and actin cytoskeleton rearrangement, resulting in invasome-mediated bacterial aggregates for bacterial internalisation[65,66]. Induction of the NF-κB pathway results in increased secretion of IL-8, causing angiogenesis and secretion of adhesion molecule ICAM-1 to facilitate proinflammatory response[65]. The Trw T4SS does not secrete any proteins into the host cell, but rather facilitates the adhesion and invasion of erythrocytes. It also functions as a key factor for reservoir host specificity by expressing a wide variety of lengths and number of pili to adapt to specific erythrocyte surface of reservoir hosts[67]. *B. henselae* have a small molecule called deformin, which deforms the membrane of erythrocytes to also facilitate the bacterial invasion of erythrocytic cells[68].

Lipopolysaccharide (LPS) is another factor contributing to pathogenesis in *B. quintana* and *B. henselae.* LPS in these bacteria have unique lipid A along with a long fatty chain without an O-chain polysaccharide. This structure makes their LPS less recognisable by Toll-like receptor 4 (TLR4), therefore contributing to low levels of inflammation and reduced efficiency of phagocytosis[69]. *B. quintana* LPS has also been shown to downregulate the immune system by inhibiting the production of proinflammatory cytokines, including IL-1β, IL-6 and tumour necrosis factor α that are generated from TLR4 and its pathway[70–72].

B. henselae also have a trimeric autotransporter adhesin (TAAs) called BadA that facilitates the adhesion to the host cell. Other than facilitating adhesion and autoaggregation, BadA also expresses a wide range of motifs that enable escape from phagocytosis[73]. *B. henselae* in macrophages can form a unique vacuole inside called *Bartonella*-containing vacuole, or BCV, that causes a delay in lysosome targeting[74]. TAAs also contribute to virulence in *B. quintana.* Variably expressed outer membrane proteins, or VOMPs, bind to collagen in the extracellular matrix of the host and mediate adhesion and autoaggregation[75]. Other studies reveal that VOMPs in these bacteria also play a role in the reprogramming of angiogenesis[76].

Furthermore, *B. quintana* modulates both apoptotic and anti-apoptotic signals at different times when invading endothelial cells. In early infection, *B. quintana* induces apoptosis of the endothelial cells by causing them to overexpress caspase 8 and Apaf-1.

However, when *B. quintana* internalisation is completed, they switch to inhibit apoptotic signals, such as p38 MAPK and SAPK/JNK, and induce antiapoptotic signals[77]. This promotes survival and proliferation in their primary niche.

B. quintana is able to obtain nutrients from hemin by expressing hemin-binding proteins (Hbp). There are five different Hbp in *B. quintana* and they all are expressed in different conditions. For example, expression of HbpC increases 100-fold at 30°C compared to 37°C, which indicates greater expression of HbpC in in the louse gut over the human bloodstream. Also, HpcC and HpcB tend to be more highly expressed in high concentrations of haem. The reverse is true for HbpA, HbpD, and HbpE[78]. The adaptation of *B. quintana* to the body louse gut is also facilitated by an extracytoplasmic function sigma factor called RpoE[79]. *B. quintana* also triggers overproduction of IL-10 by host macrophages, which attenuates the inflammatory response. This is important for the persistence of *B. quintana* and for long-term bacteraemia[80].

B. quintana utilises a wide variety of virulence factors to facilitate invasion of erythrocytes, evasion of the host immune system, and persistence in niche without causing too much damage. One intriguing possibility is that control of the *Bartonella* cell cycle also contributes to their success as a persistent pathogen. Notably, once inside the erythrocyte, the bacteria stop replication after only a few rounds, and thus avoid lysing the cells. This is likely a critical adaptation that enables the bacteria to persist in the host, reduces the harm caused to the host, and enhances the likelihood of transmission to a new host. Very little is known about regulation of the cell cycle in *Bartonellae*. However, other alpha-proteobacteria have long been used as model organisms for studying regulation of the bacterial cell cycle.

1.2 Cell Cycle in Bacteria

Most bacterial cells divide by binary fission and produce daughter cells, which undergo additional rounds of binary fission to produce progeny; thus bacterial growth typically occurs in an exponential manner. It is critical for bacteria to ensure precise timing and order in the cell cycle, to avoid an incorrect number of chromosomes or damage to the DNA. The bacterial cell cycle involves DNA replication, chromosome segregation, cytokinesis, and septum formation and division; all of these processes need to be under spatial and temporal control.

1.2.2 Alpha-proteobacteria cell cycle regulation

Alpha-proteobacteria are a Gram-negative class of proteobacteria. The alpha-proteobacteria class is comprised of diverse species, including phototrophic genera, symbionts of plants and animals, pathogens, and genera metabolising C1-compounds. The focus of this thesis, the *Bartonella* genus, also belongs to this group of bacteria. Although the alpha-proteobacteria have diverse lifestyles and environmental niches, some of their cell cycle regulation and control mechanisms are conserved[81,82]. For example, CtrA (cell cycle transcriptional regulator A), an important cell cycle regulator, is conserved in multiple alpha-proteobacterial species. Regulation of the cell cycle has not been described in the *Bartonella* genus but has been studied in detail in other alpha-proteobacteria, including *Caulobacter crescentus* and *Brucella* spp.

C. crescentus has a dimorphic cell cycle and asymmetric cell division that results in a motile, swarmer daughter cell, and a non-motile, stalked cell. The swarmer cell expresses a flagellum and pili, whereas the stalked cell has a stalk at one pole, which is a thin and long extension of the cell envelope[83]. The main difference between those two cells, in addition to their morphology, is their ability to replicate. The swarmer cell is unable to replicate its chromosome and divide, while the stalked cell is able to replicate its chromosomal DNA and complete cell division[83]. As the stalked cell replicates its chromosome, the body is elongated into a pre-divisional cell, where a flagellum is constructed at one pole. Pili and membrane phage receptors start to accumulate at the same time around the flagellum side of the pre-divisional cell. When the cells divide, two morphologically different cells are produced. After a short period of time, the swarmer daughter cell undergoes maturation and differentiates into a stalked cell by disassembling the flagellum, and pili and extending the newly formed stalk

(Figure 1-3). As soon as the cells are differentiated into stalked cells, they start chromosomal replication immediately to prepare for the next cell cycle [83,84].

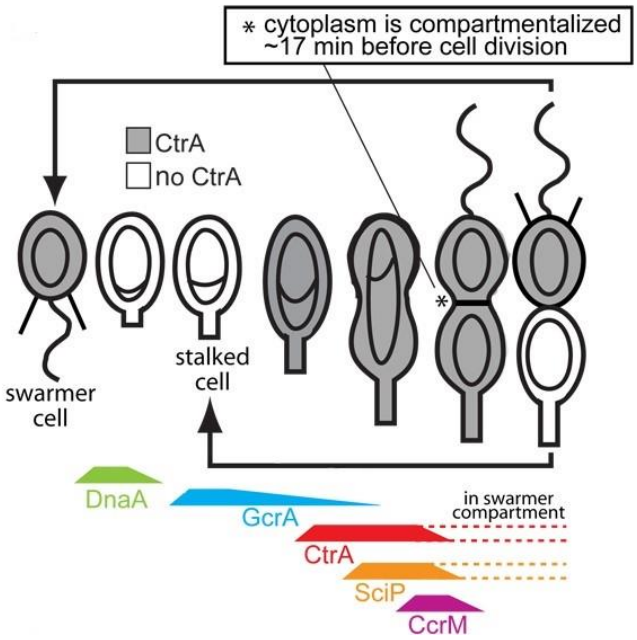

Figure 1-3:Master regulatory proteins in *C. crescentus*. This diagram shows dimorphic life cycle of *C. crescentus* and the concentration and presence of five master regulatory proteins involved in the cell cycle. The shading in the cell shows the localization of CtrA throughout the cell cycle. This diagram was reproduced from McAdams and Shapiro[85] with permission from Elsevier.

C. crescentus provides an excellent model system for studying cell cycle regulation and the mechanisms behind alpha-proteobacterial growth and cell division. Their asymmetric division and dimorphic life cycle, with distinct cell polarity producing two daughter cells exhibiting different controls in their replication, combined with the availability of genetic information, has made it possible to investigate cell cycle regulation[84,86]. In addition, the purification of swarmer cells by synchronisation makes these bacteria well-suited for studying cell cycle regulation and its surrounding events[86,87].

1.2.3 Circuitry cell cycle control in *C. crescentus*

The cell cycle in *C. crescentus* is controlled by phospho-signalling networks and five master regulatory proteins, which are essential for the cell cycle to progress in the proper

order and for steps to occur at the appropriate time[85]. These proteins include DnaA, GcrA, CtrA, CcrM and SciP, as shown in Figure 1-4. These master regulatory proteins regulate the expression of more than 200 genes related to DNA replication and polar differentiation, including flagellar and pili biogenesis[88,89]. DnaA has two functions, the first of which is to initiate chromosome replication. DnaA directly binds the origin the replication of the bacterial chromosome and activates the DNA polymerase to initiate the DNA replication. DnaA also controls the expression of approximately 40 genes as a transcription factor. For example, DnaA positively regulates transcription of the *hdaA* and *ftsZ* genes, while the resulting proteins, HdaA and FtsZ, inactivate DnaA to prevent further initiation of DNA replication and promote cytokinesis, respectively[90]. Only a small amount of inactivated DnaA is present in the swarmer cell, preventing the initiation of replication. DnaA starts to accumulate during the transition of the swarmer cell to the stalked cell, resulting in high DnaA concentration in the early stalked cell, levels that correspond to the initiation of DNA replication[85,91]. DnaA activates the transcription of GcrA, which regulates crucial genes in the S-phase, including CtrA[92]. Activated CtrA controls the transcription of numerous genes, including the gene encoding CcrM, a DNA methyltransferase that is transcribed towards the end of chromosome replication to re-methylate the DNA. Production of CcrM also results in the reactivation of DnaA transcription to prepare for the next cell cycle in newly produced stalked cells[92]. The last master regulatory protein, SciP, is activated when phosphorylated CtrA accumulates in pre-divisional cells. SciP then accumulates in the swarmer cell after cell division and represses transcription of at least 58 genes that are activated by CtrA. SciP protein also binds to CtrA, without influencing its phosphorylation status or stability, thus preventing CtrA from recruiting RNA polymerase[93,94].

In *C. crescentus*, CtrA binds tightly to the chromosomal origin of replication, preventing the initiation of replication. Therefore, the clearance of CtrA and accumulation of DnaA is critical for initiating DNA replication. The cell cycle controls allow the cell to only initiate chromosomal replication when the conditions are right for replication and ensure that there is only one chromosomal replication per cell cycle[85,92]. CcrM, a DNA methylase, also limits cells to one chromosomal replication per cell cycle, by methylating DNA and inhibiting DnaA transcription on the same chromosome[92]. After the replication of DNA, chromosomes segregate and the cytoplasm is divided to make two separate compartments. This cytoplasmic compartmentalization results in a division of genetic programs in the cell, with swarmer cells controlled via their own network without interacting with the stalked

cells[95,96]. Additionally, when carbon and nitrogen are depleted from the environment, proteolytic turnover of DnaA increases and CtrA is further stabilised, inhibiting the initiation of DNA replication in this stressful environment[97].

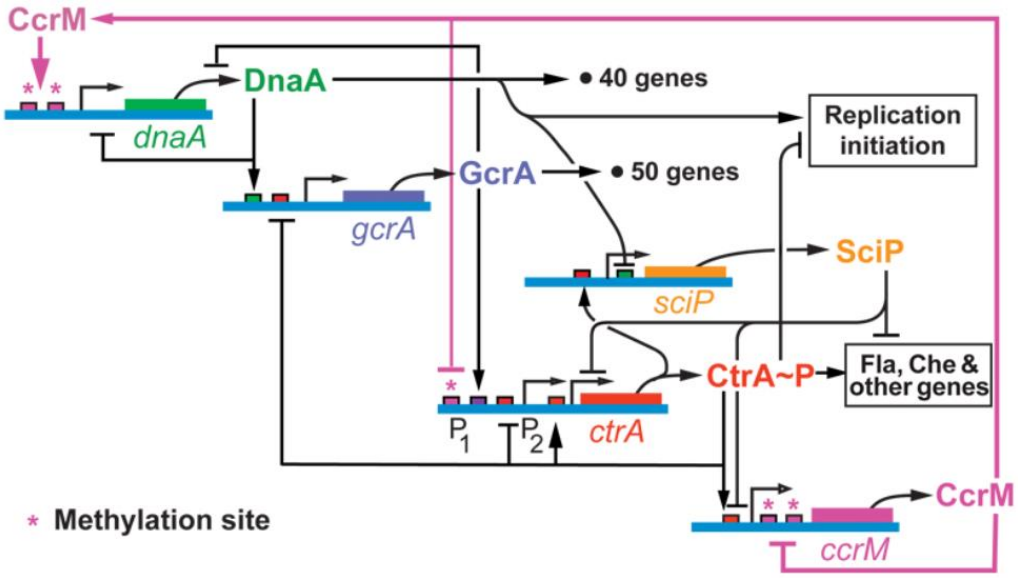

Figure 1-4: Schematic diagram of the cyclic genetic circuitry system for five master regulatory genes. This system provides the core regulation of the *C. crescentus* cell cycle. This diagram was reproduced from McAdams and Shapiro[85] with permission from Elsevier.

Meanwhile, phospho-signalling networks function to keep track of the progression of the cell cycle, specifically by managing the correct time and place of chromosomal replication initiation, cytokinesis, and polar organelle development[85]. This network is critical for establishing asymmetry during cell division. Here, multiple important proteins are involved as well. One of them is CckA, a histidine kinase that is present in all the stages of the cell cycle but localised in the swarmer cell pole during the pre-divisional stage. The phospho-signaling network relies on the localization and phosphorylation status of CckA. CckA also determines the stability and activation status of CtrA by phosphorylation and a protease called ClpXP. ClpXP is controlled by its phosphorylation status and is responsible for rapidly degrading and clearing the CtrA protein when it is no longer needed. CckA localisation results in a phosphorelay from CckA, to ChpT, a phosphotransferase, to CtrA. CpdR is also phosphorylated by ChpT which prevents proteolysis of CtrA via ClpXP. When the cell is differentiated into a stalked cell, CpdR is rapidly de-phosphorylated and localises itself to the stalked cell pole, resulting in ClpXP protease degrading and removing CtrA. This results in the chromosome now being able to initiate replication (Figure 1-5) [90,98,99].

1.2.4 Role of CtrA in *C. crescentus*

The main focus of this thesis, the CtrA master cell cycle regulator, belongs to the response regulator family of two-component signal transduction systems[100]. Two-component systems are major transcriptional regulators in bacteria and include a sensor kinase and response regulator. The sensor kinase can sense changes in the environment and the response regulator controls transcription of genes in response to environmental changes and stress[100]. CtrA is known to directly control the expression of over 90 genes. This includes the *ftsZ* gene, which encodes protein components of the Z-ring, a structure that is essential for cellular cytokinesis[101,102]. Furthermore, microarray experiments revealed that the regulatory components of over 25% of cell cycle-regulated genes interact with CtrA directly or indirectly[103]. Those genes are involved in a wide range of functions, including DNA replication and methylation, cytokinesis and polar differentiation. For example, *ftsQ*, *ftsA* and *ftsW*, which are essential genes for cell division, are regulated by CtrA expression. These interactions allow the cells to divide in the right orientation with the correct timing[101,104].

The activation status of CtrA is determined by phosphorylation. CtrA expression is driven from two promoters. The first promoter is activated by GcrA when swarmer cells differentiate into stalked cells. Phosphorylated CtrA then activates positive autoregulation, driving strong expression from the second promoter. At the same time, expression of CtrA from the first promoter is inhibited in pre-divisional and swarmer progeny cells[85,105–107]. This system allows CtrA levels to rise rapidly to activate downstream genes. In swarmer cells, CtrA is activated through phosphorylation, which enables it to bind to five distinct sites in the chromosomal origin of replication and contribute to repressing DNA replication in swarmer cells[108]. Therefore, CtrA must be deactivated and unbound from the origin of replication in order to initiate DNA replication. At the appropriate time, CtrA is deactivated by dephosphorylation and DnaA is synthesised to bind the origin of replication instead of CtrA, resulting in the initiation of DNA replication[90]. Once deactivated, CtrA is degraded by the ClpXP ATP-dependent protease. CtrA is phosphorylated and activated in swarmer cells by the polar kinase CckA after DNA replication, preventing premature initiation of chromosomal replication. Activated CckA also prevents CtrA from lysing by activating CpdR to inactivate ClpXP protease (Figure 1-5)[90,101].

Ultimately, CckA control of CtrA is regulated via the DivK signalling pathway, as shown in Figure 1-5. CtrA is activated and phosphorylated at the flagellar pole. PleC, a histidine kinase, is expressed to dephosphorylate DivK and PleD. This results in DivL

interacting with CckA to initiate phosphorelay to CtrA through ChpT. ChpT also phosphorylates CpdR to prevent it from recruiting RcdA, PopA and CtrA to a protease called ClpXP, shown as a pacman in Figure 1-5. Therefore, this signalling pathway also prevents degradation of activated CtrA. In stalked cells, however, CtrA is dephosphorylated and degraded to initiate chromosome replication. DivJ, another histidine kinase, phosphorylates DivK and PleD. Phosphorylated DivK binds to DivL. This results in higher levels of the small signalling molecule cyclic-di-GMP, which triggers CckA to enter a phosphatase mode, resulting in dephosphorylation of CtrA. ChpT also dephosphorylates CpdR, which triggers recruitment of RcdA and PopA, which bring CtrA to the ClpXP protease. This results in degradation of CtrA[109,110].

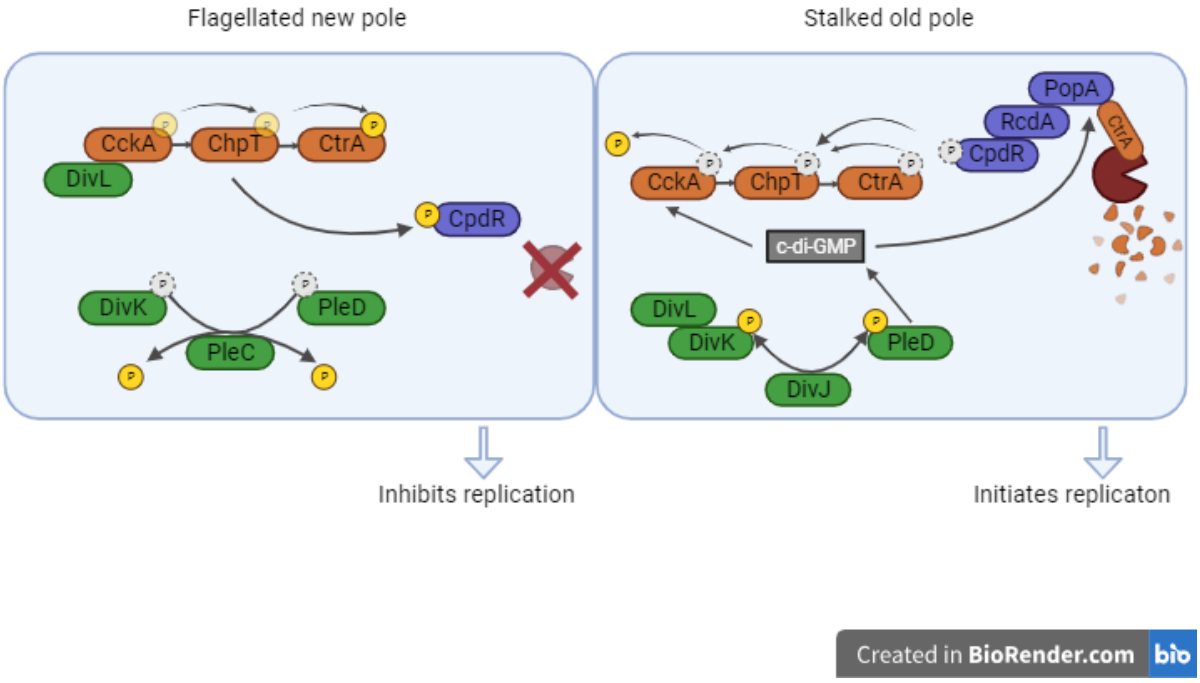

Figure 1-5: Diagram of CtrA controls in morphologically different cells Schematic diagram of the CtrA controls in morphologically different cells, created by BioRender.com. In the flagellated pole where the chromosome cannot be replicated, PleC dephosphorylates both DivK and PleD. DivL interacts with CckA to initiate the Cck-ChpT phosphorelay to phosphorylate CtrA, instead of interacting with DivK. In this phosphorelay, ChpT also phosphorylates CpdR to prevent recruiting CtrA to the proteolysis module, shown in purple, preventing the proteolysis of CtrA. On the other hand, in the stalked cells, DivJ phosphorylates DivK and PleD; phosphorylated DivK interacts with DivL instead of CckA. Phosphorylated PleD synthesises cyclic-di-GMP (c-di-GMP) to set CckA to the phosphatase mode and results in dephosphorylation of CtrA. ChpT dephosphorylates CpdR to recruit RcdA and PopA. This results in CtrA proteolysis and chromosome replication is initiated.

1.2.5 Role of CtrA in Other Bacteria

Many proteins utilised in the cell cycle, especially five master regulatory proteins in *C. crescentus*, are conserved among many alpha-proteobacteria, although their precise functions and interactions differ between species. CtrA is exclusively found in alpha-proteobacteria and is well-conserved among this bacterial group[85,111]. CtrA is found in over thirty different species in alpha-proteobacteria and has been shown experimentally to be an essential protein and to play a central role in the cell cycle in six alpha-proteobacteria, including *Caulobacter crescentus, Sinorhizobium meliloti, Rickettsia prowazekii, Brucella melitensis, Mesorhizobium loti* and *Agrobacterium tumefaciens*[85,112]. There are also alpha-proteobacteria that have a CtrA orthologue that does not appear to be essential or to play a central role in cell cycle, such as that found in *Rhodobacter capsulatus*[113].

CtrA is present in *Sinorhizobium meliloti* and its promoter structure is similar to that of *C. crescentus*[114]. Previous studies showed that *S. meliloti* CtrA also acts as a transcriptional regulator that coordinates cell division and the cell cycle [115]. A downregulated level of CtrA is required for nitrogen-fixing bacteroid differentiation inside the host plants[116]. CtrA is also conserved in *Rickettsia prowazekii*, the causative agent of epidemic typhus. The function of CtrA is relatively similar to *C. crescentus*, with five binding sites in the origin of replication[117]. In *Brucella abortus*, CtrA is essential and *ctrA* mutants are non-viable. CtrA in *B. abortus* plays an essential role in the cell cycle and its overexpression causes the cells to become elongated and branched, indicating dysregulation of the cell cycle [118,119]. *B. abortus* CtrA also regulates genes encoding outer membrane components and proteins involved in lipopolysaccharide synthesis and membrane protein export[119]. CtrA is not essential in *Rhodobacter capsulatus*, indicating it does not regulate the cell cycle, despite the fact that its sequence is highly similar to that of *C. crescentus* CtrA. Instead, in *R. capsulatus*, CtrA controls the expression of gene transfer agents, which allows genetic exchange between bacterial cells[113]. Also, CtrA loss seems to affect the flagellar motility gene but does not affect any genes involved in the cell cycle[120]. Similarly, CtrA in *Rhodobacter sphaeroides* upregulates polar flagella genes and stress responses and downregulates genes involved in photosynthesis and CO_2 fixation to contribute to adapting into a particular niche[121]. *Ehrlichia chaffeensis* also utilises CtrA to adapt to an ROS-rich environment by regulating synthesis of an antioxidant. This system is crucial for *E. chaffeensis* survival in the host, as the bacteria infect human monocytes and macrophages that produce ROS to eliminate any invaders[122].

For *B. quintana* to survive in human host erythrocytes and to avoid immune surveillance, their cell cycle must be tightly regulated. This is particularly true when the bacteria are inside red blood cells, as halting their cell division is critical to prevent lysis or destruction of host cells. Although cell cycle regulation, including the role of CtrA, has not previously been studied in *B. quintana* in detail, the CtrA protein in *B. quintana* exhibits more than 80% amino acid identity with the one in *C. crescentus*[123]. This identity is relatively high among alpha-proteobacteria with CtrA functioning as a central regulator; *S. meliloti* has 82% amino acid identity, *B. abortus* has 81% and *R. prowazekii* shows 58% amino acid identity with CtrA in *C. crescentus*[114,117,118]. Also, the *ftsE* gene, which encodes a protein that is part of the Z-ring, has previously been shown to be regulated positively by CtrA in *B. quintana*[123]. Interestingly, CtrA binding sites were not found near the *B. quintana* chromosomal origin of replication, similar to what was found in *S. meliloti,* even though CtrA inhibits *C. crescentus* DNA replication by binding the origin of replication [123].

1.3 Research Aims

As CtrA serves as a transcription factor and represses cell division by directly binding the origin of replication in swarmer cells of *C. crescentus,* we asked if CtrA in *B. quintana* also regulates cell division. The specific cell cycle regulatory and signalling mechanisms that enable *B. quintana* to halt replication erythrocytes remain unknown. To shed light on the role of CtrA in *B. quintana*, three research aims were established.

1. To use a bioinformatics approach to identify candidate *B. quintana* genes that may be regulated by CtrA. Reporter plasmids would then be constructed and used to quantify the effect of CtrA on target gene expression, using LacZ reporter *Escherichia coli* strains.

2. To investigate the functional role of CtrA in *B. quintana* by constructing a conditional CtrA mutant strain.

3. To investigate the effect of CtrA loss or overexpression in *Bartonella quintana*, using growth assays and microscopy, to detect changes in cell viability and morphology, and flow cytometry, to detect aberrations in chromosomal replication.

2 Materials and Methods

2.1 Bacterial Strains

Table 2-1: Bacterial strains used in this project

E. coli Strain	Source
DH-5α	Life Technologies
HI-Control BL21(DE3)	Lucigen
S17-1	Donated by Owen lab. Original source from Simon et al. 1983[124]
Top10	Life Technologies
K12 ER2420	New England BioLabs (#E4152S),

B. quintana Strain	Source
JK-31	BEI Resources, NIAID[75]
JK-7	BEI Resources, NIAID[75]

2.2 Bacterial Growth Media

2.2.2 Solid Media

2.2.2.1 LB agar

To culture *Escherichia coli*, Lysogeny Broth (LB) agar from Acumedia was used. To prepare plates, powder was mixed with distilled water and autoclaved at 121 °C for 15 min. After autoclaving, LB agar was cooled to 50°C in a water bath, and antibiotics or supplements were added and mixed well. The molten agar was poured into Petri dishes and stored at 4°C for up to one month. Solidified LB agar was also kept at room temperature until needed, then melted in a microwave and cooled to 50°C before proceeding as described above.

When blue-white colony screening was conducted, 40 µl of 20 mg/ml 5-bromo-4-chloro-3-indolyl-β-D-galactopyranoside (X-gal) and 40 mg/ml Isopropyl β-D-1-thiogalactopyranoside (IPTG) was spread on each LB agar plates 30 min before bacteria were inoculated. The plates were dried for 5-10 min at room temperature and stored at 37°C for 20 min or until bacteria were ready to be inoculated.

2.2.2.2 Chocolate agar

Solid cultures of *Bartonella quintana* were cultivated on plates made with GC (*Neisseria gonorrhoeae*) agar base (Oxoid) and freeze-dried BBL bovine haemoglobin (Becton Dickinson). GC agar base powder (18 g) was combined with 250 ml distilled water and vigorously stirred with a magnetic stir bar on a hot plate until it just reached the point of boiling. In a separate flask, 5 g freeze-dried bovine haemoglobin powder was manually mixed into a small amount of water, using a serological pipette to ensure the dispersion of haemoglobin clumps. The remaining water was then added to a final volume of 250 ml, and the solution was blended using a magnetic stir bar without applying heat. The two solutions were autoclaved at 121 °C for 15 min, then cooled to 55 °C in a water bath for 30 min. The haemoglobin solution was then carefully poured into the GC agar flask and mixed thoroughly. The combined solution was further cooled to 45 °C in the water bath for 30 min. Subsequently, 5 ml of reconstituted BBL IsoVitaleX Enrichment (Becton Dickinson), along with antibiotics, was introduced into the agar solution and gently mixed through swirling. All of the chocolate plates contain vancomycin, to suppress Gram-positive bacterial contamination, and cycloheximide and amphotericin B to suppress fungal and yeast growth on the plates. The molten agar was then pipetted into Petri dishes (28 ml per plate) and dried, with the plate lids askew, in the biosafety cabinet for 15 minutes. The plates were stored for up to one week at 4°C until use.

2.2.3 Liquid Media

2.2.3.1 LB broth

To prepare broth for *E. coli*, 32 g of dehydrated LB broth powder (Invitrogen) was mixed with 1 L of distilled water and autoclaved at 121 °C for 15 min. The broth was stored in small batches, using 50-ml Falcon tubes, at room temperature until needed.

2.2.3.2 Heart Infusion Broth

Bacto Heart Infusion Broth (HIB; Becton Dickinson) was prepared by combining 25 g of powder was mixed with 1 L of distilled water and autoclaved at 121 °C for 15 min, then stored at room temperature until needed.

2.2.3.3 Schneider's Drosophila Medium

Schneider's Drosophila Medium (ThermoFisher) was combined with 10% foetal calf serum (FCS) and appropriate antibiotics, then filtered through a disposable, sterile 0.22 µm vacuum filter. The filtered media was stored at 4°C until use.

2.2.4 Supplements

Table 2-2: Antibiotics and supplements used for media

Antibiotics/supplements (Source)	Stock Solution	Final Concentration required	Storage
Kanamycin (Fluka BioChemika)	50 mg/mL in water	50 µg/mL	-20 °C
Gentamicin (Sigma-Aldrich)	25 mg/mL in water 12.5 mg/mL in water	25 µg/mL (LB agar) 12.5 µg/mL (LB broth) 10 µg/mL (chocolate agar)	-20 °C
Chloramphenicol (Sigma-Aldrich)	40 mg/mL in absolute ethanol	35 µg/mL (LB agar) 15 µg/mL (chocolate agar)	-20 °C
Vancomycin (Cayman Chemical)	5 mg/mL in water	5 µg/mL	-20 °C
Nalidixic acid (Acros Organics)	20 mg/mL in NaOH/water – see below	20 µg/mL	-20 °C
Cefazolin (Cayman Chemical)	2 mg/mL in water	2 µg/mL	-20 °C
Cycloheximide (Cayman Chemical)	10 mg/mL in water	10 µg/mL	-20 °C
Amphotericin B (Cayman Chemical)	8 mg/mL in DMSO	8 µg/mL	-20 °C
IPTG (Invitrogen)	0.1 M in water 1 M in water	0.04 mM (Miller Assay) 1 mM (IPTG overexpression)	4 °C or -20 °C
Glucose (Sigma-Aldrich)		2 mg/mL in LB media	15~25 °C

Nalidixic acid stock solutions were made by adding 100 mg to 2 ml dH_2O, then 1N NaOH was added dropwise and the solution mixed until the powder dissolved. The volume was then brought to 5 ml with dH_2O. The stock was filter sterilized with a 10 ml disposable syringe fitted with a disposable filter (0.22 µm pore size), dispensed into sterile Eppendorf tubes, and frozen at -20°C.

2.3 Culture conditions

2.3.2 *E. coli*

E. coli liquid cultures were incubated with continuous shaking at 200~225 RPM and aeration at 37 °C. *E. coli* was cultured on plates at 37 °C. Generally, *E. coli* cultures were grown overnight, unless otherwise noted. Glycerol stocks were made by combining 500 µl of an overnight culture with 500 µl of sterile 25% glycerol solution in cryopreservation tubes (Tarsons) and storing at -80 °C.

2.3.3 *B. quintana*

B. quintana was cultured on fresh (<1 week old) chocolate agar plates in a sealed candle jar at 36.5 – 37 °C. After positioning plates inside the jar, the candle was ignited and sealed in the jar, ensuring the flame was extinguished before the jar was placed into the incubator. Long-term -80°C freezer stocks of *B. quintana* were made by combining bacteria, scraped from a plate, into HIB media, with 25% glycerol, in cryopreservation tubes. All procedures involving live *B. quintana* were carried out within a Class II biosafety cabinet.

2.4 Plasmids

Table 2-3: Plasmids produced or used for this research

Plasmid	Size	Features	Source
pET28a(+)	5367 bp	Kanamycin resistance; optimised for protein overexpression in *E. coli*	Novagen
pET28a(+)-*ctrA*	6063 bp	*ctrA* gene, amplified from JK-31 *B. quintana*, inserted into the expression site	From Thomson, R. H[123].
pACYC184	4246 bp	Chloramphenicol resistance; p15 *ori*, compatible with other plasmids.	New England Biolabs
pACYC184-*lacZ*	7236 bp	*lacZ* gene, amplified from the SOS-R2 genome, cloned into HindIII and XbaI restriction sites	From Thomson, R. H[123].
pACYC184-*lacZ-ftsH*	7446 bp	Promoter region of *fstH* from *B. quintana* JK-31, cloned immediately upstream of the *lacZ* gene of pACYC184-*lacZ*	This study
pACYC184-*lacZ-ftsK*	7435 bp	Promoter region of *fstK* from *B. quintana* JK-31, cloned immediately upstream of the *lacZ* gene of pACYC184-*lacZ*	This study
pSRKKm	5775 bp	Broad-host-range plasmid Kanamycin resistance IPTG-inducible promoter	Kind gift from Clay Fuqua (Indiana University). Originally from Khan et al. 2008[125]
pSRK-*ctrA*	6380 bp	*ctrA* gene, amplified from *B. quintana* JK-31, cloned adjacent to IPTG-inducible promoter in pSRKKm	This study
pEX18Gm	5831 bp	Suicide plasmid in *B. quintana* Gentamicin resistance *sacB* gene for counterselection	Kind gift from the Ackerley lab (Victoria University of Wellington). Originally from Hoang et al. 1998[126]
pEX18-*ctrA*	7839 bp	~1000 bp homology arms of sequence flanking the *ctrA* gene from JK-31 *B. quintana*	This study

pRK2013	48 kb	Helper plasmid for triparental conjugation Kanamycin resistance	Biomedal, Spain. Originally from Figurski et al. 1979[127]
pSIM7	5676 bp	pBBR1 plasmid for expressing phage λ Red system Contains temperature-sensitive lambda repressor Chloramphenicol resistance	National Cancer Institute. Originally from Datta et al. 2006[128]

2.5 Oligonucleotides Primers

All of the primers contained tags to enable Gibson assembly and were designed using the NEBuilder tool (https://nebuilder.neb.com/#!/).

To make sure they were suitable, online tools such as NEB Tm calculator (https://tmcalculator.neb.com/#!/main) and Benchling[129] were used to optimize their length, GC content, and melting temperature. All of the primers were ordered from Integrated DNA Technologies. Lyophilised primers were resuspended at 100 µM concentration and stored at -20°C. Working stocks of 10 µM were used routinely.

All the primers used are listed up below. Restriction sites are underlined. Plasmid annealing sections for Gibson assembly are in bold and bases to amplify *B. quintana* sequence are in italic (Table 2-4)

Table 2-4: Primers used for this project

Name	Sequence	GC content	Tm (°C)	Restriction Enzyme	Product Size
FtsH-For	**5' TA AAC TAC CGC ATT AAA GCT TC***C ATA AAG CGG ATT ATG GC* 3'	44%	58	HindIII	219 bp
FtsH-Rev	5' **AG TGA ATC CGT AAT CAT ATG CA***T CAT ATT AAG CCC ACT TTA AAA TAC* 3'	28%	58	NdeI	
FtsK-For	5' **TA AAC TAC CGC ATT AAA GCT TC***A TAC CTT CAT TGA GAT CAG AAT AC* 3'	33%	59	HindIII	208 bp
FtsK-Rev	5' **AG TGA ATC CGT AAT CAT ATG CA***G CAT CCA TCA ATT CCA AAT AC* 3'	38%	59	NdeI	
CtrA-pSRK-For	5' **TAA CAA TTT CAC ACA GGA AAC AG**C ATA TG*C GCG TAT TAT TAA TTG AAG A* 3'	31%	61	NdeI	700 bp
CtrA-pSRK-Rev	5' **GAT ATC GAA TTC CTG CAG CCC GGG G***TA AGC GGT TTT ACG TAC* 3'	41%	55		
CtrA-pEX18-US-For	5' **GCA TGC CTG CAG GTC GAC TCT AGA G**GA TC*C AAG TCA AGT ATC GCA AG* 3'	45%	63	BamHI	1 kb
CtrA-pEX18-US-Rev	5' **TTT CAC TGC TTA** *TTT ATA TCC CTC ACT TTG TTC* 3'	33%	56		
CtrA-pEX18-DS-For	5' **TGA GGG ATA TAA A***TA AGC AGT GAA AAT GCA C* 3'	39%	57		1 kb
CtrA-pEX18-DS-Rev	5' **GGA AAC AGC TAT GAC CAT GAT TAC G***AA TTC AAA AAT AAG ACG TAA GGT TAT TTA AAT TC* 3'	21%	60	EcoRI	

2.6 DNA manipulation

2.6.2 Polymerase Chain Reaction

2.6.2.1 PCR for Gibson Assembly

PCR reactions for Gibson assembly were conducted with the Q5® High-Fidelity DNA polymerase (New England Biolabs). Genomic DNA from the *B. quintana* JK-31 strain was generously provided by Dr. Jane Koehler (University of California, San Francisco) or was purified according to the protocol below. Reagents (Table 2-5) were combined and gently mixed by tapping and collected at the bottom of the tube with a quick spin. The thermocycling conditions are detailed in Table 2-6. The annealing temperatures varied depending on the primers used.

Table 2-5: PCR mix using the Q5 high-fidelity polymerase

Reagent	**Volume**
Nuclease- Free water	32.5 µL
5x Q5 reaction buffer	10 µL
10 mM dNTPs	1 µL
10 µM Forward primer	2.5 µL
10 µM Reverse primer	2.5 µL
Template DNA (*B. quintana* JK-31 genomic DNA)	1 µL
Q5 DNA Polymerase (NEB)	0.5 µL
Total	50 µL

Table 2-6:Thermocycling conditions for a Q5 high-fidelity polymerase PCR reaction

Step	Temperature	Time
Initial Denaturation	98 °C	30 sec
35 cycles	98 °C	10 sec
	50-72 °C	30 sec
	72 °C	30 sec/kb
Final Extension	72 °C	2 min
Hold	4 °C	Infinite

2.6.2.2 Genomic DNA Extraction

Genomic DNA extracted from *B. quintana* JK-31 was purified using the Monarch® Genomic DNA Purification Kit (New England Biolabs). *B. quintana* was scraped from plates

and resuspended in 1 ml of PBS at a concentration of about 2 x 10^9 cells/ml in an Eppendorf tube. The rapid protocol for Gram-negative bacteria, using lysozyme, was used to purify *B. quintana* genomic DNA. After the purification procedure, the resultant DNA was eluted with 100 µL of Elution Buffer from the kit.

2.6.3 DNA Purification

PCR and restriction digest products were purified using the Zymo DNA Clean & Concentrator™-5 kit (Ngaio Diagnostics). DNA was eluted using 10 µL of Elution Buffer.

2.6.4 Plasmid Extraction

For plasmid extraction from bacteria, either overnight cultures or colonies resuspended in LB broth were used with the Monarch® Plasmid Miniprep Kit (New England Biolabs). The purified plasmids were eluted with 50 µL of Elution Buffer.

2.6.5 Plasmid DNA Sequencing

Full plasmid sequences were obtained from Plasmidsaurus (Oregon, USA). Purified plasmids were quantified with a Qubit Fluorometer (Invitrogen). Plasmid concentration was adjusted to 30 ng/µL, and quality was assessed using a NanoDrop spectrophotometer (ThermoFisher Scientific), ensuring that the 260/280 ratio was above 1.8 and the 260/230 ratio fell between 2.0-2.2. Subsequently, 10 µL of the sample was dispatched to Plasmidsaurus for whole plasmid sequencing.

Plasmids were occasionally sent to Macrogen (South Korea) and were quantified using a NanoDrop spectrophotometer. Subsequently, 10-20 µL of each sample was dispatched for Sanger sequencing.

The obtained results were analysed in Benchling[129] by importing the DNA sequence and using the alignment function for further analysis.

2.6.6 Agarose Gel Electrophoresis

DNA analysis was carried out with 1% or 2% agarose gels (LE Agarose Hyagarose, Hydragene), prepared with 1X TAE buffer and supplemented with 1x RedSafe Nucleic Acid Staining Solution (iNtRON, Ngaio Diagnostics). DNA samples were mixed with 5% glycerol, which works as loading buffer in 6:1 ratio and loaded into the well along with 1 KB DNA reference ladder (Hyperladder, Bioline). Once all samples were loaded, electrophoresis was conducted at around 100-110V for 60-90 min.

2.6.7 Gibson Assembly

Gibson Assembly was used to engineer plasmids. A molar ratio of 3:1 for the insert to the vector was determined using the NEBioCalculator (https://nebiocalculator.neb.com/#!/ligation). A consistent amount of 100 ng of vector was used for all Gibson Assembly reactions. The vector and inserts were combined with the Gibson Assembly Master Mix (New England Biolabs) and water in a PCR tube (Table 2-7). Samples were incubated at 50 °C for 60 min. Following incubation, the samples were either stored at -20 °C or kept on ice until the subsequent transformation step was ready to proceed.

Table 2-7: Gibson Assembly reaction mixture

Reagent	Volume
Purified, digested vector	Equivalent to 100 ng
Purified, digested insert	Varies
Gibson Assembly Master Mix	10 µL
Water	As needed to bring to 20 µL
Total	20 L

2.6.8 Restriction Enzyme Digestions

DNA products or plasmids were digested with either 2 µL of NEB buffer 3.1r or CutSmart buffer, along with either 0.5 or 1 µL of the appropriate restriction enzymes (New England BioLabs) in a final volume of 20 µl. The resulting mixtures were incubated at 37°C overnight, for cloning, or 1-3 hours, for diagnostic restriction digests. At the conclusion of the reaction, the samples were incubated at 65°C for 20 min to deactivate the enzymes. In cases where the restriction enzyme was heat-resistant (e.g., BamHI), the Zymo DNA Clean & Concentrator™-5 kit (Ngaio Diagnostics) was used to remove the enzymes.

2.6.9 Chemical Transformation

1.6.8.1 Preparation of Chemically Competent Cells

To prepare chemically competent bacteria, an overnight *E. coli* culture was diluted 1:100 in 100 ml of LB broth the following morning and further incubated at 37°C with 200 rpm agitation until the OD_{600} reached 0.4~0.6. The culture was placed on ice for 10 min, then 25 ml of the culture was transferred into two separate 50 ml Falcon tubes and centrifuged at 2500 × *g* for 10 minutes at 4°C. The supernatant was poured off and an additional 25 ml of the culture was transferred into each tube, followed by centrifugation. The resulting pellets were then washed twice with 25 ml of ice-cold 100 mM $MgCl_2$, with each wash followed by centrifugation. The pellets were resuspended in 1 ml of ice-cold 85 mM $CaCl_2$ diluted in 15% glycerol solution. These cells were then aliquoted into 100 µl portions and stored at -80°C until they were ready for use.

1.6.8.2 Chemical Transformation

Chemically competent cells retrieved from -80°C freezer were placed on ice, along with Gibson Assembly product, allowing both to thaw. Two microlitres of the Gibson Assembly mixture was added to the chemically competent cells. The combined cells and reaction mixture were incubated on ice for 10 min, then heat-shocked at 42°C in a water bath for 90 seconds, followed by immediate cooling on ice for 60 seconds.

Following the heat shock, the cells were recovered in 900 µl of LB broth and incubated at 37 °C, with shaking, for 1 hour. Subsequently, the cells were spread onto LB plates with appropriate supplements and/or antibiotics and were incubated overnight.

2.6.10 Electroporation of *Bartonella quintana*

A target plasmid was extracted from *E. coli* overnight culture. The plasmid was quantified via a nanodrop to ensure an optimal amount of at least 100 ng/µl. These plasmids were desalted through dialysis with nitrocellulose filter paper with a pore size of 0.025 µm for 30 min.

Concurrently, *B. quintana* was collected from 2-3 plates into 1 ml of pre-chilled 15% glycerol. This bacterial suspension was centrifuged at maximum speed for 2 min at 4°C to pellet the bacteria. The pellet was washed twice with 1 ml of 15% glycerol at 4°C. After these

washes, the pellet was resuspended in a small volume of pre-chilled 15% glycerol depending on the number of electroporation experiments planned.

Next, 50 µl of the bacterial suspension was mixed with the prepared plasmid and gently combined, followed by a brief incubation on ice. The entire mixture was then transferred into the 0.2 cm gap electroporation cuvettes (Bio-Rad) and electroporated at 2.5 kV, ensuring that the time constant was approximately 5 milliseconds. The cells were immediately recovered by adding 600 µl of warmed HIB, then 300 µl of the bacterial suspension was plated on a non-selective (no antibiotics) chocolate plate and allowed to air dry for 5 min. These plates were incubated overnight in a candle jar at 36.5~37°C to allow recovery.

The following day, bacteria were scraped from the recovery plates and resuspended in 300 µl HIB. Then 100 µl of resuspended bacteria were plated onto selective chocolate plates, which were incubated for at least 14 days in a candle jar.

Once colonies formed, each colony was patched into a small compartment on selective chocolate plates further incubated for 7 days to make cryopreservation stocks.

2.6.11 Conjugation of *B. quintana*

2.6.11.1 pSRK-*ctrA* bi-parental conjugation

S17-1 containing the pSRK-*ctrA* plasmid was cultured overnight in LB broth with kanamycin. The following morning, 500 µl to 2 ml of the cultures were washed with 10 mM $MgSO_4$ and resuspended in HIB to achieve an OD_{600} of 1.0. Concurrently, *B. quintana* cells were harvested from multiple plates and resuspended in HIB to a final OD_{600} of 8.0 or a value close to it. The *B. quintana* suspension and donor *E. coli* S-17 suspension were mixed at a volume ratio of 10:1. Then 100 µl of the mixture was applied to the centre of non-selective chocolate plates and allowed to air dry for 30 min. Subsequently, these plates were incubated for 7 hours at 36.5~37°C in a candle jar.

After this initial incubation, the conjugated cells were collected onto multiple chocolate plates containing vancomycin, nalidixic acid, cefazolin, and kanamycin. *B. quintana* is inherently resistant to nalidixic acid and cefazolin, which were added to eliminate the *E. coli* donor. Kanamycin was added to select for *B. quintana* containing pSRK-*ctrA* plasmid. These plates were incubated in a candle jar for 14 days at 36.5~37°C.

When colonies formed, each colony was patched onto a small section of chocolate plates with vancomycin, nalidixic acid, cefazolin, and kanamycin. These plates were further incubated for 7 days to make cryopreservation stocks and for further analysis.

2.6.11.2 pEX18-*ctrA* conjugation

Bi-parental

These conjugations followed the protocol described above (2.6.11.1), except the recipient *B. quintana* strain used already expressed the pSRK-*ctrA* plasmid. The procedure was the same up to the 7-hour incubation, after which the conjugation mixture was carefully scraped onto new plates containing vancomycin (to reduce contamination), nalidixic acid and cefazolin (to eliminate the *E. coli* donor), and kanamycin (tom maintain the pSRK-*ctrA* plasmid). These plates were incubated further overnight to eliminate any remaining *E. coli*. The next morning, the remaining *B. quintana* was resuspended on 400 µl HIB. Then 100 µl of the suspension and of a 1:10 dilution of it, were plated onto chocolate plates with vancomycin, nalidixic acid, cefazolin, kanamycin, and gentamicin. Kanamycin was used to maintain the replicating pSRK-*ctrA* plasmid, while gentamicin was used to select for integration of the pEX18-*ctrA* plasmid. These plates were incubated in a candle jar for 14 days at 36.5~37°C.

When colonies formed, each colony was patched onto a small section of chocolate plates with vancomycin, nalidixic acid, cefazolin, kanamycin, and gentamicin. These plates were further incubated for 7 days to make cryopreservation stock for further analysis.

Tri-parental

The protocol is quite similar to the bi-parental conjugation but with a few alternations. In tri-parental conjugation, the S17-1 *E. coli* strain containing pEX18-*ctrA* is replaced with a Top10 strain as the donor strain. Additionally, a pRK2013 helper strain was introduced to facilitate the transfer of plasmid from donor to the recipient *B. quintana.* After adjusting the OD_{600}, the helper and donor strain suspensions mixed in a volume ratio of 1:1. This mixture was then combined and incubated with *B. quintana* suspension.

Lawn method

In this simplified conjugation protocol, S17-1 *E. coli* harbouring pEX18-*ctrA* plasmid was cultured overnight with LB medium and gentamicin. The next day, the overnight culture was centrifuged at maximum speed for 2 min to pellet the bacteria. The bacterial pellets were washed twice with 1 ml of HIB and finally resuspended in 500 µl of HIB. Next, 20 µl of the bacterial suspension was mixed with another 500 µl of HIB and thoroughly resuspended. The entire mixture was pipetted directly onto a 4-5 day old chocolate plate with confluent *B. quintana* growing as a lawn. The *E. coli* suspension was spread evenly over the plate for 5 min and allowed to air dry for an additional 10 min. These plates were then incubated for 7 hours in a candle at 36.5~37°C. The rest of the procedure is the same as described for the biparental conjugations.

2.7 Bioinformatics

A bioinformatics methodology was employed to identify putative DNA sequence motifs that were similar to both full-length (TTAAN$_7$TTAAC) and half-length (TTAACCAT) CtrA binding sites within all predicted promoter sequences in the complete genome of *B. quintana* Toulouse (NCBI Reference sequence NC_005955.1)[101]. The genomic data and its annotation were downloaded from NCBI in FASTA and GFF formats, respectively[130]. After extracting the gene and pseudogene entries from the GFF file, the refined file was stored. The refined GFF file was then imported into the "usegalaxy.org" platform to acquire flanking regions for each gene, utilizing the "get flank" and "GetFastaBed" tools in the platform[131]. These flanking regions were designed to include the initial 50 base pairs of an open reading frame, along with 400 base pairs upstream, totalling 450 base pairs.

The resulting FASTA file from the "usegalaxy.org" platform was then transferred to the MEME suite (http://meme-suite.org), where the Find Individual Motif Occurrence (FIMO) function was used to conduct the motif search[132]. The genes obtained through the FIMO analysis were examined via the *B. quintana* Toulouse RefSeq link (NC_005955.1) within the NCBI open database, aiming to identify CtrA binding motifs located either in promoter regions or early within coding regions[130]. The Uniprot open database was used to extract further details of the predicted gene products associated with the binding motif[133].

To evaluate the similarity in amino acid sequence and protein function between the *B. quintana* gene homologs in *C. crescentus*, I carried out an alignment comparison using the

NCBI BLAST tool[134]. Based on this comparative analysis, the final candidates that produce proteins similar to those found in *C. crescentus* were selected for further investigation.

2.8 Beta-galactosidase Assay

2.8.2 Buffers

2.8.2.1 Permeabilization Buffer

The permeabilization buffer consisted of the following chemicals, dissolved in water: Na_2HPO_4 (100 mM), KCl (20 mM), $MgSO_4$ (2 mM), hexadecyltrimethylammonium bromide (CTAB; 0.8 mg/mL), sodium deoxycholate (0.4 mg/mL), and beta-mercaptoethanol (5.4 µl/mL).

To make 250 ml of permeabilization buffer, 200 mg of CTAB was independently dissolved in distilled water with a slight heat applied. Once it dissolved, the following chemicals were poured into graduated cylinder: 125 ml of 0.2M Na_2HPO_4, 5 ml of 1M KCl, 0.5 ml of 1M $MgSO_4$, and 25 ml of 4 mg/ml sodium deoxycholate. Subsequently, the solution was adjusted to the final volume of 250 ml using distilled water. This final media was filtered and stored at room temperature. Finally, aliquots of the buffer were dispensed into smaller tubes and beta-mercaptoethanol was introduced (5.4 µl/ml final concentration) immediately before use in an assay.

2.8.2.2 Ortho-nitrophenyl-β-galactoside (ONPG) Substrate solution

The substrate solution was made by combining the following chemicals in distilled water: Na_2HPO_4 (60 mM), NaH_2PO_4 (40 mM), o-nitrophenyl-β-D-Galactoside (ONPG) (1 mg/mL), and beta-mercaptoethanol (2.7 µl/mL).

To make 100 ml of substrate solution, the following chemicals were poured into graduated cylinder; 30 ml of 0.2M Na_2HPO_4, 20 ml of 0.2M NaH_2PO_4, and 100 mg of ONPG. Then the solution was adjusted to the final volume of 100 ml using distilled water. This final media was filtered with a 0.22 µm filter and stored in 10 mL aliquots within 15 mL Falcon tubes at -20 °C. Finally, 2.7 µl/mL volume of beta-mercaptoethanol was introduced into the thawed solution immediately before use in an assay.

2.8.2.3 Stop Solution

This stop solution consisted of 1 M of sodium carbonate dissolved in distilled water. The resulting media was then filtered with a 0.22 µm filter and stored at room temperature until use.

2.8.3 Assay

E. coli strains carrying the CtrA expression and LacZ reporter plasmids were incubated overnight, then diluted back to an OD_{600} of 0.1 the following morning. CtrA expression was induced with IPTG (0.04 mM) or suppressed with glucose (2 mg/ml) in LB broth with appropriate antibiotics. Cultures were incubated at 37 °C until they reached an OD_{600} of 0.5-0.7. For each sample, 10-20 µl of liquid culture was combined with 80-90 µl of Permeabilization Buffer in a microcentrifuge tube and incubated at 30°C for 20-30 min to facilitate cell membrane disruption and halt translation. After this, 600 µl of ONPG Substrate solution was added to each sample. After sufficient colour development, 700 µl of Stop Solution, 1M Na_2CO_3, was introduced to terminate the reaction, and the total reaction time was recorded. Samples were centrifuged for 10 min at maximum speed to pellet any debris, and the OD_{420} of the supernatants was measured. Miller units were calculated using the following equation:

$$Miller\ Units = 1000 \times \frac{(Abs_{420})}{(Abs_{600} \times V \times T)}$$

In this equation, T represents the reaction time in minutes and V represents the volume of the culture assayed in millilitres. Each condition was analysed in triplicate.

2.8.4 Data Analysis

Excel was used to calculate Miller Units and to evaluate the statistical significance using a T-test or multiple comparison with one-way ANOVA test. The normality of the data was visually inspected by a residual plot and QQ plot when ANOVA test was carried out. Graphs were generated using Prism[135].

2.9 CtrA Overexpression Analysis of *B. quintana* with pSRK-*ctrA*

2.9.2 Liquid culture growth curve

Five to seven-day-old plates with confluent *B. quintana* growth were used, with the bacteria scraped from the plates and resuspended in 1 ml filtered Schneider's Drosophila Medium containing 10% FCS. The OD_{600} absorbance was measured and recorded. Ten to fifteen millilitres of filtered Schneider's Drosophila Medium with FCS was aliquoted into a 25 ml tissue culture flask (JET BIOFIL). Each condition had three biological replicates. A final concentration of 50 μg/mL of kanamycin was added to flasks for *B. quintana* with pSRK-*ctrA* to maintain this plasmid. Additionally, a final concentration of 1 mM of IPTG was introduced into flasks for the induced CtrA condition. The final OD_{600} in all of the flasks was consistently 0.05 for all conditions. As a negative control, I included a flask with filtered Schneider's Drosophila Medium with FCS without any bacteria inoculation. All the flasks' lids were loosely fastened and placed upright in a candle jar. The jar was placed in a shaking incubator at 60 rpm 37°C for 7 days. Each day, 1 ml of media was taken in a biosafety cabinet to measure the OD_{600}. The OD_{600} measurements were recorded, and data analysed in Excel and Prism[135].

2.9.3 Bacterial Chromosome Analysis

2.9.3.1 FACS Buffer

Fluorescence-Activated Cell Sorting (FACS) buffer was used when bacterial cells were stained for flow cytometry. FACS buffer consisted of PBS with 1% of FCS. The resulting solution was filtered through a 0.22 μm vacuum bottle filter and stored at 4 °C until use.

2.9.3.2 Flow cytometry

One millilitre of *B. quintana*, grown in Schneider's supplemented media, at an OD_{600} of around 0.4, was centrifuged at 6,000 × *g* for 5 min. Pelleted bacteria were resuspended in 1 ml PBS and transferred into 4 ml of ice-cold 100% ethanol drop-by-drop, with continuous vortexing, to avoid any clumps when fixing and permeabilising the bacterial cells. The cells were incubated at -20°C for 15 min, then centrifuged at 3,000 × g for 5 min. The pelleted bacteria were then resuspended in 5 ml PBS and incubated for 15 min at room temperature. The bacteria were pelleted at 3,000 × g for 5 min and resuspended in 1 ml of FACS buffer with 3 μM DAPI (Thermo Scientific). The bacteria were further incubated another 15 min

and analysed on BD LSRFortessa™ X-20 flow cytometer or BD FACSCanto™ II flow cytometer. A violet laser with 450/40 channel was used to observe the DAPI fluorescence. The data and images were analysed with FlowJo software[136].

2.9.4 Microscopy

Microscope samples were prepared using the same procedure as for flow cytometry (2.9.3.2). The one millilitre sample was pelleted at maximum speed for one minute and resuspended in a small volume of FACS buffer. Five to ten microlitres of *B. quintana* were spotted onto a 25 × 75 mm microscope slide (Citoplus) and mounted using Prolong™ Diamond Antifade Mountant (Invitrogen) according to the manufacture's instruction. The sample was covered with a coverslip (Citoglas, 22 × 22 mm) and incubated for 24 h in dark at room temperature. The sample slides were then stored at -20°C until use. All the microscope images were taken with OLYMPUS cellSens Entry 4.1.1 software. Phase-contrast images were taken on OLYMPUS CX31 microscope using 100 × oil immersion objective. Fluorescence images were taken on OLYMPUS BX61 fluorescent microscope using 100 × oil immersion objective. Confocal image was taken on OLYMPUS FLUOVIEW FV3000 confocal microscope using 100 × oil immersion objective. Images were processed and scale bar was added with ImageJ.

3 Exploring the interaction between CtrA and putative regulated genes

3.1 Introduction

The CtrA orthologues in *B. quintana* and *C. crescentus* were previously shown to exhibit relatively high levels of amino acid identity[123]. In *S. meliloti* and *B. abortus*, *ctrA* is an essential gene and CtrA plays a critical role in cell cycle. Their CtrA orthologues also exhibit over 80% of amino acid identity with that of *C. crescentus*. Therefore, I hypothesised that the CtrA in *B. quintana* may also be involved in cell cycle and its regulation. In this part of this research project, I aimed to investigate the role of CtrA as a transcriptional regulator in *B. quintana*. To do this, a bioinformatics approach was used to identify CtrA binding sites in promoter regions of the *B. quintana* genome. Candidate genes that CtrA may regulate were selected. Interactions between CtrA and the promoter regions of those genes were tested using by fusing the promoters to LacZ on a reporter plasmid, then transforming the reporter into an *E. coli* strain with inducible *ctrA* on a compatible plasmid. Finally, LacZ activity upon *ctrA* induction was measured to detect CtrA-promoter interactions. I anticipated that this project would shed light on the role of CtrA in *B. quintana*.

3.2 Results

3.2.2 CtrA Binding Motif Search

Using the bioinformatics pipeline described in the methods, promoter regions, defined as encompassing 400 bp upstream and 50 bp downstream of a start codon, were extracted from the *B. quintana* reference Toulouse strain (NCBI accession PRJNA44). These promoter sequences were searched for both full and half *C. crescentus* CtrA binding sequences. Given the high amino acid identity between the *B. quintana* CtrA homologue and *C. crescentus* CtrA (81%), it was hypothesized that they might recognize similar DNA sequence motifs[123]. This approach allowed me to identify over 100 genes that have either full or half CtrA motifs in their *B. quintana* Toulouse genome. The NCBI genome database was utilized to determine the distance of these motifs from the start site of genes, and to exclude any motifs that is within the coding regions. Furthermore, the ontology of genes predicted to be encoded by these promoters was analysed to discern the potential functions of their gene products in similar species. This allowed me to exclude any genes that are not suspected to play role in the cell cycle and its regulation and also included any genes that may be unique to *B.*

quintana. Based on this analysis, the candidate genes were narrowed down to 14. Additionally, BLAST protein tools were used to identify the homologue proteins of those candidates with *C. crescentus* amino acids sequence and their similarity was investigated (Appendix 1).

Two putative full CtrA binding motifs were found in the promoter region of BQ_RS06180 (Figure 3-1). This gene is predicted to encode the DNA translocase FtsK, exhibiting a 66.86% amino acid identity with the cell division protein FtsK in *C. crescentus*. The FtsK protein plays a crucial role in converting energy from ATP hydrolysis into the translocation of bacterial chromosomes via its C terminus, contributing to cell division, cytokinesis and chromosome segregation[137]. Furthermore, the N terminus of FtsK is necessary for constructing and maintaining FtsZ rings required for bacterial cell division[138]. The sporulation protein SpoIIIE in *Bacillus subtilis* belongs to the FtsK family and also functions for translocation of chromosomes via ATPase machinery and is required for chromosome segregation[139]. In *C. crescentus*, FtsK is also found on the division plane prior to cell division in the predivisional cells. FtsK C-terminus-depleted *C. crescentus* revealed up to 20% defects in cell segregation and a *ftsK* mutated strain showed elongated filament with random distribution of FtsZ rings. Therefore, FtsK is necessary for cell division through the translocation of chromosome segregation as well as the formation of FtsZ ring[138,140]. I anticipated that BQ_RS06180 in *B. quintana*, homologue to the *ftsK* gene in *C. crescentus*, could play a critical role in the cell cycle and could be regulated by CtrA. Since BQ_RS06180 does not have a name in *B. quintana*, it is denoted as FtsK hereafter.

Similarly, two CtrA binding motifs were found in the promoter region of BQ11750 or *ftsH* though they are likely a single palindromic binding site (Figure 3-1). FtsH is an ATP-dependent metalloprotease that is important for quality control and regulation of proteins. It degrades unnecessary or damaged proteins and contributes to bacterial homeostasis. Mutation in the *ftsH* gene causes defects in cell division in *E. coli* and *C. crescentus* and arrested growth[141,142]. FtsH is conserved in other bacteria such as *Bacillus subtilis*. FtsH is not an essential protein in this bacterium but lack of FtsH causes a filamentous phenotype[143]. FtsH is also involved in the cell cycle and development of *C. crescentus* as mutations in the *ftsH* gene resulted in severe defects in cell division and inefficient synthesis of stalks. Mutants in *ftsH* are also more sensitive to heat, salts, and antibiotics, indicating a role in the general stress response. Although the *C. crescentus* FtsH protease controls the timing of cell differentiation, it apparently does not interact with CtrA[144,145]. I selected this gene as the second candidate for

this project because it plays a role in cell growth and division and has a relatively high amino acid identity with the *ftsH* gene in *C. crescentus.* It was also of interest to determine if *B. quintana* CtrA binds to the *ftsH* promoter, in contrast with *C. crescentus*.

In addition, consistent with previous work, this bioinformatic result did not show the CtrA binding motifs within the origin of replication regions in *B. quintana*[123].

Table 3-1: Promoters of interest determined from bioinformatics search.

Gene locus tag or name	Predicted gene product	Binding site distance	Homologous gene in *C. crescentus*	Amino acid identity
FtsK	DNA translocase FtsK	61 bp & 139 bp	Cell division protein FtsK	66.86 %
FtsH	ATP-dependent zinc metalloprotease FtsH	0 bp &1 bp	ATP-dependent zinc metalloprotease FtsH	69.33 %

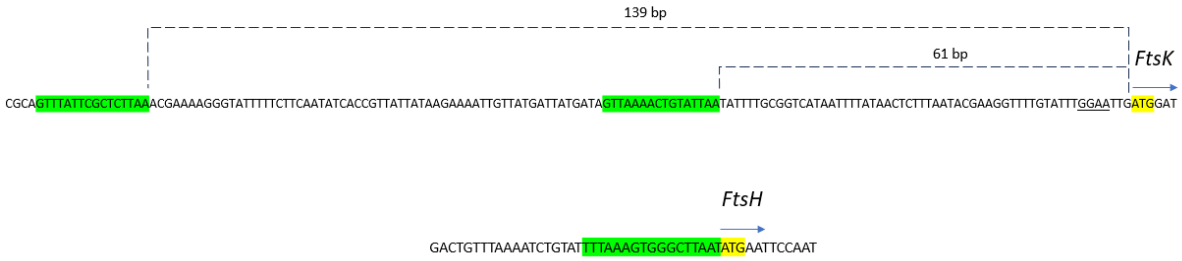

Figure 3-1: Sequence of promoter region for genes of interest. Full binding motifs are highlighted in green. Coding regions are represented in blue arrow and start codon is represented in yellow highlights. Dot lines represent the distance of the motif from the start codon of the genes. FtsH contains CtrA full binding motif in opposite strands. Underline GGAA in FtsK sequence, right before the start codon represents a possible sequence for the 16S ribosomal binding site.

3.2.3 Plasmid Construction

To investigate interaction between CtrA and the promoters of interest, I employed a beta-galactosidase reporter gene expression assay, as described previously[123]. This method requires two different types of plasmids. The first is pET28a(+)-*ctrA*, which encodes an IPTG-inducible CtrA from *B. quintana*, and a pACYC184-*lacZ* reporter plasmid, into which the promoters were cloned. Both plasmids have compatible origins, f1 and p15A,

respectively, so they can both be maintained in a single cell. The candidate promoter regions were cloned immediately upstream of the reporter *lacZ* gene. The constructed reporter plasmids were then transformed into an *E. coli* BL21(DE3) strain containing the pET28a(+)-*ctrA* inducible plasmid

pACYC184-*lacZ*, illustrated in Figure 3-2, was constructed previously in the MacKichan lab[123]. This plasmid, featuring a p15A origin of replication, confers resistance to chloramphenicol. The start codon (ATG) of the *lacZ* gene is strategically located within the NsiI restriction site (ATGCA▼T), to facilitate cloning of promoter sequences upstream.

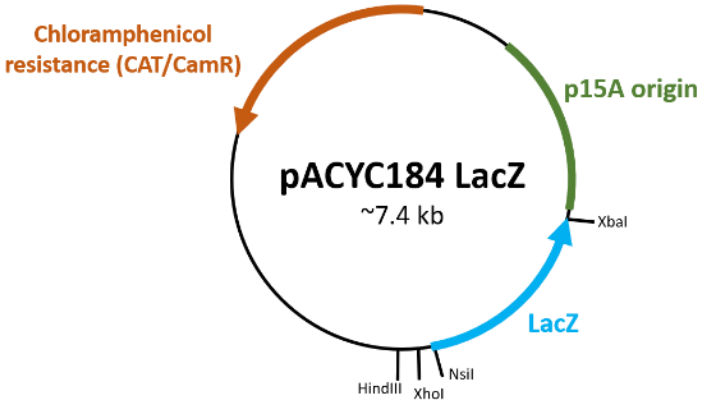

Figure 3-2: A diagram of the pACYC184-*lacZ* plasmid

The candidate promoter regions were amplified from *B. quintana* JK-31 genomic DNA by PCR, using the primers FtsH-For and FtsH-Rev (*ftsH* promoter) and FtsK-For and FtsK-Rev (*ftsK* promoter), as listed in Table 2-4. Following PCR, the products were confirmed through agarose gel electrophoresis and purified.

The purified pACYC184-*lacZ* plasmid (100 ng) of the pACYC184-*lacZ* plasmid was double-digested with the restriction enzymes NsiI and XhoI. The promoter sequence PCR products were cloned into the digested pACYC184-*lacZ* plasmid via Gibson Assembly. This product was chemically transformed into *E. coli* Top10 chemical competent cells and selected on chloramphenicol LB agar plates. On the following day, multiple colonies were screened through double digestion using XbaI and XhoI restriction enzymes (Figure 3-3). This digestion strategy was employed to rule out the presence of empty plasmids as the XhoI restriction site is no longer conserved in the plasmid once an insert is present and would produce different pattern in electrophoresis analysis from empty plasmid.

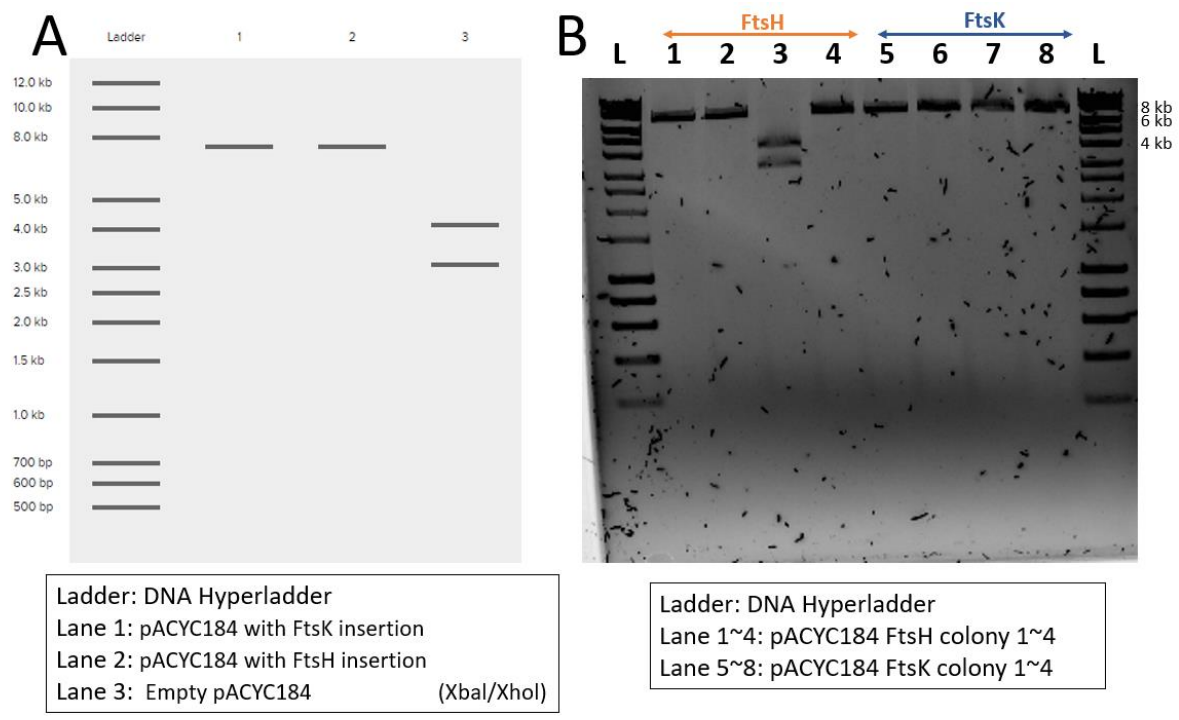

Figure 3-3: Promoter region of FtsH and FtsK insert restriction digest screen

Figure 3-3 A shows a virtual gel, produced by Benchling, with the predicted band locations for each condition with double digests. An insertion of either the *ftsK* or *ftsH* promoter would result in one band just below 8 kb, whereas the pACYC184-*lacZ* plasmid without any insertion should show two bands around 3 kb to 5 kb. Figure 3-3 B shows the result of the restriction digest of the plasmid from four colonies. All but one colony appeared to have the insertion. Following this screening, the *ftsH* and *ftsK* promoter regions were confirmed by Plasmidsaurus sequencing as having been successfully inserted into pACYC184-*lacZ*.

These reporter pACYC184-*lacZ* plasmids with FtsK or FtsH promoters were then introduced into *E. coli* BL21 strain carrying pET28a(+)-*ctrA* plasmid by chemical transformation. The resultant bacteria were selected on LB agar plates supplemented with kanamycin and chloramphenicol. Total plasmid content was recovered from some of the resultant colonies, then digested with XhoI and XbaI restriction enzymes to confirm that the plasmids were correct (Figure 3-4).

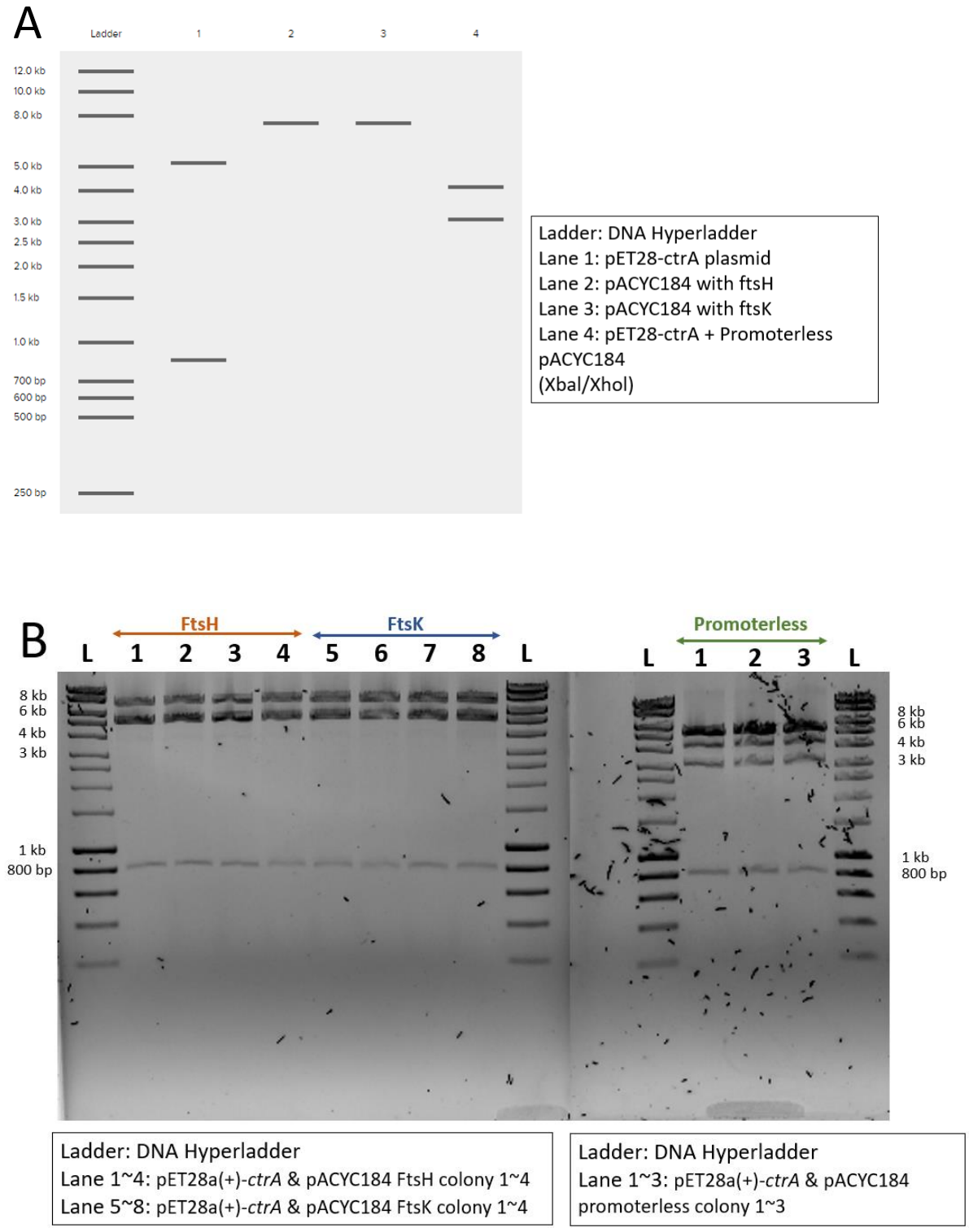

Figure 3-4: pET28a(+)-*ctrA* and pACYC184-*lacZ* reporter with insert restriction digest screen

Figure 3-4 A shows a virtual gel with predicted band locations for each plasmid with double digests. pET28a(+)-*ctrA* plasmid produces two bands around 5 kb and below 1 kb when restricted with XbaI and XhoI. Therefore, an *E. coli* that contains the pET28a(+)-*ctrA* plasmid and pACYC184-*lacZ* with the correct inserts should produce three bands in total (~8,

5, and <1 kb). In contrast, an *E. coli* that contains two plasmids, including pACYC184-*lacZ* without an insert, produces four bands. Figure 3-4 B shows the result of this screening. All of the colonies appear to have two plasmids, with bands of the expected sizes. I also produced an *E. coli* BL21 strain that contains pET28a(+)-*ctrA* and pACYC184-*lacZ* plasmid without any insert (Figure 3-4 B), which was included as a promoterless negative control. The resulting strains were frozen down and used for beta-galactosidase assays.

3.2.4 Gene Expression Assays via Beta-galactosidase Activity

E. coli BL21(DE3) strains, containing both the CtrA expression plasmid (pET28a(+)-*ctrA*) and the pACYC184-*lacZ* reporter plasmid with or without inserts, were used for a beta-galactosidase assay to assess *lacZ* expression levels and investigate the impact of *B. quintana* CtrA on the promoters of the genes of interest. By SDS-PAGE analysis, pET28a(+)-*ctrA* was confirmed to produce a protein consistent with CtrA when induced (Appendix 2).

To investigate whether *ftsH* and *ftsK* promoter regions interact with CtrA, both induction and repression media were created to control CtrA expression. The induction medium consists of LB media, kanamycin, chloramphenicol, to maintain both plasmids, and 0.04 mM ITPG to induce CtrA production. The repression medium is similar but replaces IPTG with 2 mg/ml glucose to repress CtrA expression. The beta-galactosidase activity was calculated as Miller unit, using the equation in Section 2.8.3. Higher Miller units correspond to greater beta-galactosidase activity. Three technological replicates were examined for each sample.

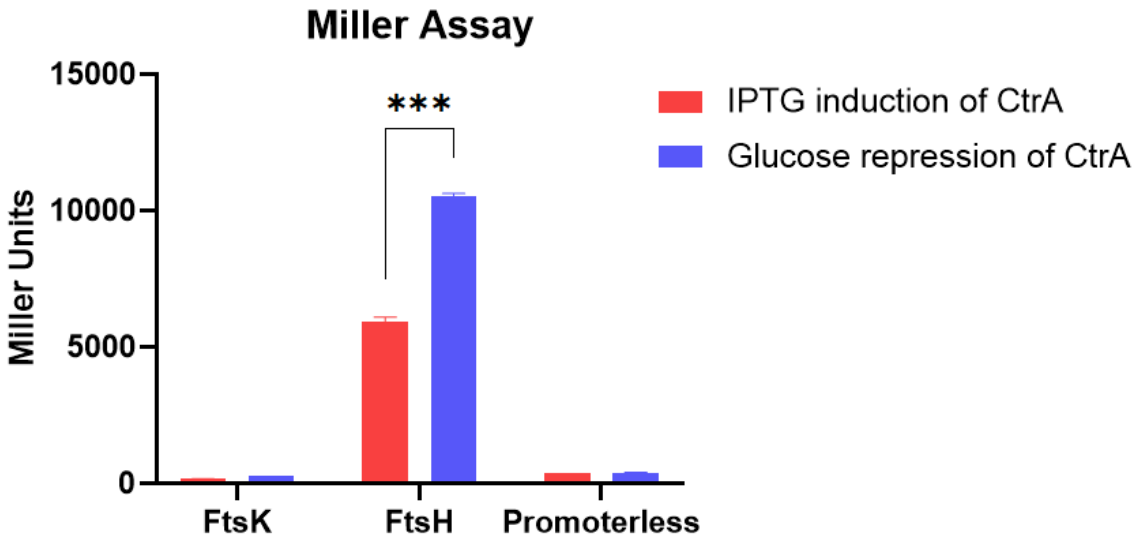

Figure 3-5: Preliminary Miller Assay result using cuvette. Red bars represent the average beta-galactosidase activity when CtrA was induced with IPTG. Blue bars represent the average beta-galactosidase activity when CtrA was repressed with glucose. Three asterisks (***) represents $P \leq 0.001$.

Initially, the beta-galactosidase assay was carried out in Eppendorf tubes and activity was measured by optical density. The initial attempt showed that the reaction time of FtsK was extremely fast. Therefore, the reaction volume was reduced by half to slow the reaction time and to minimise errors.

The summarized graph of results is shown above (Figure 3-5). The promoterless negative control lacks a promoter to express *lacZ*, therefore it indicates the baseline of the beta-galactosidase activity from the strain. The bar shows the mean and error bars the standard deviation of three data replicates. The data was analysed with an independent T-test. As seen in Figure 3-5, the beta-galactosidase activity driven by the *ftsH* promoter was significantly higher when the CtrA was repressed by glucose ($P \leq 0.001$). The overall activity of beta-galactosidase was high for *ftsH*, both with CtrA induced or repressed, suggesting that this is a strong and constitutive promoter in *E. coli*. As expected, the promoterless control resulted in extremely low beta-galactosidase activity for both CtrA induction and repression. Even lower beta-galactosidase activity was observed with the *ftsK* promoter, with both CtrA induction and repression. Several technical replicates confirmed that lower beta-galactosidase activity resulted from the *ftsH* promoter when CtrA expression was induced. The beta-galactosidase activity from the *ftsK* and promoterless controls remained extremely low,

however, the impact of CtrA induction or repression varied between assays with little consistency.

An alternative protocol was trialled for the beta-galactosidase assay, which was performed in 96-well plates instead of Eppendorf tubes and cuvettes. Due to the capacity of the 96-well plates, the assay was run on a smaller scale, approximately 1/7 the volume of the Eppendorf assay.

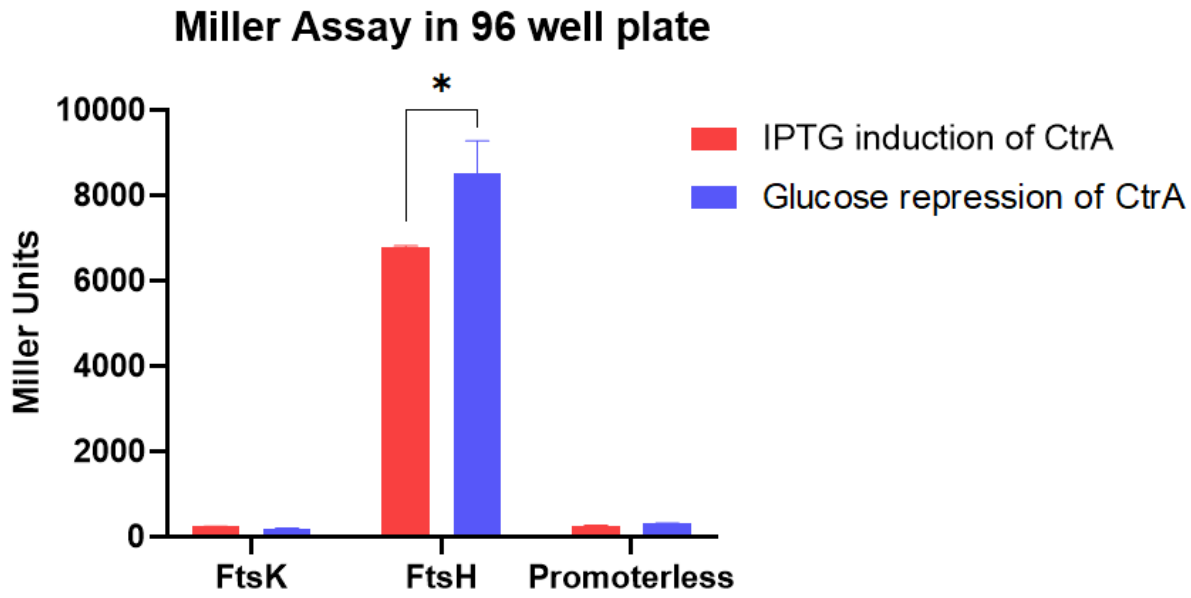

Figure 3-6: Miller Assay result using a 96-well plate. Red bars represent the average beta-galactosidase activity when CtrA was induced with IPTG. Blue bars represent the average beta-galactosidase activity when CtrA was repressed with glucose. One asterisk (*) represents $P \leq 0.05$.

As shown in Figure 3-6, there is a significant difference in beta-galactosidase activity from the *ftsH* promoter when CtrA is induced or repressed, as indicated by the asterisk ($P \leq 0.05$). Consistent with the assay done on cuvettes, the beta-galactosidase activity on promoterless negative control and FtsK remains extremely low. Although there is a difference in the scale of Miller units, the overall relationship between each promoter and the presence of CtrA seemed to be consistent with the assay done with Eppendorf tubes and cuvettes.

The spectrophotometer and the plate reader had differences in their readings of the OD_{600} due to differences in the light path length. After 3~3.5 hours of incubation for the *E.*

coli to be in the log phase, the spectrophotometer usually gave OD_{600} of 0.5~0.7, while the plate reader only gave 0.2~0.4. Therefore, for this assay, the absorbance was measured using cuvettes and the spectrophotometer.

Since the *ftsH* promoter seemed to drive less expression of *lacZ* when CtrA was induced, I investigated *lacZ* expression at different levels of CtrA induction. To achieve this, a range of IPTG concentrations (0.04 mM, 0.1 mM and 0.4 mM), were used to induce CtrA, with the expectation that higher IPTG concentration would result in lower beta-galactosidase activity.

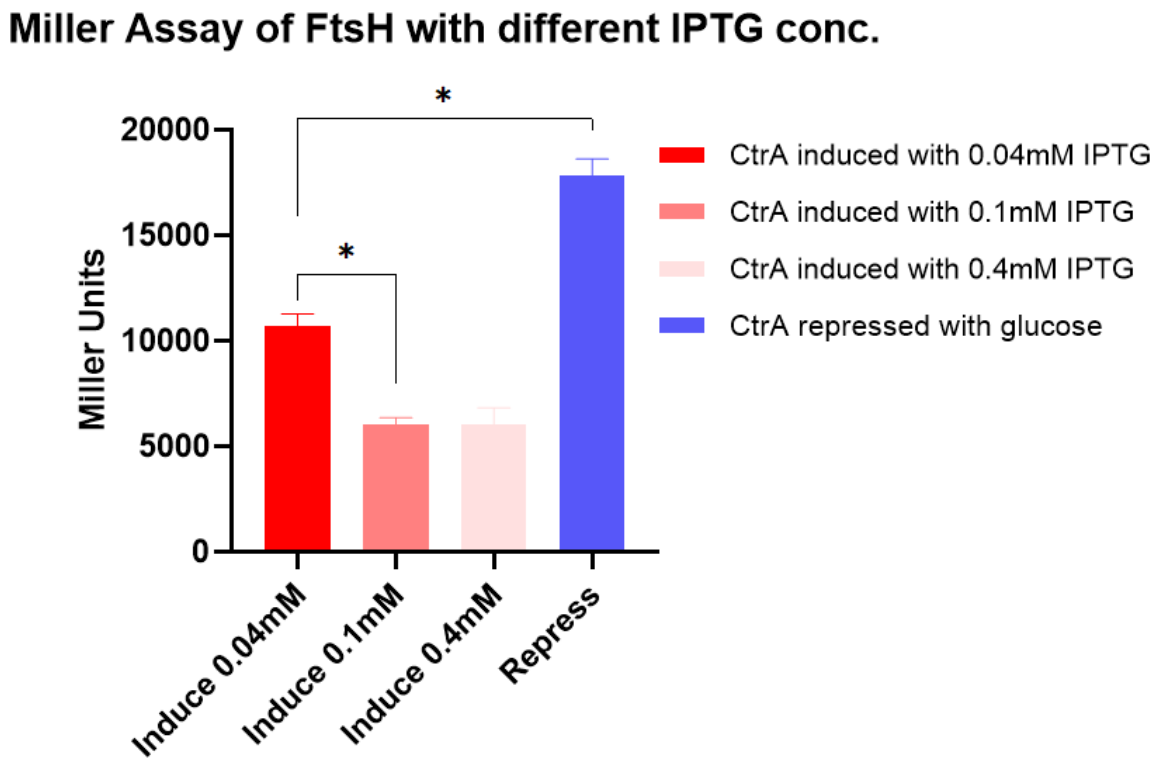

Figure 3-7: Miller Assay result on FtsH with different IPTG concentration. The three bars on the left of the graph, coloured red to pink, represent the average beta-galactosidase activity when CtrA was induced with IPTG. Blue bars represent the average beta-galactosidase activity when CtrA was repressed with glucose. One asterisk (*) represents $P \leq 0.05$.

Figure 3-7 shows the result of beta-galactosidase assay with the *ftsH* promoter driving *lacZ*, in the presence of a range of IPTG concentrations and, for comparison, glucose repression. The bar shows the mean and the error bars indicate standard deviations of three data replicates. The data was analysed with a one-way ANOVA test. The normality of those

data was verified with residual plot and QQ plot. As expected from the previous assay, there was a significant difference in the induced sample with the original IPTG concentration (0.04 mM) and the repressed sample ($P \leq 0.05$). Furthermore, we observed a significant difference in the induced sample with 0.04 mM of IPTG and 0.1 mM of IPTG ($P \leq 0.05$) but not in the sample with 0.1 mM of IPTG and 0.4 mM of IPTG ($P \geq 0.05$). A higher level of induced CtrA correlates with a reduction in beta-galactosidase activity up to a certain IPTG concentration (0.1 mM), after which higher IPTG levels do not have any further impact. This is probably due to the fact that the system was saturated, e.g. they reached the maximum CtrA production from pET28a(+) plasmid on *E. coli*.

These beta-galactosidase assays suggest an interaction between CtrA and the *ftsH* promoter, specifically, with CtrA repressing expression of the LacZ reporter in *E. coli,* and possibly the *ftsH* gene in *B. quintana*. Meanwhile, the very low activity of the *ftsK* promoter in *E. coli* prevents me from drawing any conclusions as to whether it interacts with CtrA.

3.3 Discussion

The goal of this project was to investigate the relationship between CtrA and its putative regulon in *B. quintana*, using a beta-galactosidase reporter assay.

The bioinformatics results revealed a wide range of possible genes that may be regulated by CtrA *B. quintana.* This includes a few *fts* cell cycle genes, DNA repair genes and hemin-degrading factors (Appendix 1). However, this result did not suggest any CtrA binding sites around the chromosomal origin of replication in *B. quintana,* in contrast to *C. crescentus,* but consistent with previous findings[123].

One of the gene candidates, BQ_RS06180, is predicted to encode the DNA translocase FtsK, sharing over 66% amino acid identity with the cell divisional FtsK in *C. crescentus*. FtsK protein is involved in harnessing energy from ATP hydrolysis to facilitate the translocation of bacterial chromosomes, thus playing a pivotal role in cell division and chromosomal segregation. FtsK is also responsible for assembly and maintenance of FtsZ rings, which are crucial for bacterial cell division. CtrA has been shown to bind to the *ftsK* promoter and control its expression in *S. meliloti*, *B. abortus*, and *C. crescentus*[146]. Furthermore, bioinformatics analyses suggest interactions between CtrA and the *ftsK* promoters of other diverse alpha-proteobacteria, including *Agrobacterium tumefaciens*,

Ehrlichia chaffeensis, *Wolbachia*, and *Rickettsia prowazekii*[146]. However, the overall beta-galactosidase activity, when driven by the *B. quintana ftsK* promoter, was too low to detect any changes when CtrA was induced. We were therefore not able to reach any conclusions about interactions of CtrA with the *ftsK* promoter. Alternative approaches, such as ChIP-Seq or electrophoretic mobility shift assays, would be useful to demonstrate a direct interaction between CtrA and the *ftsK* promoter.

Another gene candidate, *ftsH*, encodes an ATP-dependent metalloprotease crucial for protein quality control and regulation in bacteria by degrading damaged or unnecessary proteins. Multiple studies demonstrated that mutations in *ftsH* gene result in cell division and stress response defects, although the *ftsH* promoter is reportedly not controlled by CtrA in *C. crescentus* [144,145]. However, the beta-galactosidase assay demonstrated a robust impact of CtrA on expression from the promoter of the *B. quintana ftsH* gene. Notably, the beta-galactosidase activity was significantly diminished when CtrA was induced with higher levels of IPTG. This implies that CtrA acts as a repressor of the *ftsH* gene in *B. quintana*. CtrA has been reported to act as both a repressor and an activator in *C. crescentus*[101]. For example, CtrA acts as a repressor of a *hemE* gene to control the DNA replication[147] whereas CtrA also acts as an activator of the *fliQ* flagellar gene[148]. Furthermore, a single gene, such as *ctrA* and *ftsZ* can also be activated or repressed by CtrA at different points in the cell cycle[101,102,106].

There are a few limitations of this beta-galactosidase assay. First, positive controls, either a high-activity promoter or a promoter known to be activated by CtrA, were not included in this experiment. Although high-activity promoters in *E. coli* are available, there are no *B. quintana* promoters known to be activated by CtrA. The promoterless negative control exhibited very low expression of *lacZ*, regardless of whether CtrA was induced or repressed.

Second, this system could be influenced by other regulatory elements in the *E. coli* host. Finally, although this system demonstrated the impact of higher CtrA induction on the *ftsH* promoter, it is important to note that direct interactions between CtrA and regulated promoters were not detected using this approach. Therefore, future studies should employ methods that enable detection of DNA-protein interactions.

The next step could involve Chromatin Immunoprecipitation (ChIp) analysis enabling the identification of promoters that physically interact with CtrA. This would enhance our

understanding of protein-DNA interactions and may unveil a wider range of DNA binding sites for CtrA. Additionally, RNA-seq analysis would help investigate gene expression patterns and identify differences in gene expression under CtrA upregulation, further deepening our understanding of the underlying cellular processes and potential pathways involved.

4 Constructing a conditional CtrA mutant strain in *B. quintana*

4.1 Introduction

CtrA is exclusively found in alpha-proteobacteria, where it is usually an essential gene whose product functions as a central regulator of the cell cycle. We hypothesised that CtrA is likely important in *B. quintana* as well, and may play a role in the tight cell cycle regulation that occurs in the intraerythrocytic niche. Without halting replication and limiting the number of bacteria, *B. quintana* would lyse erythrocytes and cause a debilitating illness that might limit the ability of the bacteria to persist or be to transmitted to a new host. In this part of the research project, I aimed to construct a conditional null *ctrA* mutant *B. quintana* strain. This project employed a conditional knockout, rather than a simple deletion, because I assumed that *ctrA* is also likely essential in *B. quintana*. Therefore, the *ctrA* gene needed to be introduced on a plasmid before it could be deleted from the chromosome. This approach has been used in the study of *ctrA* orthologues from other alpha-proteobacteria, including *Sinorhizobium meliloti* and *Brucella abortus*[115,119]. A series of conjugations were required for this approach, as summarised in Figure 4-1.

Briefly, a conjugation with the *E. coli* donor, harbouring a broad-host-range pSRKKm plasmid with IPTG-inducible *ctrA*, was carried out with a wild type JK-31 *B. quintana* as the recipient. The pSRK plasmids are able to replicate in *B. quintana*. The resulting colonies, selected on kanamycin, would then be used for the next round of conjugation. In the second conjugation, the *E. coli* donor would be carrying a pEX18 mutagenesis plasmid, which includes homologous flanking regions (~1000 bp) up- and downstream of the chromosomal *ctrA* gene, the *sacB* levansucrase counterselection gene, and gentamicin resistance. This plasmid is unable to replicate in *B. quintana*, so selection of gentamicin-resistant colonies selects for integration of the plasmid, forming a merodiploid strain. The resulting colonies would be maintained on kanamycin and gentamicin, to maintain the replicating pSRK-*ctrA* plasmid and the integrated pEX18 plasmid. Finally, because SacB in Gram-negative bacteria is lethal in the presence of sucrose, loss of the integrated plasmid would be selected on sucrose plates. Loss of the integrated plasmid may lead to reversion to the wild type or to loss of the *ctrA* gene, so sucrose-sensitive colonies would need to be screened to distinguish between these two outcomes. At the same time, IPTG would be added to plates to induce CtrA expression from the pSRK-*ctrA* plasmid. The goal of this project was to generate the conditional CtrA mutant strain and use it to observe the effect of CtrA loss on *B. quintana*

after removing IPTG from the media. The effect of CtrA overexpression could also be studied by treating *B. quintana* with the pSRK-*ctrA* plasmid with IPTG.

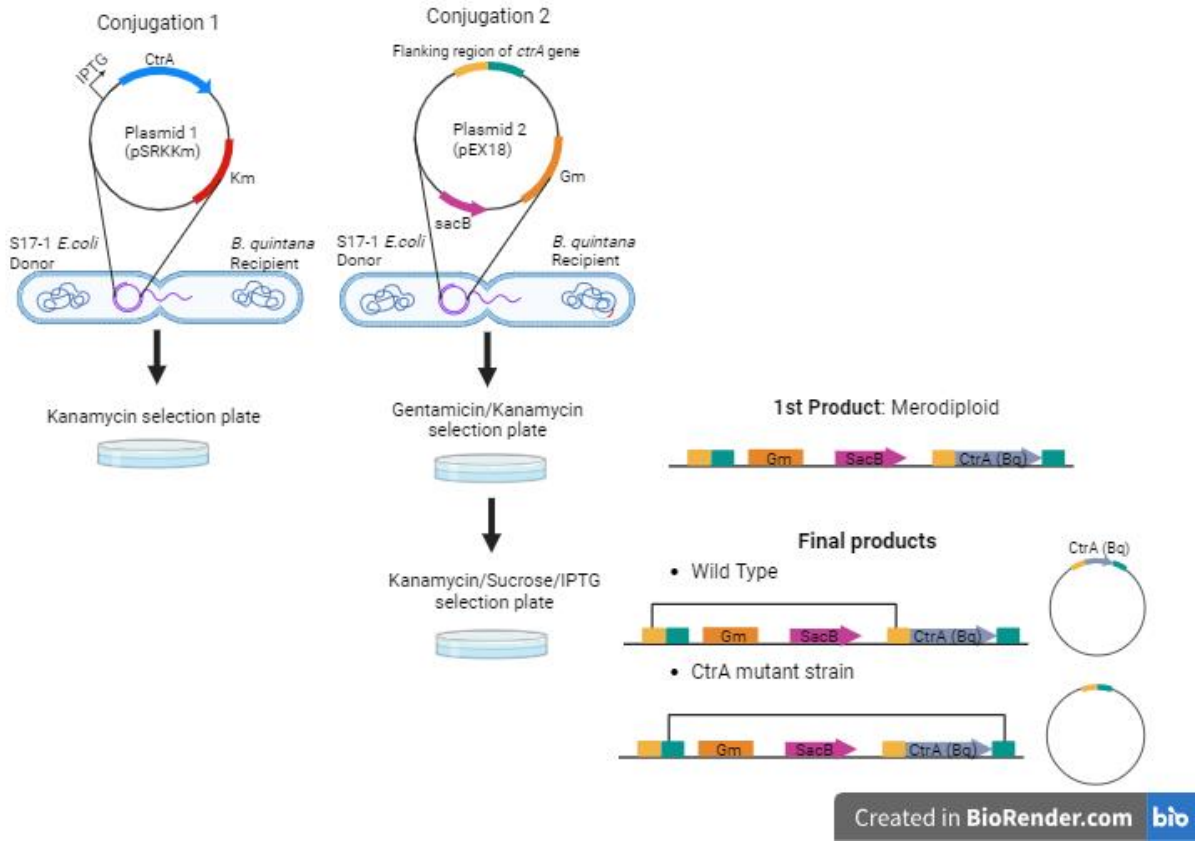

Figure 4-1: Schematic diagram of constructing a CtrA conditional mutation in *B. quintana*. Plasmid 1 is a replicating plasmid that provides an inducible *ctrA* gene in trans, before Plasmid 2, a non-replicating mutagenic plasmid, is introduced to delete the chromosomal copy of *ctrA*.

It is noteworthy that this project would be the first instance of the generation of a conditional null mutant strain in *B. quintana*.

4.2 Results

4.2.2 Construction of the *ctrA* complementation plasmid

In order to make a conditional mutant *ctrA* strain in *B. quintana*, I first needed to construct the complementation plasmid. To do this, I started with pSRKKm, a plasmid that confers kanamycin resistance and possesses a broad-host-range origin of replication, allowing this plasmid to replicate in *B. quintana* [125] (Figure 4-2).

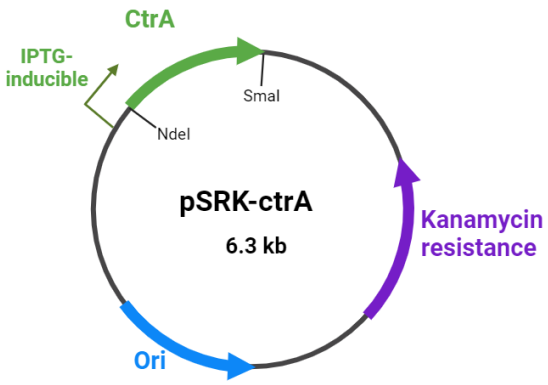

Figure 4-2: A diagram of the pSRK-*ctrA* plasmid

The *B. quintana ctrA* gene was identified by analysis of the *B. quintana* Toulouse genome in NCBI (NCBI Reference sequence NC_005955.1) and is annotated as "response regulator transcription factor", at locus BQ09460. The gene was amplified from *B. quintana* JK-31 genomic DNA by PCR, using the CtrA-pSRK-For and CtrA-pSRK-Rev primers (Table 2-4). The CtrA-pSRK-For primer was engineered to include an NdeI restriction site, with the ATG bases in the NdeI restriction site designed to incorporate the ATG start site of the *ctrA* gene, ensuring the correct final orientation. The PCR result was confirmed by agarose gel electrophoresis and purified (Figure 4-3).

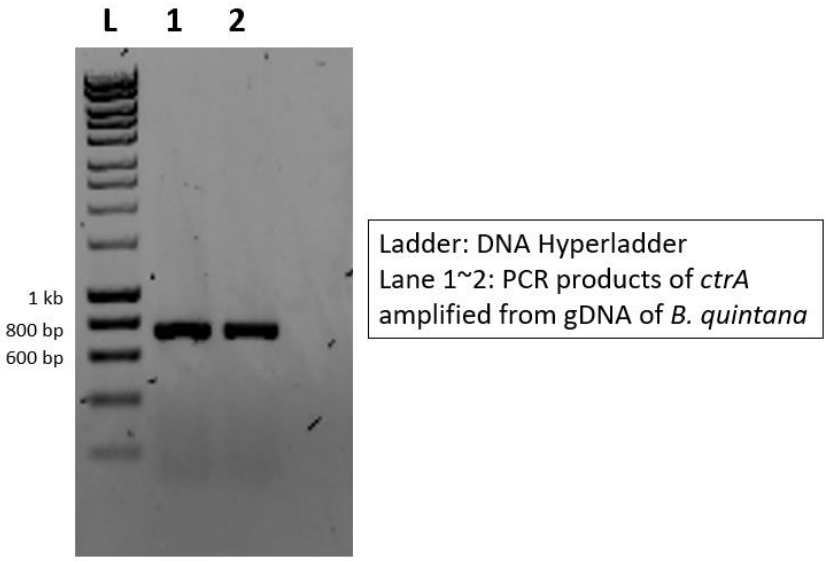

Figure 4-3: *ctrA* gene PCR product screen

Figure 4-3 shows the PCR product of *ctrA* gene amplified from *B. quintana* gDNA, which was around the expected size of 700 bp. This PCR product was then cloned into the pSRKKm plasmid, linearised by digesting with NdeI and BamHI, by Gibson Assembly. The assembled plasmid was then transformed into the *E. coli* Top10 chemically competent cells and selected on kanamycin LB agar. Insertion of the *ctrA* gene resulted in the destruction of the BamHI restriction site. Therefore, another restriction enzyme, SmaI, was used to confirm the *ctrA* insertion in cloning (Figure 4-4).

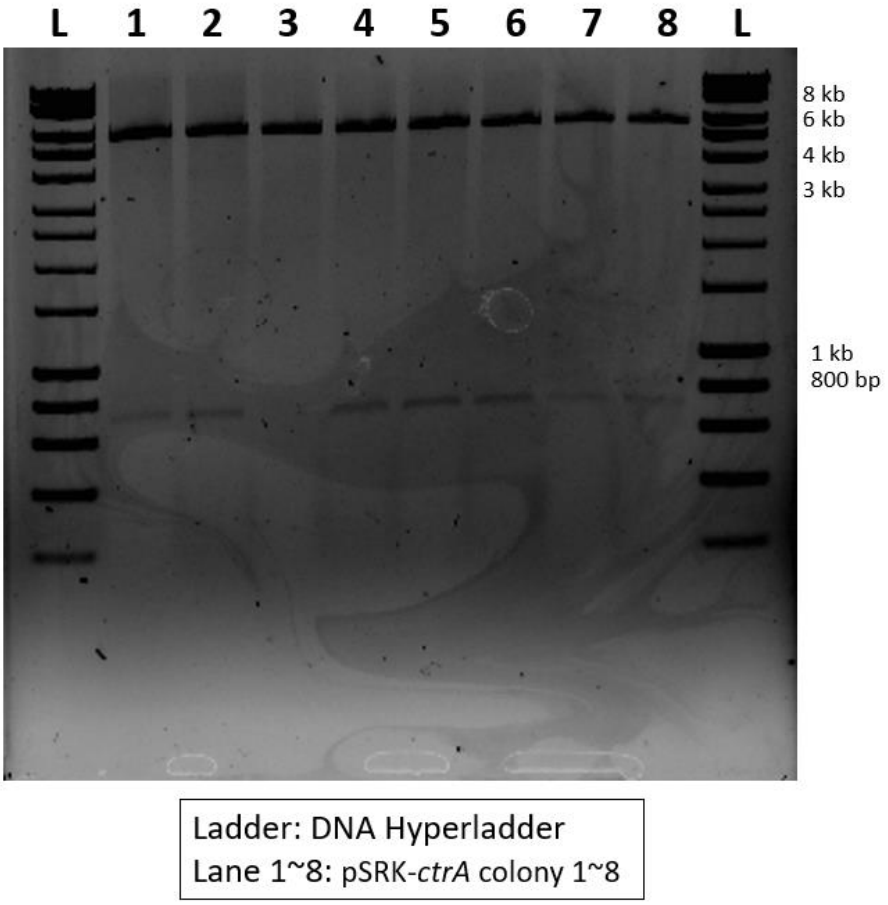

Figure 4-4: *ctrA* insert in pSRK plasmid restriction digest screen

Figure 4-4 shows plasmid screening by digesting with NdeI and SmaI restriction enzymes. The pSRK vector is 5.8 kb and the insert is 700 bp. All of the colonies, apart from colony 3 (lane 3) have bands of about 6 kb and 6-800 bp, as expected. The full plasmid sequence for colonies 1 and 2 (lane 1 and 2) was confirmed (Appendix 5) therefore, those plasmids were purified and transformed into the *E. coli* S17-1 conjugation strain, which was used to carry out a conjugation with *B. quintana*.

4.2.3 Mutagenesis Plasmid Construction

The mutagenic pEX18-*ctrA* plasmid was constructed to delete the chromosomal copy of *ctrA* gene from *B. quintana* that was carrying the complementation pSRK-*ctrA* plasmid. The pEX18-*ctrA* plasmid confers gentamicin resistance but is unable to replicate in *B. quintana*. Therefore, bacteria acquire gentamicin resistance only if this plasmid is integrated into the chromosome. This plasmid is also equipped with the *sacB* gene, which encodes the enzyme levansucrase. Levansucrase converts sucrose into a lethal compound for Gram-

negative bacteria, therefore *sacB* was used for counterselection, to obtain colonies that had lost the integrated plasmid. The flanking regions of the *B. quintana ctrA* gene were cloned next to each other utilising EcoRI and BamHI restriction sites. This arrangement enables integration of the plasmid into the *B. quintana* chromosome, by homologous recombination, at site of the chromosomal *ctrA* gene (Figure 4-5).

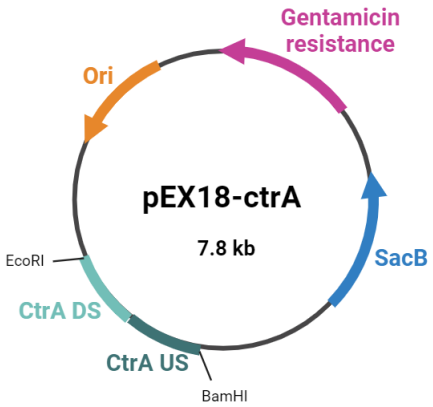

Figure 4-5: A diagram of the pEX18-*ctrA* plasmid

To construct the mutagenesis plasmid, pEX18-*ctrA*, PCR was used to amplify approximately 1,000 base pairs of flanking regions of the *ctrA* gene from *B. quintana* JK-31 genomic DNA. The amplification of the upstream region was carried out using primers CtrA-pEX18-US-For and CtrA-pEX18-US-Rev, and the amplification of the downstream region was carried out using the CtrA-pEX18-DS-For and CtrA-pEX18-DS-Rev, as listed in Table 2-4. To simplify the process of verifying colonies later on, the BamHI site was retained in the upstream forward primer. The downstream reverse primer included an EcoRI site for the same purpose. The PCR result was confirmed through agarose gel electrophoresis (Figure 4-6).

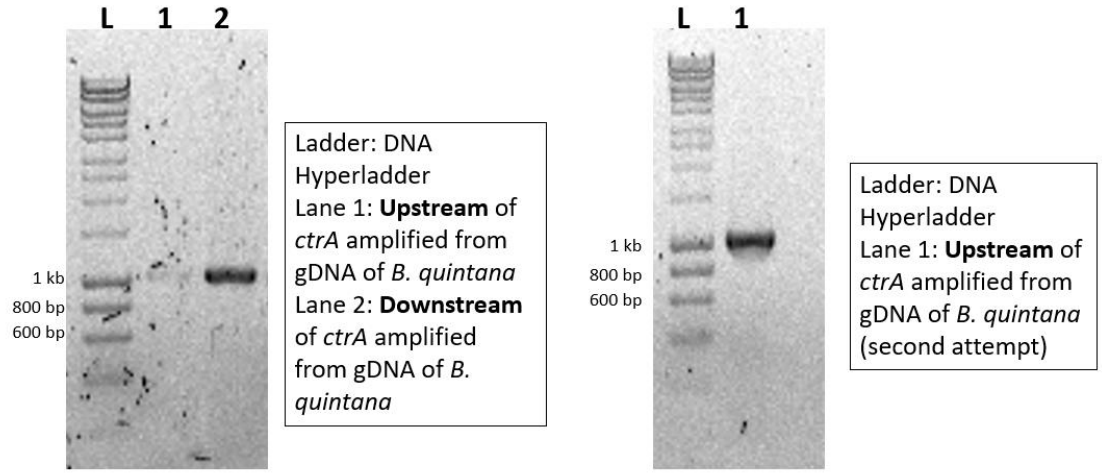

Figure 4-6: *ctrA* flanking regions PCR product screen

Figure 4-6 shows the PCR products of the *ctrA* flanking regions amplified from *B. quintana* gDNA. The PCR yielded products of the expected size for both reactions. The PCR products were then cloned into pEX18Gm plasmid, linearised by digest with EcoRI and BamHI, by Gibson Assembly. The assembled plasmid was then transformed into Top10 chemically competent cells and selected on gentamicin LB agar. Purified plasmids from the colonies obtained were digested with EcoRI and BamHI, to confirm the presence of flanking regions of *ctrA* in pEX18 plasmid.

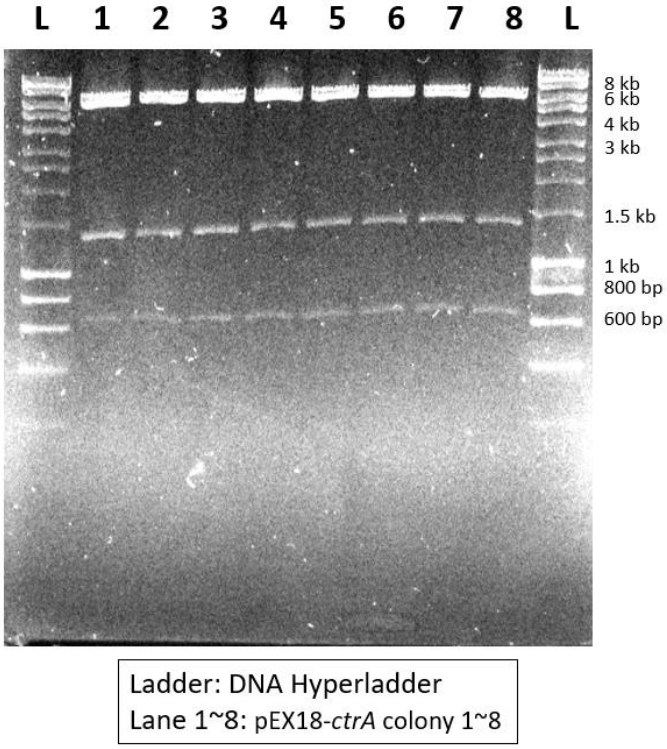

Figure 4-7: *ctrA* insert on pEX18Gm plasmid restriction digest screen

Figure 4-7 shows the restriction digest of the purified plasmids. The EcoRI restriction enzyme cleaves inside the insert, therefore, double digestion is expected to result in three bands (of 5.8 kb, 1.5 kb, and ~600 bp) if the pEX18 plasmid has both inserts. All the colonies had band sizes consistent with having both flanking regions inserted. Full plasmid sequencing was carried out on purified plasmids from colonies 2, 4, 5, 6 and 7, confirmed the correct insertion of the flanking regions. Those plasmids were purified and transformed into the *E. coli* S17-1 conjugation strain, to carry out the second conjugation with *B. quintana*.

4.2.4 Conjugation and Electroporation

Biparental conjugation for complementation

Before the conditional *ctrA* mutant could be made, a plasmid-borne copy of *ctrA*, under the control of an inducible promoter, needed to be introduced into wild type JK-31 *B. quintana*. To do this, a biparental conjugation was carried out, using the S17-1 *E. coli* strain containing the pSRK-*ctrA* plasmid as a donor, and wild type JK-31 *B. quintana* as the recipient. After 14 days of incubation, I observed multiple white colonies on chocolate plates consistent with the appearance of *B. quintana* (Figure 4-8). The kanamycin resistance of this *B. quintana* was confirmed by passaging to fresh selective chocolate plates. Therefore, these bacteria were likely to contain pSRK-*ctrA* plasmid.

Figure 4-8: Chocolate agar and colonies from the conjugation of pSRK-*ctrA* plasmid in *B. quintana* JK-31

To further confirm that these colonies contained the plasmid, a colony was expanded on a separate plate and grown to confluence. The resulting confluent bacteria were scraped from the plate, resuspended in 400 µl of HIB, and the plasmid extracted with a Monarch Miniprep kit. The purified plasmid was then assessed by restriction digest.

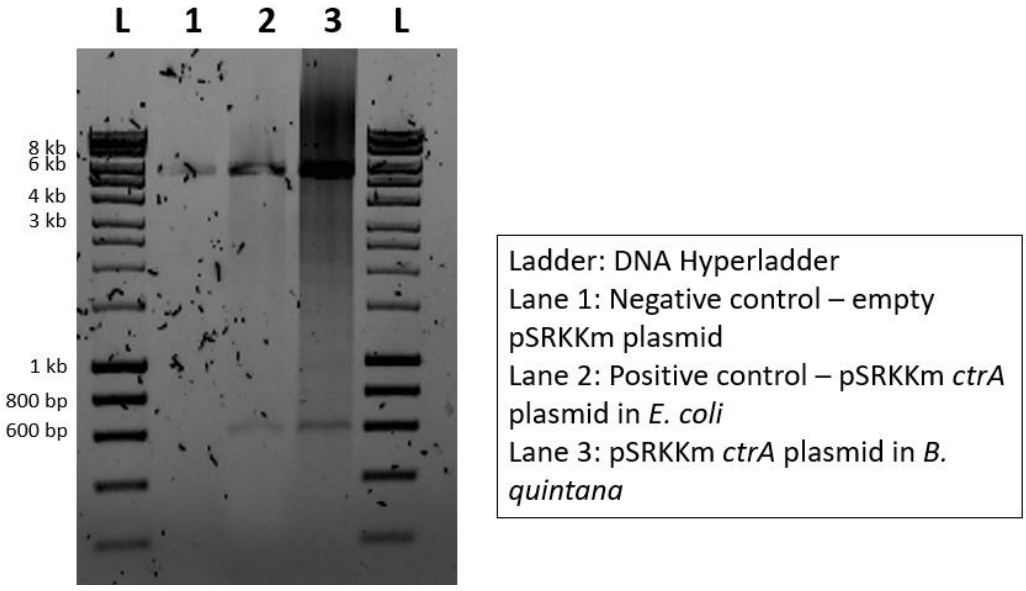

Figure 4-9: pSRK-*ctrA* on *B. quintana* JK-31 restriction digest screen with NdeI and HindIII.

Figure 4-9 shows the *B. quintana* plasmid, with controls, digested with NdeI and HindIII restriction enzymes. The HindIII restriction enzyme cleaves inside the insert, therefore, double digestion results in two separate bands, of around 6 kb, corresponding to the vector, and another one at around 600 bp. The profile of the *B. quintana*-derived plasmid was consistent with that of the pSRK-*ctrA* plasmid extracted from *E. coli*; both were distinct from the negative control with an empty pSRK plasmid. Therefore, *B. quintana* seemed to have a pSRK-*ctrA* plasmid. This purified plasmid was additionally confirmed with sequencing, and found to be the same as the one extracted from *E. coli.* From here forward, the wild type strain carrying the pSRK-*ctrA* plasmid was used as the recipient for conjugations with the mutagenesis plasmid.

Quality controls before mutagenesis conjugation.

Before proceeding with the conjugation of the mutagenic plasmid into the complemented strain, I carried out some tests to ensure that the plasmid retained essential

functions and could be mobilised by S17-1. These tests included a test conjugation, into an *E. coli* recipient strain, and confirmation that the *sacB* gene in the plasmid conferred lethality on *E. coli* in the presence of sucrose.

① Test conjugation

Since conjugations into *B. quintana* can be difficult, we first used an *E. coli* recipient to check that our S17-1 strain and the mutagenic plasmid could be mobilised. In this case, the recipient strain used was an *E. coli* K12 strain containing the pACYC184 plasmid. The mutagenic plasmid, pEX18-*ctrA* and pACYC184 are compatible plasmids, as they have different types of origin of replication. This is important because, in contrast with the situation in *B. quintana*, pEX18-*ctrA* can replicate in *E. coli*. Also, pACYC184 is selected with chloramphenicol and pEX18-*ctrA* is selected for on gentamicin. Therefore, transconjugants could be selected on LB plates with gentamicin and chloramphenicol. Confirming the ability S17-1 with pEX18-*ctrA* plasmid to mobilise its plasmid via conjugative transfer is important, especially as it can take more than 14 days to know if a *B. quintana* conjugation has been successful. The pACYC184 recipient and S17-1 donor were conjugated on nitrocellulose filter paper (0.22 µm pore size) on LB agar with no antibiotics. After 5-6 h incubation at 37°C, the bacteria were dissociated from the filter paper and transferred onto LB plates with gentamicin and chloramphenicol. Two negative controls, donor only (S17-1 with pEX18-*ctrA*) and recipient only (*E. coli* K12 with pACYC184), were included. Results are shown in Figure 4-10.

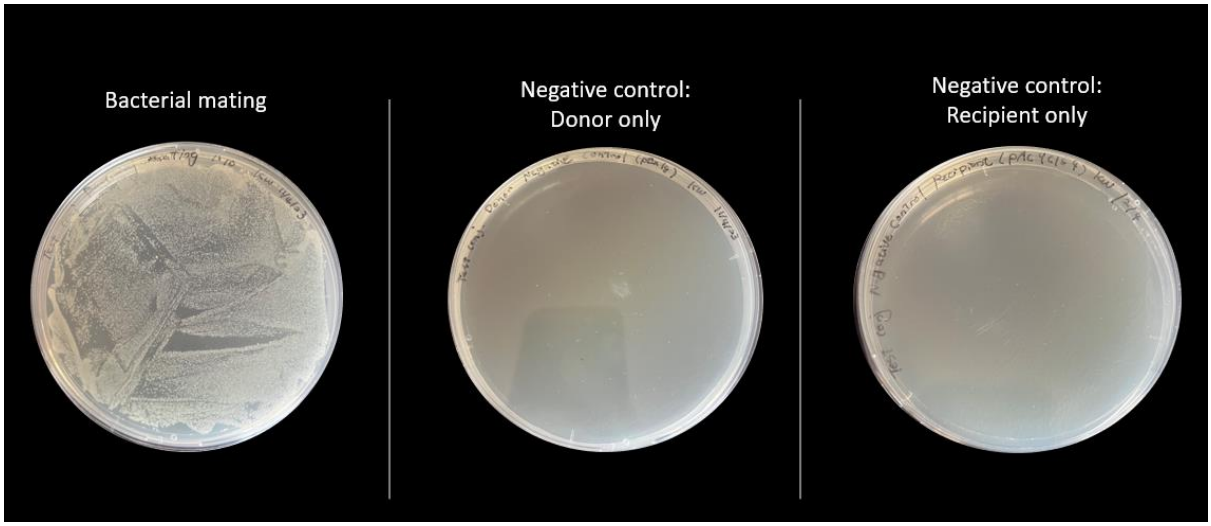

Figure 4-10: LB agar (chloramphenicol/gentamicin) to examine the ability of S17-1 *E. coli* to donate its plasmid

As shown above, the number of transconjugants was so numerous that nearly a lawn of bacteria were recovered on the bacterial mating plate. By contrast, no growth was observed in either of the negative controls. This assured us that S17-1 with pEX18-*ctrA* certainly retains its ability to mobilise its plasmid to a recipient.

② Test SacB activity on pEX18-*ctrA*

Constructing CtrA conditional mutant involves a counterselection of sucrose to screen bacterium that undergoes second recombination. The activity of SacB is critical for obtaining mutants, but point mutations in *sacB* can easily arise during cloning. Therefore, it is important to confirm the lethality of *sacB* on pEX18-*ctrA*. To examine this, Top10 cells with pEX18Gm or pEX18-*ctrA* were spread onto LB agar containing gentamicin only, or gentamicin and 5% sucrose. If SacB is functional, there should be no or minimal growth on gentamicin and sucrose LB agar. Top10 cells with pEX18-*ctrA* were grown with gentamicin only to confirm that the *E. coli* is viable and contains the plasmid.

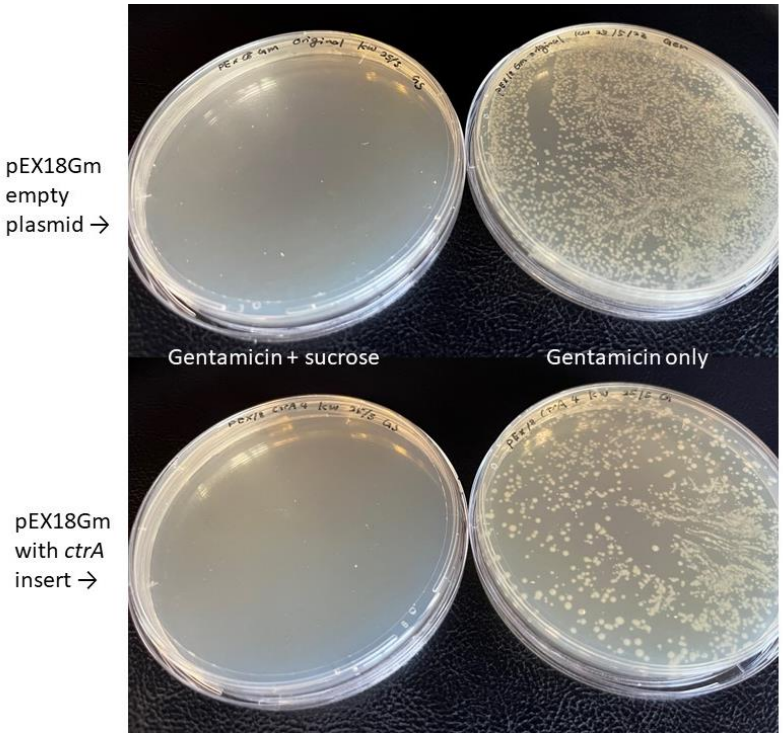

Figure 4-11: Confirmation of *sacB* gene in pEX18Gm plasmid

As shown in Figure 4-11, *E. coli* with either pEX18Gm or pEX18-*ctrA* could not grow on LB plates with sucrose and gentamicin, while robust growth was seen on LB plates with gentamicin only. The functionality of SacB was checked for the pEX18-*ctrA* plasmid from colony numbers 2, 4, 5, 6 and 7 (see Figure 4-7); SacB activity was confirmed for all of them,

apart from colony 2, which wasn't used any further. Total inhibition of growth was not observed for any the LB plates with gentamicin and sucrose, even with the pEX18 empty plasmid, indicating the occasional sporadic appearance of point mutations in the *sacB* gene. However, this was relatively rare and still shows >95% clearance on sucrose supplemented plates, so the pEX18-*ctrA* plasmid from colonies 4, 5, 6 and 7 retains a functional *sacB* gene.

pEX18-*ctrA* conjugation and electroporation

Having confirmed that S17-1 could robustly mobilise pEX18-*ctrA* to an *E. coli* recipient and that the plasmid retained a functional *sacB* gene, I proceeded to introducing the mutagenic plasmid into the complemented strain via conjugation and electroporation.

Despite the ease with which a replicating plasmid could be introduced into *B. quintana* (Figure 4-8), I encountered significant challenges in introducing the pEX18-*ctrA* mutagenic plasmid into the *B. quintana* chromosome. This is likely because the integration step via homologous recombination is very inefficient in *B. quintana*; repeated attempts yielded no colonies. Multiple bi-parental and tri-parental conjugations were conducted in parallel to utilise the available time effectively. After a several attempts of tri-parental conjugation, I discovered that the helper strain, containing plasmid pRK2013, was inherently resistant to the antibiotics used to select against *E. coli* (including nalidixic acid and cefazolin). It was also resistant to gentamicin and kanamycin presumably by acquiring pEX18-*ctrA* during the conjugation. Thereafter I focused on bi-parental conjugation. I attempted various approaches, including lawn method, altering the incubation time, altering the concentration of antibiotics, introducing nitrocellulose filter paper (0.22 µm pore size), and changing equipment to maximise the bacterial collection.

A number of electroporations were conducted along with those conjugations, as we have had success with efficiently introducing replicating plasmids into *B. quintana* by electroporation. I endeavoured to optimise the electroporation by using different wash buffer formulations and by concentrating the pEX18-*ctrA* plasmid to increase the chance of integration; however, the desired outcome was not achieved.

Despite persistent efforts, integrating pEX18-*ctrA* plasmid into *B. quintana* chromosome through conjugation or electroporation remained extremely challenging. Given the successful introduction of the pSRK-*ctrA* replicative plasmid into *B. quintana*, I

anticipated that the difficulty in introducing the pEX18-*ctrA* integrative plasmid may stem from very low levels of endogenous homologous recombination within *B. quintana*.

4.2.5 Bacteriophage recombineering

Because *B quintana* homologous recombination, mediated by endogenous recombinases, had very low efficiency, I looked for an alternative method that would overcome this barrier. One well-described method for making mutants, using highly efficient bacteriophage-derived recombinases, is known as recombineering[128,149]. I opted to try the lambda red system, which uses phage recombinase genes encoded on a broad-host-range plasmid (pSIM7), as described previously[128,149]. Recombineering is an efficient approach to genetic engineering, as the lambda red recombinases allow the integration of introduced linear DNA, with precise junctions, to any desired chromosomal location, in contrast to relying on endogenous recombinases and extensive regions of homology. Linear double-stranded DNA, containing a sequence to be inserted and flanked by two 50-base homology arms on both ends, is introduced into bacteria that express the pSIM7 plasmid. Recombination of short regions of homology is catalysed by the lambda red proteins, Exo, Beta and Gam, delivered on pSIM7. Exo exhibits a 5' to 3' double-stranded DNA exonuclease activity, resulting in the generation of 3' overhangs on DNA. Beta binds to the single-stranded DNA with a 3' overhang created by Exo and facilitates single-stranded annealing and the formation of recombinant DNA structure. Finally, Gam prevents nucleases from degrading double-stranded linear DNA fragments. To prevent unintended effects on the bacterial chromosome, the pSIM7 *exo*, *bet* and *gam* genes are under control of a temperature-sensitive repressor and are only induced by incubating the system in a 42 °C for 15 min[128,149].

Lambda red recombineering has been used successfully in *B. abortus* to create a mutant strain[150]. Although this approach has not been reported in any *Bartonella* species yet, I thought this could improve the success rate of recombination to create the conditional mutant. This method has two parts; ① introduction of pSIM7 plasmid into the *B. quintana* strain containing pSRK-*ctrA* plasmid, followed by ② electroporation of DNA selectable fragment with a tag to introduce the alternation in chromosome.

The pSIM7 plasmid-containing strain was acquired from the National Cancer Institute, and the plasmid was extracted from an *E. coli* overnight culture. The concentration was recorded and 200 ng of plasmid was dialysed over distilled water to prevent arcing, then was

electroporated into *B. quintana*. After electroporation, the bacteria were recovered overnight on non-selective plates, then transferred to selective chocolate plates with vancomycin, kanamycin, and chloramphenicol. Vancomycin was included to suppress contaminants, kanamycin was included to maintain the complementation plasmid, and chloramphenicol was included to select for uptake of pSIM7. All of the incubations were done in a candle jar at 30~32°C, as recommended for keeping the temperature-sensitive repressor active for the duration of selection. After the electroporation, plates were incubated for 14-21 days.

Several attempts of electroporation of pSIM7 plasmid into *B. quintana* containing pSRK-*ctrA* plasmid were conducted, without obtaining any colonies. Because pSIM7 and pSRK-*ctrA* share an origin of replication, even though can be selected with different antibiotics, I thought that plasmid incompatibility could mean that both plasmids couldn't be present in the same cell. To test this, I carried out several electroporations of the pSIM7 plasmid into wild type *B. quintana* strains JK-31 and JK-7. However, none of these attempts yielded colonies either. Unfortunately, time constrains impeded further progress on this attempt.

4.3 Discussion

The replicative pSRK-*ctrA* complementation plasmid was successfully introduced into *B. quintana* JK-31 through bi-parental conjugation. However, introduction of the pEX18-*ctrA* mutagenic suicide plasmid was extremely challenging, despite numerous attempts and varied approaches. I suspected that this was due the rarity of recombination events that relied on endogenous recombinases. The pEX18-*ctrA* mutagenic plasmid contained homology arms of 1,000 bp of flanking sequence around *ctrA*. Expanding the length of the homology arms in the mutagenic plasmid, for example to 1,500 bp, could enhance the likelihood of successful recombination events. Given that the integrative conjugation was successfully generated in other *B. quintana* strains (JK-7 and JK-63) by others, it could have been worthwhile to attempt creating a mutant in another strain if time had permitted.

The recombineering approach using pSIM7 plasmid and lambda red system was employed to enhance the efficiency and the likelihood of chromosomal recombination. Nonetheless, the initial step of introducing pSIM7 into *B. quintana* with pSRK-*ctrA* remained challenging. This could have been due to plasmid incompatibility of the pSRK and pSIM7 plasmids, but pSIM7 could not be introduced into wild type *B. quintana* either. Another issue

was the low temperature (30-32°C) incubation required following electroporation, to maintain activity of the temperature-sensitive repressor. *B. quintana* grows more slowly at lower temperatures[151], potentially prolonging the recovery and selection periods after electroporation. This extended selection period may require over a month, which was the longest period of time the pSIM7 electroporated bacteria were incubated. Introducing pSIM7 into *B. quintana* wild type was also challenging. pSIM7 plasmid confers a resistance to chloramphenicol, but the optimal chloramphenicol concentration for selection of *B. quintana* is not known. The recommended chloramphenicol concentration, 15 µg/ml, was used in the chocolate plates. However, this may have been too concentrated for *B. quintana.* A previous study selected chloramphenicol-resistant *B. quintana* on only 1 µg/ml chloramphenicol[152]. Recombineering using pSIM7 and the lambda red system has never been reported in *B. quintana*, and lack of time precluded additional optimisation of the process.

5 Investigating the effect of CtrA overexpression in *B. quintana*

5.1 Introduction

Construction of a conditional *ctrA* mutant was not successful in *B. quintana,* so I was not able to assess the impact on the bacteria in the absence of CtrA. However, given that the complementation pSRK-*ctrA* plasmid was successfully introduced into *B. quintana*, I opted to use this strain to study CtrA overexpression instead. The *ctrA* gene in this plasmid can be induced with IPTG, allowing us to look at the effect of higher than usual levels of CtrA. In this part of the research project, I aimed to investigate the effect of CtrA overexpression on *B. quintana*. Considering that CtrA may play an essential role regulating in the *B. quintana* cell cycle, I hypothesised that the overexpression of CtrA would adversely affect the growth of *B. quintana* or result in an abnormal morphology. I also expected that overexpression of CtrA could cause the cell to have abnormal number of chromosomes as a consequence of the disruption of the cell cycle. The goal of this project was to elucidate the potential functions of CtrA in *B. quintana*, focusing on three aspects: growth rate, morphology and chromosomal content.

5.2 Result

5.2.2 Growth in liquid culture

The growth of wild type JK-31 was compared to the strain expressing *ctrA,* either in the presence or absence of IPTG. Although *B. quintana* grows poorly in most liquid microbiology media, it has been shown to grow in 10% FCS-supplemented Schneider's Drosophila Medium, which was originally created for culturing insect cells[153,154].

Three conditions were included in this experiment: ① *B. quintana* JK-31 pSRK-*ctrA* with IPTG, ② *B. quintana* JK-31 with pSRK-*ctrA* without IPTG, ③ wild type *B. quintana* JK-31. A pilot experiment was conducted initially to confirm that the protocol would detect bacterial growth (Figure 5-1). The *B. quintana* liquid culture was started from OD_{600} of 0.01 and to reduce potential contaminations, I included 8 µg/ml amphotericin B, 5 µg/ml vancomycin along with kanamycin for the strain carrying the plasmid, and IPTG to induce *ctrA*.

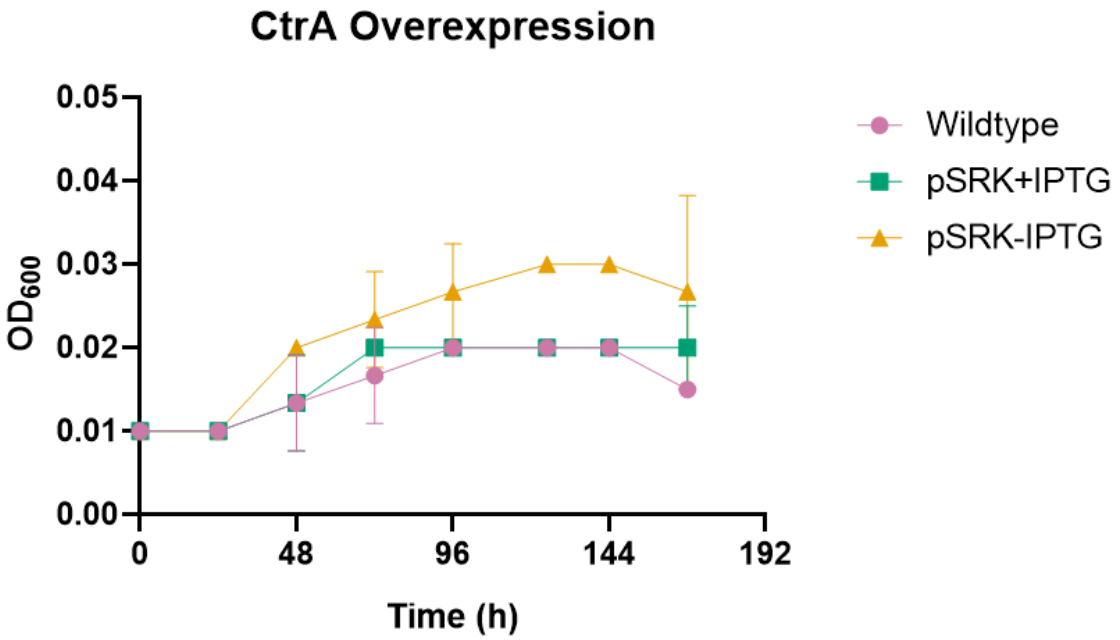

Figure 5-1: Pilot experiment of IPTG overexpression on *B. quintana* with pSRK-*ctrA* plasmid. Wild type strain is represented by pink circles. The strain with pSRK-*ctrA* plasmid with IPTG induction is represented by green squares. The strain with pSRK-*ctrA* plasmid without IPTG induction is represented by yellow triangles. One millilitre of the culture was taken from the cell culture flask every 24 h to monitor growth.

Each shape shows the mean and the error bars represent the standard deviations of three data replicates. The pilot experiment showed a slight increase of growth over 7 days, though the overall growth remains lower than expected. Interestingly, the *B. quintana* with pSRK-*ctrA* without IPTG showed the most growth 5-6 days of incubation. *B. quintana* with pSRK-*ctrA* with IPTG and wild type seemed to grow at a similar rate over 7 days. Given the poor growth of *B. quintana* observed across all conditions, I wanted to optimise the system. In the optimised protocol, the initial OD_{600} was increased to 0.05, instead of 0.01, in order to facilitate more pronounced growth changes over time. To enhance gas exchange within the system, the caps of the culture flasks were partially loosened. Additionally, vancomycin and amphotericin B were omitted, as antibiotics and antifungals could inhibit growth..

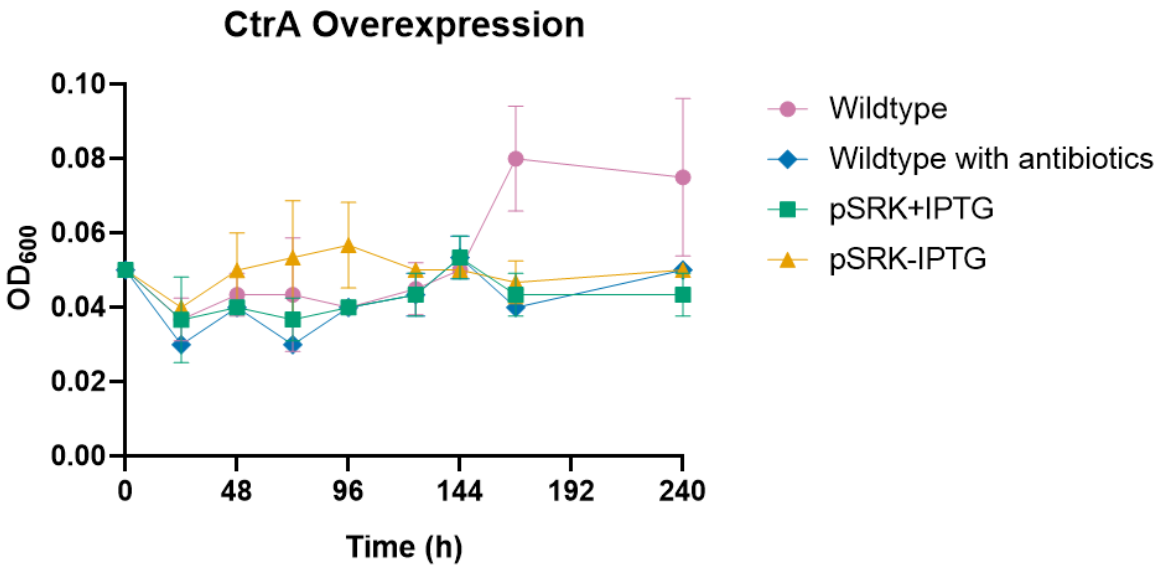

Figure 5-2: Optimised experiment of CtrA overexpression on *B. quintana* with pSRK-*ctrA* plasmid. Wild type strain is represented by pink circles. Strain with pSRK-*ctrA* plasmid with IPTG induction is represented by green squares. Strain with pSRK-*ctrA* plasmid without IPTG induction is represented by yellow triangles. Wild type with antibiotics (vancomycin and amphotericin B) is represented by blue rhombus. The wild type does not contain any antibiotics whereas strains with pSRK-*ctrA* only contain kanamycin to maintain the plasmid. One millilitre of culture was sampled from the cell culture flask every 24 h.

The growth curve using a more optimised protocol is shown in Figure 5-2. Each shape shows the mean and the error bars represent standard deviations of three data replicates. The wild type strain exhibited greater growth between 7 to 10 days compared to the strain with pSRK-*ctrA*. Moreover, notably reduced growth was observed in the wild type strain treated with antibiotics, suggesting a significant hindrance to growth due to antibiotic presence. Interestingly, during days 2 to 4, the strain with pSRK-*ctrA* without IPTG exhibited enhanced growth compared to other conditions. However, OD_{600} declined thereafter. The strain with pSRK-*ctrA* treated with IPTG appeared to maintain its initial OD_{600} and no significant growth was observed over 10 days.

The strain with pSRK-*ctrA* without IPTG demonstrated greater growth at specific time points in the second growth curve assay and consistently in most time points during the pilot experiment, compared to pSRK-*ctrA* with IPTG, suggesting that CtrA overexpression may hinder the growth of *B. quintana*. It was unexpected, however, to find that the strain with pSRK-*ctrA* without IPTG exhibited greater growth than the wild type strain.

5.2.3 Morphology

The morphological changes upon CtrA overexpression were analysed by microscopy techniques that were available.

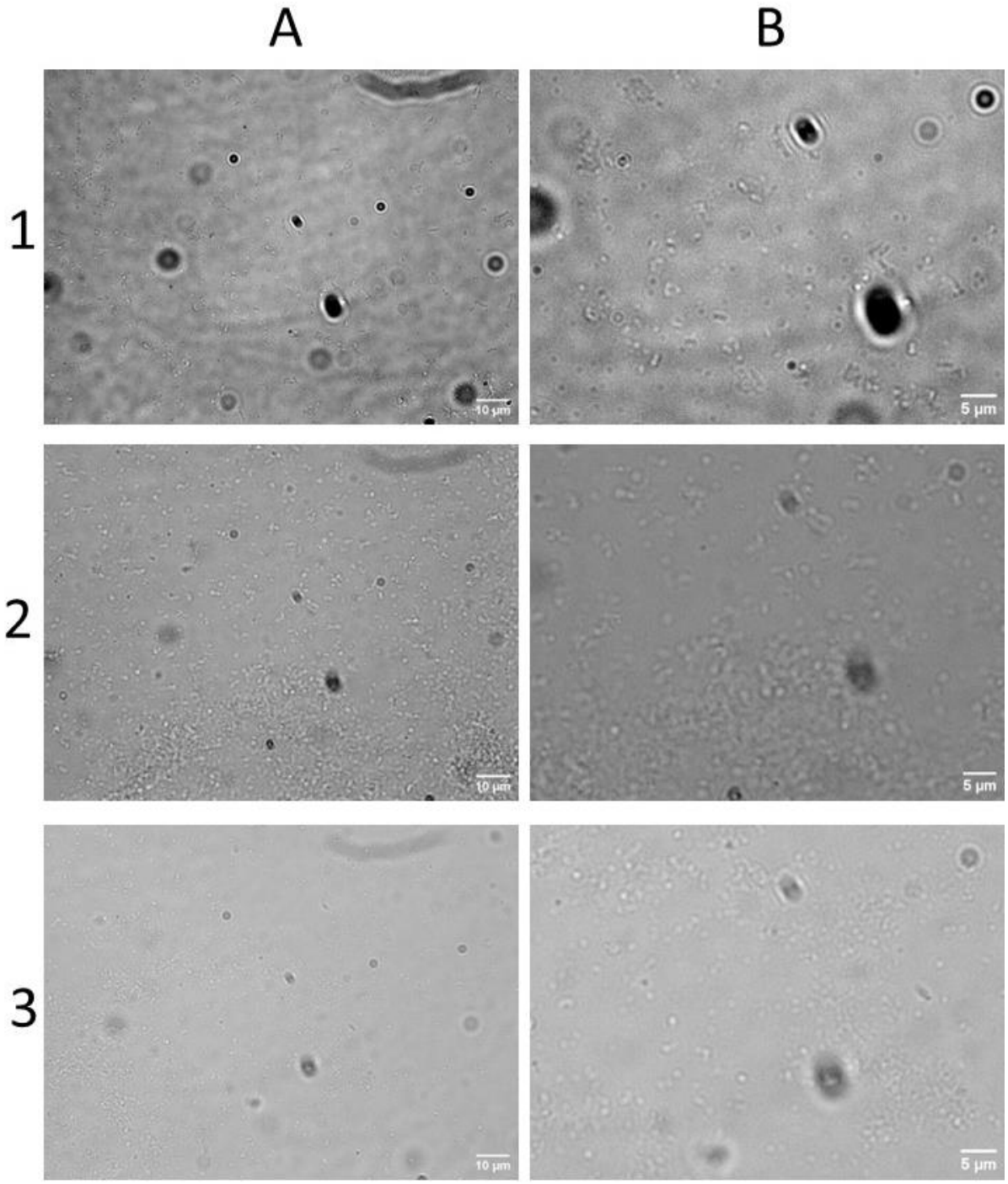

Figure 5-3: Phase-contrast microscope images of *B. quintana* upon CtrA overexpression. Section A is the original images from 100× objective. Section B is the close-up cropped version of section A. 1. Wildtype JK-31, 2. JK-31 pSRK-*ctrA* with IPTG induction, 3. JK-31 pSRK-*ctrA* without IPTG induction. The scale bar indicates 10 µm in section A and 5 µm in section B.

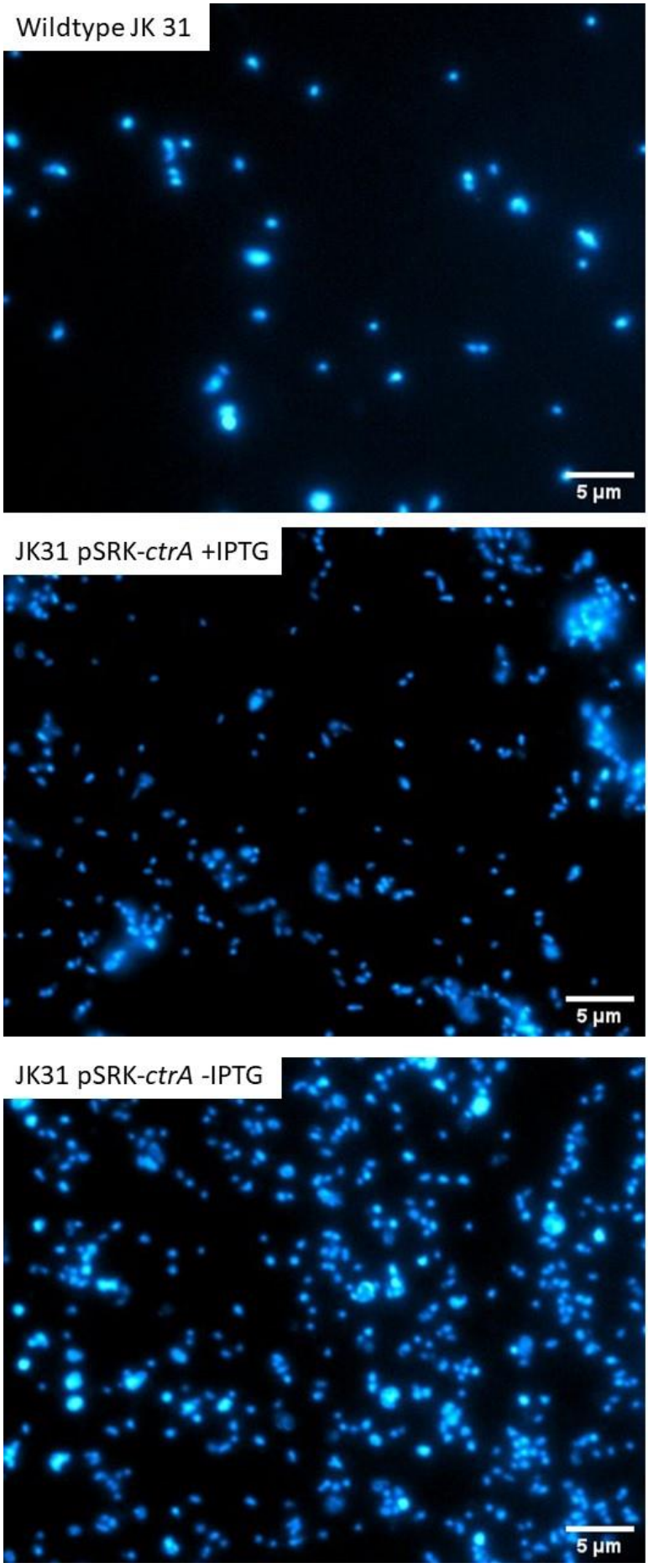

Figure 5-4: Fluorescence microscope images of *B. quintana* upon CtrA overexpression. Blue represent DAPI stained bacteria. The scale bar indicates 5 µm.

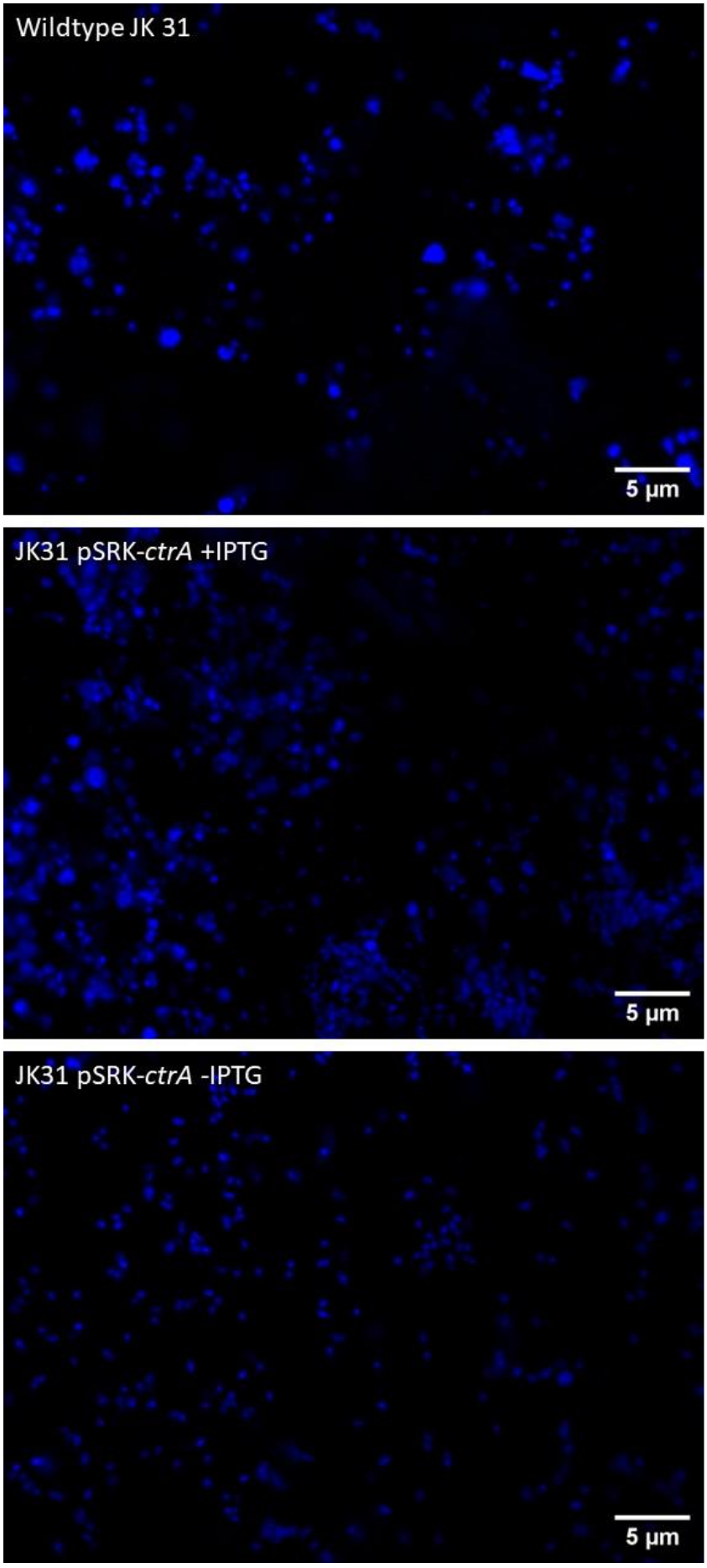

Figure 5-5: Confocal microscope images of *B. quintana* upon CtrA overexpression. Blue represent DAPI stained bacteria. The scale bar indicates 5 µm.

First, the bacteria were viewed using phase-contrast light microscopy (Figure 5-3). Fluorescence (Figure 5-4) and confocal (Figure 5-5) microscopy was also done following staining of the bacteria with DAPI. As previously described, loss of CtrA induces an abnormal morphology in *B. abortus* and *S. meliloti* [115,155], and I anticipated overexpression of CtrA might do the same in *B. quintana*. However, upon observation, none of the images revealed distinct morphological changes as a result of CtrA overexpression. Overall, the cells appeared to be of similar size and shape. I observed that the strain containing pSRK-*ctrA* with IPTG tended to exhibit a higher tendency for aggregation, relative to the wild type strain or the one without IPTG induction (Figure 5-6).

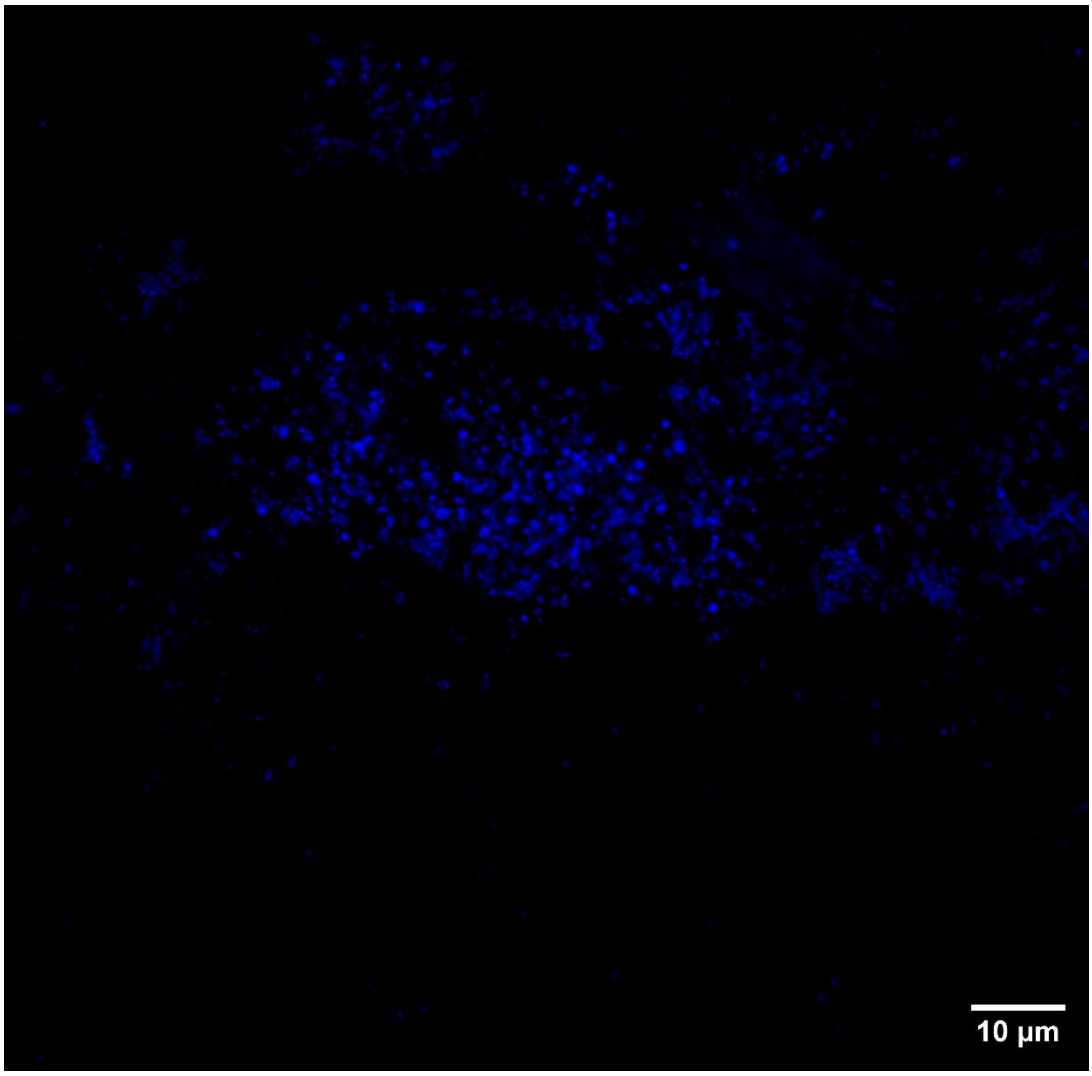

Figure 5-6: Confocal microscope images of *B. quintana* harbouring pSRK-*ctrA* plasmid upon CtrA overexpression with IPTG induction. Blue represent DAPI stained bacteria. The scale bar indicates 10 µm.

5.2.4 Flow Cytometry Analysis

The chromosomal contents of bacterial cells can be assessed with a nuclear dye and flow cytometry. Most bacterial cells would be expected to have a single chromosome. However, a subset of cells could be in the process of cell division; after the DNA has replicated but before completion of the septum, cells could have two chromosomes. If there is a problem with completion of cell division, the chromosomal contents can become very high, as DNA continues to replicate but new cells are not formed. Therefore, the chromosomal contents following CtrA overexpression were analysed and compared with uninduced control and wild type via flow cytometry. As it was expected that CtrA overexpression causes disruption of the cell cycle and division, an abnormal number of chromosomes could accumulate in the strain with pSRK-*ctrA* upon IPTG induction. First, an initial experiment was conducted to examine the difference of the total DNA quantity between each condition (Figure 5-7). The bacterial cells were gated using forward scatter (FSC-A) and side scatter (SSC-A) to remove as much acellular debris as possible. The resulting single cell populations were then analysed with a DAPI log scale vs cell count on a histogram and overlayed together. There was a clear shift in DAPI signal throughout the conditions. The wild type had the lowest amount of DNA, while the strain with pSRK-*ctrA* without IPTG induction had the most DNA, per single cell. The DAPI signal of the strain with pSRK-*ctrA* with IPTG induction is in the middle of those two conditions. The median fluorescence intensity also shows the clear increase in strain with pSRK-*ctrA* plasmid, with the no treatment of IPTG being the highest.

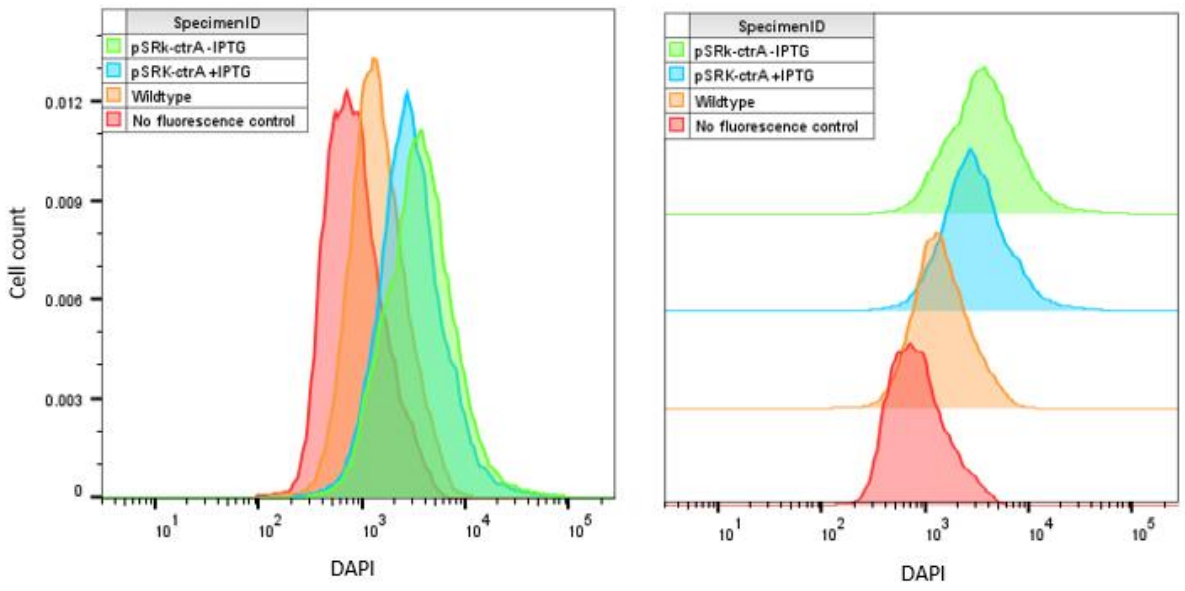

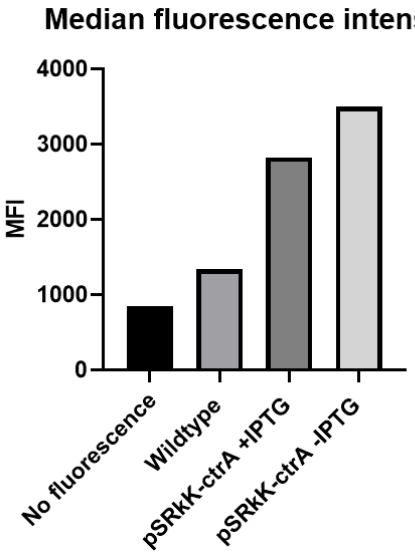

Figure 5-7: Flow cytometry profiles on overall DNA contents upon CtrA overexpression. Wild type and JK-31 with pSRK-*ctrA* was treated with 1 mM of IPTG for 18 h in a candle jar. The cells were fixed and stained with DAPI, and subsequently visualised by flow cytometry immediately. Histogram overlays show wild type (orange), pSRK-*ctrA* without IPTG induction (green), pSRK-*ctrA* with IPTG induction (blue) and no fluorescence control (red). Both histogram overlays at the top show the same data with a slightly different representation. The bar graph at the bottom shows the median fluorescence intensity over all conditions.

A second flow cytometry experiment was conducted and used to examine the difference in chromosomal DNA between each condition (Figure 5-8). The bacterial cells were gated to remove as much debris as possible and to select for single cells. Single cell populations were used to represent the size of the DNA, thus chromosomes (DAPI-A vs DAPI-W on linear scale). DNA populations were further gated out by excluding the population that was located at the very left on the DAPI-A axis. Those DNA populations were finally presented with DAPI linear scale vs cell count on histogram and overlayed together. In this experiment, the wild type has distinct two peaks: one around 20-30K DAPI-A and the other one around 50K on DAPI-A. These peaks likely correspond to the number of chromosomes present in one bacterial cell as the second peak is almost double the size of the first one. In this case, most of the wild type cells have a single chromosome, with a subset of these having two. By contrast, the strains with pSRK-*ctrA*, with or without IPTG induction, exhibit different flow cytometry profiles. There is one peak around 20-30K DAPI-A hidden in the large peak next to it, shown in red arrow in the figure. Interestingly, the large peak that sits around 50K on DAPI-A are larger than that the first peak of those conditions, which is different from the wild type. Assuming those two peaks correspond to one or two

chromosomes, the strains with pSRK-*ctrA* seemed to accumulate more chromosomes per cell. The largest peak corresponds to two chromosomes, but some cells have more than this. This could be because the presence of the pSRK-*ctrA* plasmid accelerates chromosomal replication or hinders cell division, or both. It is difficult to make any conclusive statement from this result, but there is clearly a difference in chromosome content between the wild type and *B. quintana* with pSRK-*ctrA* plasmid. The overlay of these results (Figure 5-8) demonstrates this clearly.

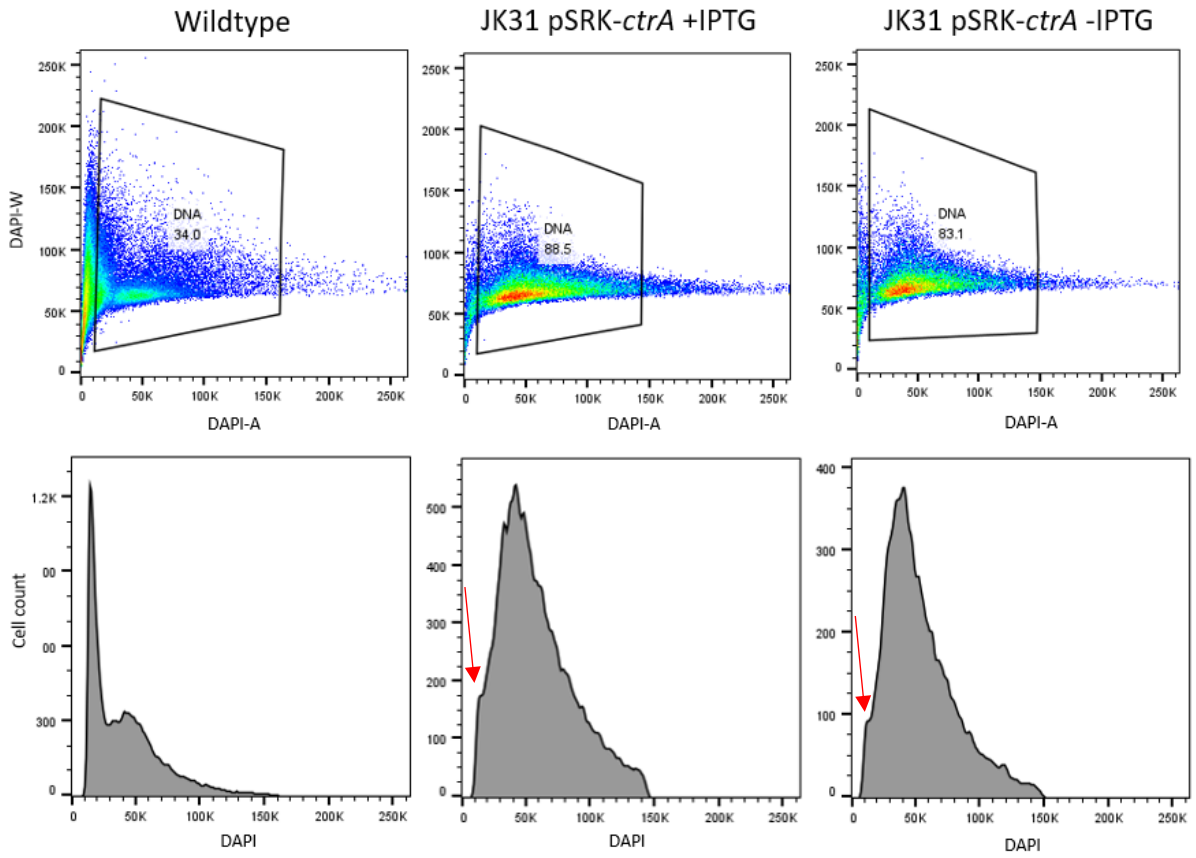

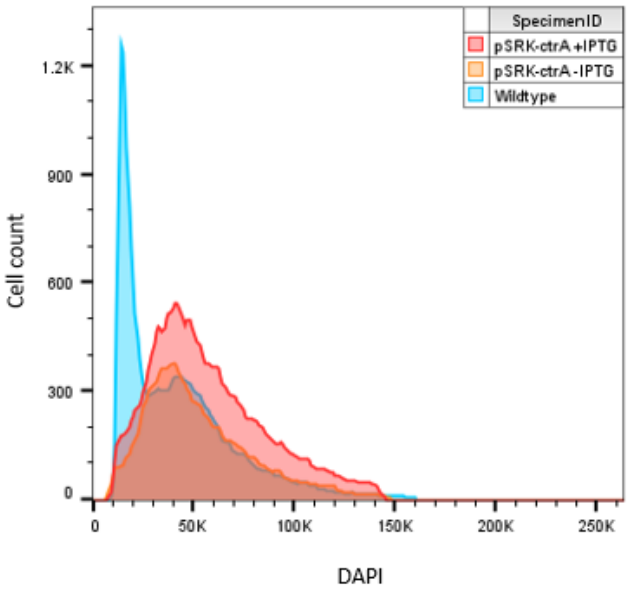

Figure 5-8: Flow cytometry profiles on chromosomal contents upon CtrA overexpression. Wild type and JK-31 with pSRK-*ctrA* was treated with 1 mM of IPTG for 10 days in a candle jar. The cells were fixed and stained with DAPI, and subsequently visualised by flow cytometry. The flow cytometry profile was recorded in DAPI area vs DAPI width on linear scale. The bacterial DNA population was gated according to the wild type population. Histogram overlays show wild type (blue), pSRK-*ctrA* without IPTG induction (orange), pSRK-*ctrA* with IPTG induction (red).

5.3 Discussion

The effect of CtrA overexpression, utilising *B. quintana* carrying the pSRK-*ctrA* plasmid, was analysed by examining the growth rate, the morphology by microscopy, and chromosomal contents by flow cytometry. This project successfully provides a preliminary study of CtrA overexpression on *B. quintana.*

The growth rate analysis revealed some growth in strains harbouring the pSRK-*ctrA* plasmid without IPTG induction from days 2 to 4, but overall, there was a decrease in the growth rate observed in strains with both induced and uninduced pSRK-*ctrA* plasmids compared to the wild type after 7-10 days. This finding is concerning, as it suggests that the introduction of the pSRK-*ctrA* plasmid may have adversely affected the growth of *B. quintana*. This could explain the challenges encountered in introducing another plasmid into this strain or in achieving chromosomal recombination within it.

Microscopy images did not exhibit discernible morphological changes across any conditions, with cells appearing similar in size and shape. However, limited time precluded the optimisation of microscopy to assess bacterial morphology. Differential interference contrast (Nomarski) microscopy is useful to assess bacterial cell morphology, but there was not sufficient time to try this. It is noteworthy that increased aggregation was observed in strains containing the pSRK-*ctrA* plasmid with IPTG induction. Bacterial autoaggregation is frequently mediated by surface-exposed envelope proteins. It would be worthwhile to investigate the role of CtrA in regulating surface protein expression, as CtrA in *Brucella* has been shown to do this[119]. Furthermore, autoaggregation can be quantified through techniques such as a sedimentation assay, to explore this phenomenon in more depth.

The overall flow cytometry analysis revealed a distinct difference in DNA quantity between the wild type and strains containing the pSRK-*ctrA* plasmid. Specifically, the flow cytometry profile, which assesses chromosomal contents within individual cells, indicated that there was an increase in the second peak in strains with the pSRK-*ctrA* plasmid compared to the wild type. This suggests that the mutant strains may carry two chromosomes within a single cell more frequently than is observed with the wild type. However, additional biological replicates are needed to average the fluorescence intensity, and the experiment needs to be repeated more times. Furthermore, it is essential to optimize the quality control of stained cells and the gating methodology of flow cytometry to draw any conclusive statements from the analysis.

Overall, there seemed to be minimal differences between the pSRK-*ctrA* strain with, or without, IPTG induction. This phenomenon suggests that the activity of the IPTG-inducible promoter should be confirmed in *B. quintana*.

The level of CtrA expression was not confirmed in this analysis. This would be helpful to investigate how much CtrA was present in each condition and to confirm they all produced different amounts of CtrA. This could be done via Western blot or quantitative real-time PCR.

6 Discussion

B. quintana is yet to be fully understood, particularly regarding its cell cycle, which enables persistence within the intraerythrocytic environment and may be linked to its virulence. Investigating CtrA, a master regulatory protein of the cell cycle, known to play a critical role in multiple alpha-proteobacteria, offers the opportunity to gain insights into the cell regulatory system of *B. quintana* and its virulence mechanisms. Ultimately, the goal of this project was to explore the interactions between CtrA and *B. quintana* genes and to examine the impact of CtrA overexpression on *B. quintana*. This research has the potential to enhance our understanding of *B. quintana* biology and its implications for human health.

6.1 Key Findings

6.1.2 Expression of CtrA-Regulated Genes

Multiple putative CtrA binding motifs were identified in *B. quintana* str. Toulouse promoter sequences. The gene BQ_RS06180 (*ftsK*) was selected as a candidate for the beta-galactosidase assay. This gene exhibits over 66% amino acid identity with the cell division protein FtsK in *C. crescentus*, which is responsible for the cytokinesis and chromosome segregation. I anticipated that homologue protein in *B. quintana* may also plays a critical role in the cell cycle. Furthermore, *ftsK* has been shown to be regulated by CtrA in multiple alpha-proteobacteria[146]. A LacZ reporter plasmid with *ftsK* promoter region insertion was generated by Gibson Assembly. Another gene candidate was chosen from the list of putative DNA binding motifs of CtrA that were investigated in the previous project; the *ftsH* gene was selected as this protease protein is responsible for controlling the timing of the cell differentiation in *C. crescentus* and exhibited 69% of amino acid similarity to the homologue protein in *C. crescentus.*

The beta-galactosidase assay revealed an interaction between CtrA and the promoter of the *ftsH* gene. The beta-galactosidase activity was significantly lower when CtrA was induced through IPTG, suggesting that CtrA acts as a repressor for this promoter. Increasing concentrations of IPTG, presumably resulting in higher expression of CtrA, resulted in lower beta-galactosidase activity. This finding is consistent with studies of CtrA in other bacteria, which have found that it can act as either transcriptional activator or a repressor[101].

Minimal beta-galactosidase activity was detected when induced from the *ftsK* promoter, or from the promoterless control. The overall low level of beta-galactosidase activity from the *ftsK* promoter meant that no conclusions could be drawn about its interaction with CtrA.

6.1.3 Constructing a conditional CtrA mutation strain

The replicative pSRK-*ctrA* plasmid was successfully introduced into *B. quintana* JK-31 through bi-parental conjugation. This strain therefore had the *ctrA* gene complemented, which is necessary for deletion of a gene that, like *ctrA*, is presumed to be essential. To generate the mutant from this complemented strain, I attempted several strategies, including bi- and tri-parental conjugations, lawn method of conjugation, electroporation and recombineering using pSIM7 plasmid. However, despite employing numerous approaches from various angles, the introduction of the pEX18-*ctrA* integrative plasmid proved to be extremely challenging, and a *ctrA* mutant strain is yet to be produced in *B. quintana*.

6.1.4 Effect of CtrA overexpression in *B. quintana*

The effect of CtrA overexpression using *B. quintana* carrying the pSRK-*ctrA* plasmid was analysed by examining growth, morphology, and chromosomal contents. This project has provided some initial insights into the impact of CtrA overexpression on *B. quintana*. The growth assays showed some initial growth in strains harbouring the pSRK-*ctrA* plasmid without IPTG induction. However, overall, there was a decrease in growth observed in strains with both induced and uninduced pSRK-*ctrA* plasmids compared to the wild type. Microscopic observation did not reveal noticeable alterations in morphology under any conditions, as cells appeared consistent in size and shape. Nevertheless, enhanced aggregation was noted in strains harbouring the pSRK-*ctrA* plasmid with IPTG induction, and this result should be investigated further. Flow cytometry analysis unveiled a clear contrast in DNA content between the wild type and strains harbouring the pSRK-*ctrA* plasmid. Specifically, an elevation in the second peak in strains possessing the pSRK-*ctrA* plasmid, in comparison to the wild type, indicated a potential increase in the number of chromosomes within single cells in the *ctrA* overexpressing strains. Overall, minimal differences were observed between IPTG-induced and uninduced conditions in strains containing the pSRK-*ctrA* plasmid. However, growth assays and analysis of the chromosomal

contents revealed distinct outcomes observed between wild type *B. quintana* and those carrying pSRK-*ctrA* plasmid.

6.1.5 Implications

The overall results of this project partially suggest that CtrA in *B. quintana* may be involved in the cell cycle, based on the bioinformatics studies and some of the CtrA overexpression analysis outcomes. However, there were unexpected findings, such as the repression of the *ftsH* gene, which produces a protease for quality control, by CtrA. The promoter of the *ftsK* gene, expected to be responsible for cell division and chromosome segregation, yielded very low activity, precluding any observations about its interaction with CtrA. Therefore, further experiments are needed to conclusively shed light on the possibility that CtrA in *B. quintana* plays an essential role or is involved in cell cycle regulation.

While CtrA in multiple alpha-proteobacteria is known to play a central role in the cell cycle, there are other alpha-proteobacteria in which CtrA does not participate in the cell cycle. It may be worthwhile to revisit the function of CtrA in *R. capsulatus*, where it plays a crucial role in facilitating genetic exchange between bacterial cells through gene transfer agents. Indeed, gene transfer agents have been documented in *Bartonella* species, facilitating efficient horizontal gene transfer and enabling adaptive evolution to thrive within the complex facultative intracellular lifestyle of these bacteria within mammalian hosts[156]. This mechanism likely plays a crucial role in the ability of *Bartonella* species to adapt and persist within their host environments[157]. Exploring this perspective of CtrA in *B. quintana* further in the future could provide valuable insights into its function and mechanisms of action.

6.2 Future Directions

6.2.2 RNA-Seq and ChIP-Seq

RNA-Seq analysis is a powerful technique to reveal the transcriptome of a biological sample through next-generation sequencing. This provides comprehensive insights into gene expression through the analysis of presence and quality of RNA molecules in the sample. Researchers utilise RNA-Seq to study the gene expression pattern and to identify the differences in gene expression under certain conditions. This will contribute to a deeper understanding of the underlying cellular processes and potential pathways involved. Therefore, as a future direction, the relationship between the CtrA protein and gene expression in *B. quintana* could be elucidated through RNA-Seq analysis. Such an approach could enable the identification of genes affected by CtrA upregulation and offers insights into the transcriptional regulation of these genes. Additionally, analysis of hierarchical clustering maps of gene expression profiles facilitates our understanding of the regulatory networks and potential pathways modulated within the system. By contrast, ChIP-Seq is a powerful method to identify promoters that physically interact with a transcriptional regulator, such as CtrA. In this method, the cell is fixed and interacting DNA and proteins are cross-linked. The protein of interest, such as CtrA, can be immunoprecipitated, and associated DNA can be identified through high-throughput sequencing. This technique has been used to study the regulons of CtrA in multiple species[115].

6.2.3 CRISPRi system

Producing a *ctrA* null conditional mutant strain in *B. quintana* remained challenging in this project despite multiple different approaches. An alternative gene editing approach utilising CRISPR interference (CRISPRi) system, described and applied to *C. crescentus* previously[158] may offer a solution to this challenge. Original CRISPR system is commonly used as a gene editing tool. In brief, the CRISPR system typically employs Cas9, an endonuclease, to cleave double-stranded DNA at a specified genomic location guided by a guide RNA (gRNA). Subsequent DNA repair mechanisms usually introduce mutations at the targeted site, facilitating gene editing. Precision alterations to the DNA sequence can be achieved by introducing an additional DNA template, allowing for straightforward replacement of the desired sequence. Adaptation of this mechanism to gene knockdown in bacteria, also called CRISPRi, utilises a catalytically inactive form of Cas9 (dCas9), which

lacks endonuclease activity but retains the ability to bind to specific genomic regions. Therefore, dCas9 can block the transcription of genes without cleavage of DNA[159,160].

CRISPRi has been used to deplete *ctrA* expression in *C. crescentus*, recapitulating the phenotypic consequences associated with *ctrA* depletion[158]. Use of CRISPRi technology in *B. quintana* could overcome the challenges associated with introducing foreign plasmids into the bacterium, which were encountered in this project. This approach potentially simplify the genetic manipulation process and facilitating the generation of a *ctrA*-depleted mutant strain in *B. quintana*.

6.2.4 CtrA loss analysis

The utilization of a *ctrA* null conditional mutant *B. quintana* strain presents a promising approach to investigate the effects of CtrA loss, allowing for comparison with the effects observed in wild type and CtrA overexpression strains. Similar methodologies, such as assessing growth, observing changes in morphology, and analysing chromosomal contents via flow cytometry, can be employed for comprehensive evaluation of the phenotypic consequences of CtrA depletion. Moreover, to validate CtrA production in the mutant strains, complementary techniques such as SDS-PAGE analysis or Western blotting could be utilized. This validation step ensures the accuracy of the genetic manipulation and confirms the absence of CtrA protein expression in the null mutant strain. In addition to phenotypic characterization, integrating RNA-Seq analysis would enable the exploration of global patterns of gene expression in response to CtrA loss. This comprehensive approach would provide insights into the regulatory networks of CtrA in *B. quintana*, further advancing our understanding of its biology and pathogenesis.

6.2.5 Sedimentation Assay

As microscopic observations suggested a potential increase in aggregation among *B. quintana* strains harbouring the pSRK-*ctrA* plasmid upon IPTG induction, further investigation through a sedimentation assay could offer valuable insights. This assay is commonly employed to detect clumping of bacteria, which more rapidly fall out of suspension. In brief, both wild type *B. quintana* and strains containing the pSRK-*ctrA* plasmid would be harvested into a liquid medium. Subsequently, the optical density at 600nm

of the top of the culture would be measured at regular intervals. Increased aggregation among bacterial cells would result in clumps that more rapidly fall out of suspension; this leads to a more rapid decrease in OD_{600} measurements as they settle at the bottom of the tubes. This approach provides a quantitative assessment of bacterial aggregation and can help elucidate differences in particle size between the wild type and strains with the pSRK-*ctrA* plasmid. Considering the significance of autoaggregation as a virulence factor in bacteria, which aids in protection against host immune responses and other external stresses, exploring the aggregation rate in the sedimentation assay may unveil additional roles of CtrA beyond cell cycle regulation.

6.3 Concluding Remarks

This project acknowledges the limited understanding of *Bartonella quintana* (*B. quintana*), particularly concerning its cell cycle, which is crucial for its persistence within the intraerythrocytic environment and likely intertwined with its virulence. By focusing on CtrA, a master regulatory protein known for its pivotal role in various alpha-proteobacteria, the research aims to shed light on the cell cycle regulation and its virulence mechanisms. The primary objective was to investigate the interactions between CtrA and *B. quintana* genes and to assess the effects of CtrA overexpression on the bacterium.

While some outcomes suggest that CtrA in *B. quintana* may be involved in cell cycle regulation, exploring its implications in other areas, such as its potential role in gene transfer agents, could provide valuable insights. Understanding the broader functions of CtrA in *B. quintana* will not only deepen our knowledge of its biology but also pave the way for improved medical applications in managing *B. quintana* infections.

7 Bibliography

1. Jacomo, V., Kelly, P. J. & Raoult, D. Natural History of *Bartonella* Infections (an Exception to Koch's Postulate). *Clin Diagn Lab Immunol* **9**, 8 (2002).
2. Okaro, U., Addisu, A., Casanas, B. & Anderson, B. *Bartonella* Species, an Emerging Cause of Blood-Culture-Negative Endocarditis. *Clin Microbiol Rev* **30**, 709–746 (2017).
3. Kosoy, M. *et al. Bartonella* spp. in Bats, Kenya. *Emerg Infect Dis* **16**, 1875 (2010).
4. Maggi, R. G. *et al. Bartonella henselae* in captive and hunter-harvested beluga (*Delphinapterus leucas*). *J Wildl Dis* **44**, 871–877 (2008).
5. Valentine, K. H. *et al. Bartonella* DNA in Loggerhead Sea Turtles. *Emerg Infect Dis* **13**, 949 (2007).
6. Angelakis, E. & Raoult, D. Pathogenicity and treatment of *Bartonella* infections. *Int J Antimicrob Agents* **44**, 16–25 (2014).
7. Chomel, B. B. *et al.* Dogs are more permissive than cats or guinea pigs to experimental infection with a human isolate of *Bartonella rochalimae*. *Vet Res* **40**, (2009).
8. Veikkolainen, V., Vesterinen, E. J., Lilley, T. M. & Pulliainen, A. T. Bats as Reservoir Hosts of Human Bacterial Pathogen, *Bartonella mayotimonensis*. *Emerg Infect Dis* **20**, 960 (2014).
9. Urrutia, L. C. *et al.* Oroya Fever, Verruga Peruana, and Other Bartonelloses Incidence Rates in Colombia (2009-2013). *Cureus* **10**, (2018).
10. Sanchez Clemente, N. *et al. Bartonella bacilliformis*: A Systematic Review of the Literature to Guide the Research Agenda for Elimination. *PLoS Negl Trop Dis* **6**, e1819 (2012).
11. Mada, P. K., Zulfiqar, H. & Chandranesan, A. S. J. *Bartonellosis*. *StatPearls* (StatPearls Publishing, 2023).
12. Shorbatli, L. A., Koranyi, K. I. & Nahata, M. C. Effectiveness of antibiotic therapy in pediatric patients with cat scratch disease. *Int J Clin Pharm* **40**, 1458–1461 (2018).
13. Baranowski, K. & Huang, B. *Cat Scratch Disease*. *StatPearls* (StatPearls Publishing, 2023).
14. Oskouizadeh, K., Zahraei-Salehi, T. & Aledavood, S. J. Detection of *Bartonella henselae* in domestic cats' saliva. *Iran J Microbiol* **2**, 80 (2010).
15. Harms, A. & Dehio, C. Intruders below the Radar: Molecular pathogenesis of *Bartonella* spp. *Clin Microbiol Rev* **25**, 42–78 (2012).
16. Sykes, J. E. & Chomel, B. B. *Bartonellosis*. *Canine and Feline Infectious Diseases* (W.B. Saunders, 2014). doi:10.1016/B978-1-4377-0795-3.00052-1.

17. Drali, R., Shako, J. C., Davoust, B., Diatta, G. & Raoult, D. A new clade of African body and head lice infected by *Bartonella quintana* and *Yersinia pestis*-democratic republic of the Congo. *American Journal of Tropical Medicine and Hygiene* **93**, 990–993 (2015).

18. Leulmi, H. *et al.* Competence of *Cimex lectularius* Bed Bugs for the Transmission of *Bartonella quintana*, the Agent of Trench Fever. *PLoS Negl Trop Dis* **9**, e0003789 (2015).

19. Ov, M., NIa, C. & Morozov. [Detection of the *Bartonella* DNA by the method of nested PCR in patients after tick bites in Novosibirsk region]. *Mol Gen Mikrobiol Virusol* (2005).

20. Kernif, T. *et al.* Acquisition and excretion of *Bartonella quintana* by the cat flea, *Ctenocephalides felis felis*. *Mol Ecol* **23**, 1204–1212 (2014).

21. La, V. D., Tran-Hung, L., Aboudharam, G., Raoult, D. & Drancourt, M. *Bartonella quintana* in Domestic Cat. *Emerg Infect Dis* **11**, 1287 (2005).

22. Okorji, O., Olarewaju, O., Smith, T. & Pace, W. C. *Trench Fever*. *xPharm: The Comprehensive Pharmacology Reference* (StatPearls Publishing, 2023). doi:10.1016/B978-008055232-3.60905-5.

23. Brouqui, P., Lascola, B., Roux, V. & Raoult, D. Chronic *Bartonella quintana* bacteremia in homeless patients. *N Engl J Med* **340**, 184–189 (1999).

24. Sangaré, A. K. *et al.* Detection of *Bartonella quintana* in African Body and Head Lice. *Am J Trop Med Hyg* **91**, 294 (2014).

25. Brouqui, P. *et al.* Ectoparasitism and vector-borne diseases in 930 homeless people from Marseilles. *Medicine* **84**, 61–68 (2005).

26. Chomel, B. B. *et al.* Ecological fitness and strategies of adaptation of *Bartonella* species to their hosts and vectors. *Vet Res* **40**, (2009).

27. Jackson, L. A. *et al.* Seroprevalence to *Bartonella quintana* among patients at a community clinic in downtown Seattle. *J Infect Dis* **173**, 1023–1026 (1996).

28. Shepard, Z. *et al. Bartonella quintana* Infection in People Experiencing Homelessness in the Denver Metropolitan Area. *J Infect Dis* **226**, S315–S321 (2022).

29. Tasher, D., Raucher-Sternfeld, A., Tamir, A., Giladi, M. & Somekh, E. *Bartonella quintana*, an Unrecognized Cause of Infective Endocarditis in Children in Ethiopia. *Emerg Infect Dis* **23**, 1246 (2017).

30. Knoop, F. C. Trench Fever. *Reference Module in Biomedical Sciences* (2014) doi:10.1016/B978-0-12-801238-3.05379-4.

31. Spach, D. H. *et al. Bartonella (Rochalimaea) quintana* bacteremia in inner-city patients with chronic alcoholism. *N Engl J Med* **332**, 424–428 (1995).

32. Mosepele, M., Mazo, D. & Cohn, J. *Bartonella* Infection in Immunocompromised Hosts: Immunology of Vascular Infection and Vasoproliferation. *Clin Dev Immunol* **2012**, (2012).

33. Ruiz, J. *Bartonella quintana*, past, present, and future of the scourge of World War I. *APMIS* **126**, 831–837 (2018).

34. Byam, W. *et al.* Trench fever. *Oxford (UK): Oxford University Press* (1919).

35. Maurin, M. & Raoult, D. *Bartonella (Rochalimaea) quintana* infections. *Clin Microbiol Rev* **9**, 273–292 (1996).

36. Hunt, G. H. & Rankin, A. C. Intermittent fever of obscure origin, occurring among British troops in France. The so-called 'trench fever'. *The Lancet* **186**, 1133–1136 (1915).

37. Anstead, G. M. The centenary of the discovery of trench fever, an emerging infectious disease of World War 1. *Lancet Infect Dis* **16**, e164–e172 (2016).

38. Vinson, J. W. & Fuller, H. S. Studies on trench fever. I. Propagation of Rickettsia-like microorganisms from a patient's blood. *Pathol Microbiol (Basel)* (1961).

39. Bruce, D. Trench Fever: Final Report of the War Office Trench Fever Investigation Committee. *J Hyg (Lond)* **20**, 258–288 (1921).

40. Atenstaedt, R. L. Trench fever: the British medical response in the Great War. *J R Soc Med* **99**, 564 (2006).

41. Arkwright, J. A. & Martin Duncan, F. Preliminary note on the association of rickettsial bodies in lice with trench fever. *Br Med J* **2**, 307–309 (1918).

42. Kostrzewski, J. [The epidemiology of trench fever]. *Bull Int Acad Pol Sci Let Cl Med* (1949).

43. Raoult, D. & Roux, V. The body louse as a vector of reemerging human diseases. *Clin Infect Dis* **29**, 888–911 (1999).

44. Vinson, J. W. *In vitro* cultivation of the rickettsial agent of trench fever. *Bull World Health Organ* **35**, 155 (1966).

45. Tissot-Dupont, H. *et al.* Outbreak of epidemic typhus associated with trench fever in Burundi. *Lancet* **352**, 353–358 (1998).

46. Foucault, C., Barrau, K., Brouqui, P. & Raoult, D. *Bartonella quintana* bacteremia among homeless people. *Clinical Infectious Diseases* **35**, 684–689 (2002).

47. Sasaki, T. *et al.* Detection of *Bartonella quintana* (Hyphomicrobiales: Bartonellaceae) Among Day Laborers in Osaka, Japan, 2009-2010. *J Med Entomol* **60**, 408–411 (2023).

48. Hammoud, A. *et al. Bartonella quintana* Transmitted by Head Lice: An Outbreak of Trench Fever in Senegal. *Clin Infect Dis* **76**, 1382–1390 (2023).

49. Raoult, D. *et al.* Evidence for louse-transmitted diseases in soldiers of Napoleon's Grand Army in Vilnius. *J Infect Dis* **193**, 112–120 (2006).

50. Mai, B. H. A. *et al.* Five millennia of *Bartonella quintana* bacteraemia. *PLoS One* **15**, (2020).

51. Chomel, B. B., Kasten, R. W., Sykes, J. E., Boulouis, H. J. & Breitschwerdt, E. B. Clinical impact of persistent *Bartonella* bacteremia in humans and animals. *Ann N Y Acad Sci* **990**, 267–278 (2003).

52. Birtles, R. J. *et al.* Identification of *Bartonella bacilliformis* Genotypes and Their Relevance to Epidemiological Investigations of Human Bartonellosis. *J Clin Microbiol* **40**, 3606 (2002).

53. Ihler, G. M. *Bartonella bacilliformis*: dangerous pathogen slowly emerging from deep background. *FEMS Microbiol Lett* **144**, 1–11 (1996).

54. Dehio, C. Molecular and Cellular Basis of *Bartonella* Pathogenesis. *https://doi.org/10.1146/annurev.micro.58.030603.123700* **58**, 365–390 (2004).

55. Foucault, C., Brouqui, P. & Raoult, D. *Bartonella quintana* Characteristics and Clinical Management. *Emerg Infect Dis* **12**, 217 (2006).

56. Ohl, M. E. & Spach, D. H. *Bartonella quintana* and urban trench fever. *Clin Infect Dis* **31**, 131–135 (2000).

57. Meghari, S. *et al.* Antiangiogenic Effect of Erythromycin: An In Vitro Model of *Bartonella quintana* Infection. *J Infect Dis* **193**, 380–386 (2006).

58. Smith, D. A. & Nehring, S. M. *Bacteremia*. *Pediatric Emergency Medicine* (StatPearls Publishing, 2023). doi:10.1016/B978-141600087-7.50071-4.

59. Ferløv Schwensen, J., Nielsen, H. & Helleberg, M. Bacillary angiomatosis in a solid organ transplant recipient. (2019) doi:10.1016/j.idcr.2019.e00649.

60. Jin, X. *et al.* Advancements in understanding the molecular and immune mechanisms of *Bartonella* pathogenicity. *Front Microbiol* **14**, 1196700 (2023).

61. Rolain, J. M., Foucault, C., Brouqui, P. & Raoult, D. Erythroblast cells as a target for *Bartonella quintana* in homeless people. *Ann N Y Acad Sci* **990**, 485–487 (2003).

62. Rolain, J. M. *et al. Bartonella quintana* in human erythrocytes. *The Lancet* **360**, 226–228 (2002).

63. Schülein, R. *et al.* Invasion and Persistent Intracellular Colonization of ErythrocytesA Unique Parasitic Strategy of the Emerging Pathogen *Bartonella*. *Journal of Experimental Medicine* **193**, 1077–1086 (2001).

64. Cascales, E. & Christie, P. J. The versatile bacterial type IV secretion systems. *Nature Reviews Microbiology 2003 1:2* **1**, 137–149 (2003).

65. Schmid, M. C. *et al.* The VirB type IV secretion system of *Bartonella henselae* mediates invasion, proinflammatory activation and antiapoptotic protection of endothelial cells. *Mol Microbiol* **52**, 81–92 (2004).

66. Scheidegger, F. *et al.* Distinct activities of *Bartonella henselae* type IV secretion effector proteins modulate capillary-like sprout formation. *Cell Microbiol* **11**, 1088–1101 (2009).

67. Vayssier-Taussat, M. *et al.* The Trw Type IV Secretion System of *Bartonella* Mediates Host-Specific Adhesion to Erythrocytes. *PLoS Pathog* **6**, e1000946 (2010).

68. Iwaki-Egawa, S. & Ihler, G. M. Comparison of the abilities of proteins from *Bartonella bacilliformis* and *Bartonella henselae* to deform red cell membranes and to bind to red cell ghost proteins. *FEMS Microbiol Lett* **157**, 207–217 (1997).

69. Zähringer, U. *et al.* Structure and biological activity of the short-chain lipopolysaccharide from *Bartonella henselae* ATCC 49882T. *J Biol Chem* **279**, 21046–21054 (2004).

70. Malgorzata-Miller, G. *et al. Bartonella quintana* lipopolysaccharide (LPS): structure and characteristics of a potent TLR4 antagonist for *in-vitro* and *in-vivo* applications. *Sci Rep* **6**, (2016).

71. Mosepele, M., Mazo, D. & Cohn, J. *Bartonella* infection in immunocompromised hosts: immunology of vascular infection and vasoproliferation. *Clin Dev Immunol* **2012**, (2012).

72. Popa, C. *et al. Bartonella quintana* lipopolysaccharide is a natural antagonist of Toll-like receptor 4. *Infect Immun* **75**, 4831–4837 (2007).

73. Deng, H. *et al.* Strategies of exploitation of mammalian reservoirs by *Bartonella* species. *Vet Res* **43**, (2012).

74. Kyme, P. A. *et al.* Unusual trafficking pattern of *Bartonella henselae* -containing vacuoles in macrophages and endothelial cells. *Cell Microbiol* **7**, 1019–1034 (2005).

75. Zhang, P. *et al.* A family of variably expressed outer-membrane proteins (Vomp) mediates adhesion and autoaggregation in *Bartonella quintana*. *Proc Natl Acad Sci U S A* **101**, 13630–13635 (2004).

76. Schulte, B. *et al. Bartonella quintana* Variably Expressed Outer Membrane Proteins Mediate Vascular Endothelial Growth Factor Secretion but Not Host Cell Adherence. *Infect Immun* **74**, 5003 (2006).

77. Liberto, M. C. *et al. Bartonella quintana*-induced apoptosis inhibition of human endothelial cells is associated with p38 and SAPK/JNK modulation and with stimulation of mitosis. *Diagn Microbiol Infect Dis* **50**, 159–166 (2004).

78. Minnick, M. F. *et al.* Five-member gene family of *Bartonella quintana*. *Infect Immun* **71**, 814–821 (2003).

79. Abromaitis, S. & Koehler, J. E. The *Bartonella quintana* extracytoplasmic function sigma factor RpoE has a role in bacterial adaptation to the arthropod vector environment. *J Bacteriol* **195**, 2662–2674 (2013).

80. Capo, C., Amirayan-Chevillard, N., Brouqui, P., Raoult, D. & Mege, J. L. *Bartonella quintana* Bacteremia and Overproduction of Interleukin-10: Model of Bacterial Persistence in Homeless People. *J Infect Dis* **187**, 837–844 (2003).

81. Collier, J. Cell cycle control in Alphaproteobacteria. *Curr Opin Microbiol* **30**, 107–113 (2016).

82. El Panis, G., Murray, S. R. & Viollier, P. H. Versatility of global transcriptional regulators in alpha-Proteobacteria: from essential cell cycle control to ancillary functions. *FEMS Microbiol Rev* **39**, 120–133 (2015).

83. Degnen, S. T. & Newton, A. Chromosome replication during development in *Caulobacter crescentus*. *J Mol Biol* **64**, 671–680 (1972).

84. Ely, B. [17] Genetics of *Caulobacter crescentus*. *Methods Enzymol* **204**, 372–384 (1991).

85. McAdams, H. H. & Shapiro, L. The Architecture and Conservation Pattern of Whole-Cell Control Circuitry. *J Mol Biol* **409**, 28–35 (2011).

86. Sundararajan, K. & Goley, E. D. Cytoskeletal Proteins in *Caulobacter crescentus*: Spatial Orchestrators of Cell Cycle Progression, Development, and Cell Shape. *Subcell Biochem* **84**, 103–137 (2017).

87. Schrader, J. M. & Shapiro, L. Synchronization of *Caulobacter crescentus* for investigation of the bacterial cell cycle. *J Vis Exp* **2015**, (2015).

88. Zhou, B. *et al.* The Global Regulatory Architecture of Transcription during the *Caulobacter* Cell Cycle. *PLoS Genet* **11**, e1004831 (2015).

89. Collier, J. Regulation of chromosomal replication in *Caulobacter crescentus*. *Plasmid* **67**, 76–87 (2012).

90. Curtis, P. D. & Brun, Y. V. Getting in the Loop: Regulation of Development in *Caulobacter crescentus*. *Microbiology and Molecular Biology Reviews* **74**, 13–41 (2010).

91. Quon, K. C., Yang, B., Domian, I. J., Shapiro, L. & Marczynski, G. T. Negative control of bacterial DNA replication by a cell cycle regulatory protein that binds at the chromosome origin. *Proc Natl Acad Sci U S A* **95**, 120–125 (1998).

92. Collier, J., McAdams, H. H. & Shapiro, L. A DNA methylation ratchet governs progression through a bacterial cell cycle. *Proc Natl Acad Sci U S A* **104**, 17111–17116 (2007).

93. Gora, K. G. *et al.* A cell-type-specific protein-protein interaction modulates transcriptional activity of a master regulator in *Caulobacter crescentus*. *Mol Cell* **39**, 455–467 (2010).

94. Tan, H. M., Kozdon, J. B., Shen, X., Shapiro, L. & McAdams, H. H. An essential transcription factor, SciP, enhances robustness of *Caulobacter* cell cycle regulation. *Proc Natl Acad Sci U S A* **107**, 18985–18990 (2010).

95. McGrath, P. T., Viollier, P. & McAdams, H. H. Setting the pace: mechanisms tying *Caulobacter* cell-cycle progression to macroscopic cellular events. *Curr Opin Microbiol* **7**, 192–197 (2004).

96. Judd, E. M. *et al.* Distinct constrictive processes, separated in time and space, divide *Caulobacter* inner and outer membranes. *J Bacteriol* **187**, 6874–6882 (2005).

97. Gorbatyuk, B. & Marczynski, G. T. Regulated degradation of chromosome replication proteins DnaA and CtrA in *Caulobacter crescentus*. *Mol Microbiol* **55**, 1233–1245 (2005).

98. Biondi, E. G. *et al.* Regulation of the bacterial cell cycle by an integrated genetic circuit. *Nature 2006 444:7121* **444**, 899–904 (2006).

99. Iniesta, A. A., McGrath, P. T., Reisenauer, A., McAdams, H. H. & Shapiro, L. A phospho-signaling pathway controls the localization and activity of a protease complex critical for bacterial cell cycle progression. *Proc Natl Acad Sci U S A* **103**, 10935–10940 (2006).

100. Quon, K. C., Yang, B., Domian, I. J., Shapiro, L. & Marczynski, G. T. Negative control of bacterial DNA replication by a cell cycle regulatory protein that binds at the chromosome origin. *Proc Natl Acad Sci U S A* **95**, 120–125 (1998).

101. Laub, M. T., Chen, S. L., Shapiro, L. & McAdams, H. H. Genes directly controlled by CtrA, a master regulator of the *Caulobacter* cell cycle. *Proc Natl Acad Sci U S A* **99**, 4632–4637 (2002).

102. Kelly, A. J., Sackett, M. J., Din, N., Quardokus, E. & Brun, Y. V. Cell cycle-dependent transcriptional and proteolytic regulation of FtsZ in *Caulobacter*. *Genes Dev* **12**, 880–893 (1998).

103. Laub, M. T., McAdams, H. H., Feldblyum, T., Fraser, C. M. & Shapiro, L. Global analysis of the genetic network controlling a bacterial cell cycle. *Science* **290**, 2144–2148 (2000).

104. Sackett, M. J., Kelly, A. J. & Brun, Y. V. Ordered expression of *ftsQA* and *ftsZ* during the *Caulobacter crescentus* cell cycle. *Mol Microbiol* **28**, 421–434 (1998).

105. Tomasch, J., Koppenhöfer, S. & Lang, A. S. Connection Between Chromosomal Location and Function of CtrA Phosphorelay Genes in Alphaproteobacteria. *Front Microbiol* **12**, 662907 (2021).

106. Domian, I. J., Reisenauer, A. & Shapiro, L. Feedback control of a master bacterial cell-cycle regulator. *Proc Natl Acad Sci U S A* **96**, 6648 (1999).

107. Shen, X. *et al.* Architecture and inherent robustness of a bacterial cell-cycle control system. *Proc Natl Acad Sci U S A* **105**, 11340 (2008).

108. Bastedo, D. P. & Marczynski, G. T. CtrA response regulator binding to the *Caulobacter* chromosome replication origin is required during nutrient and antibiotic stress as well as during cell cycle progression. *Mol Microbiol* **72**, 139–154 (2009).

109. Van Teeseling, M. C. F. & Thanbichler, M. Generating asymmetry in a changing environment: cell cycle regulation in dimorphic alphaproteobacteria. *Biol Chem* **401**, 1349–1363 (2020).

110. Leicht, O. *et al.* Integrative and quantitative view of the CtrA regulatory network in a stalked budding bacterium. *PLoS Genet* **16**, e1008724 (2020).

111. Brilli, M. *et al.* The diversity and evolution of cell cycle regulation in alpha-proteobacteria: a comparative genomic analysis. *BMC Syst Biol* **4**, 52 (2010).

112. Hallez, R., Bellefontaine, A. F., Letesson, J. J. & De Bolle, X. Morphological and functional asymmetry in α-proteobacteria. *Trends Microbiol* **12**, 361–365 (2004).

113. Lang, A. S. & Beatty, J. T. Genetic analysis of a bacterial genetic exchange element: The gene transfer agent of *Rhodobacter capsulatus*. *Proc Natl Acad Sci U S A* **97**, 859 (2000).

114. Barnett, M. J., Hung, D. Y., Reisenauer, A., Shapiro, L. & Long, S. R. A Homolog of the CtrA Cell Cycle Regulator Is Present and Essential in *Sinorhizobium meliloti*. *J Bacteriol* **183**, 3204 (2001).

115. Pini, F. *et al.* Cell Cycle Control by the Master Regulator CtrA in *Sinorhizobium meliloti*. *PLoS Genet* **11**, e1005232 (2015).

116. Pini, F. *et al.* The DivJ, CbrA and PleC system controls DivK phosphorylation and symbiosis in *Sinorhizobium meliloti*. *Mol Microbiol* **90**, 54–71 (2013).

117. Brassinga, A. K. C. *et al.* Conserved Response Regulator CtrA and IHF Binding Sites in the α-Proteobacteria *Caulobacter crescentus* and *Rickettsia prowazekii* Chromosomal Replication Origins. *J Bacteriol* **184**, 5789 (2002).

118. Bellefontaine, A. F. *et al.* Plasticity of a transcriptional regulation network among alpha-proteobacteria is supported by the identification of CtrA targets in *Brucella abortus*. *Mol Microbiol* **43**, 945–960 (2002).

119. Francis, N. *et al.* CtrA controls cell division and outer membrane composition of the pathogen *Brucella abortus*. *Mol Microbiol* **103**, 780–797 (2017).

120. Mercer, R. G. *et al.* Loss of the response regulator CtrA causes pleiotropic effects on gene expression but does not affect growth phase regulation in *Rhodobacter capsulatus*. *J Bacteriol* **192**, 2701–2710 (2010).

121. Hernández-Valle, J., Sanchez-Flores, A., Poggio, S., Dreyfus, G. & Camarena, L. The CtrA Regulon of *Rhodobacter sphaeroides* Favors Adaptation to a Particular Lifestyle. *J Bacteriol* **202**, (2020).

122. Liang, Q. *et al.* CtrA activates the expression of glutathione S-transferase conferring oxidative stress resistance to *Ehrlichia chaffeensis*. *Front Cell Infect Microbiol* **12**, (2022).

123. Thomson, R. H. Role of the CtrA cell cycle regulator in the bloodborne bacterial pathogen, *Bartonella quintana*. (Open Access Victoria University of Wellington | Te Herenga Waka, 2018). doi:10.26686/WGTN.17134073.V1.

124. Simon, R., Priefer, U. & Pühler, A. A Broad Host Range Mobilization System for In Vivo Genetic Engineering: Transposon Mutagenesis in Gram Negative Bacteria. *Bio/Technology 1983 1:9* **1**, 784–791 (1983).

125. Khan, S. R., Gaines, J., Roop, R. M. & Farrand, S. K. Broad-host-range expression vectors with tightly regulated promoters and their use to examine the influence of TraR and TraM expression on Ti plasmid quorum sensing. *Appl Environ Microbiol* **74**, 5053–5062 (2008).

126. Hoang, T. T., Karkhoff-Schweizer, R. R., Kutchma, A. J. & Schweizer, H. P. A broad-host-range F1p-FRT recombination system for site-specific excision of chromosomally-located DNA sequences: Application for isolation of unmarked Pseudomonas aeruginosa mutants. *Gene* **212**, 77–86 (1998).

127. Figurski, D. H. & Helinski, D. R. Replication of an origin-containing derivative of plasmid RK2 dependent on a plasmid function provided in trans. *Proc Natl Acad Sci U S A* **76**, 1648–1652 (1979).

128. Datta, S., Costantino, N. & Court, D. L. A set of recombineering plasmids for gram-negative bacteria. *Gene* **379**, 109–115 (2006).

129. Benchling [Biology Software]. https://benchling.com. (2024).

130. Bethesda (MD). National Center for Biotechnology Information (NCBI)[Internet]. *National Library of Medicine (US)* https://www.ncbi.nlm.nih.gov/ (1988).

131. Afgan, E. *et al.* The Galaxy platform for accessible, reproducible and collaborative biomedical analyses: 2018 update. *Nucleic Acids Res* **46**, 537–544 (2018).

132. Grant, C. E., Bailey, T. L. & Noble, W. S. FIMO: scanning for occurrences of a given motif. *Bioinformatics* **27**, 1017–1018 (2011).

133. Huntley, R. P., Sawford, T., Martin, M. J. & O'Donovan, C. Understanding how and why the Gene Ontology and its annotations evolve: The GO within UniProt. *Gigascience* **3**, (2014).

134. Altschul, S. F., Gish, W., Miller, W., Myers, E. W. & Lipman, D. J. Basic local alignment search tool. *J Mol Biol* **215**, 403–410 (1990).

135. GraphPad Prism for Windows Version 8.0.2. Preprint at www.graphpad.com.

136. FlowJo™ Software for Windows Version 10.10.0. Preprint at (2023).

137. Jean, N. L., Rutherford, T. J. & Löwe, J. FtsK in motion reveals its mechanism for double-stranded DNA translocation. *Proc Natl Acad Sci U S A* **117**, 14202–14208 (2020).

138. Wang, S. C. E., West, L. & Shapiro, L. The Bifunctional FtsK Protein Mediates Chromosome Partitioning and Cell Division in *Caulobacter*. *J Bacteriol* **188**, 1497 (2006).

139. Bath, J., Ling Juan Wu, Errington, J. & Wang, J. C. Role of *Bacillus subtilis* SpoIIIE in DNA transport across the mother cell-prespore division septum. *Science* **290**, 995–997 (2000).

140. Stouf, M., Meile, J. C. & Cornet, F. FtsK actively segregates sister chromosomes in *Escherichia coli*. *Proc Natl Acad Sci U S A* **110**, 11157–11162 (2013).

141. Ito, K. & Akiyama, Y. Cellular functions, mechanism of action, and regulation of FtsH protease. *https://doi.org/10.1146/annurev.micro.59.030804.121316* **59**, 211–231 (2005).

142. Bieniossek, C. *et al.* The molecular architecture of the metalloprotease FtsH. *Proc Natl Acad Sci U S A* **103**, 3066 (2006).

143. Zellmeier, S., Zuber, U., Schumann, W. & Wiegert, T. The Absence of FtsH Metalloprotease Activity Causes Overexpression of the σW-Controlled pbpE Gene, Resulting in Filamentous Growth of *Bacillus subtilis*. *J Bacteriol* **185**, 973 (2003).

144. Fischer, B., Rummel, G., Aldridge, P. & Jenal, U. The FtsH protease is involved in development, stress response and heat shock control in *Caulobacter crescentus*. *Mol Microbiol* **44**, 461–478 (2002).

145. Jenal, U. & Fuchs, T. An essential protease involved in bacterial cell-cycle control. *EMBO J* **17**, 5658 (1998).

146. Poncin, K., Gillet, S. & De Bolle, X. Learning from the master: targets and functions of the CtrA response regulator in *Brucella abortus* and other alpha-proteobacteria. *FEMS Microbiol Rev* **42**, 500–513 (2018).

147. Quon, K. C., Marczynski, G. T. & Shapiro, L. Cell Cycle Control by an Essential Bacterial Two-Component Signal Transduction Protein. *Cell* **84**, 83–93 (1996).

148. Reisenauer, A., Quon, K. & Shapiro, L. The CtrA Response Regulator Mediates Temporal Control of Gene Expression during the *Caulobacter* Cell Cycle. *J Bacteriol* **181**, 2430 (1999).

149. Sharan, S. K., Thomason, L. C., Kuznetsov, S. G. & Court, D. L. Recombineering: A Homologous Recombination-Based Method of Genetic Engineering. *Nat Protoc* **4**, 206 (2009).

150. Coloma-Rivero, R. F. *et al.* The Role of the Flagellar Protein FlgJ in the Virulence of *Brucella abortus*. *Front Cell Infect Microbiol* **10**, 178 (2020).

151. Abromaitis, S., Nelson, C. S., Previte, D., Yoon, K. S. & Clark, J. M. *Bartonella quintana* Deploys Host and Vector Temperature-Specific Transcriptomes. *PLoS One* **8**, 58773 (2013).

152. Battisti, J. M. *et al.* Transcriptional Regulation of the Heme Binding Protein Gene Family of *Bartonella quintana* Is Accomplished by a Novel Promoter Element and Iron Response Regulator. *Infect Immun* **75**, 4373 (2007).

153. Riess, T. *et al.* Analysis of a Novel Insect Cell Culture Medium-Based Growth Medium for *Bartonella* Species. *Appl Environ Microbiol* **74**, 5224 (2008).

154. Lynch, T., Iverson, J. & Kosoy, M. Combining Culture Techniques for *Bartonella*: the Best of Both Worlds. *J Clin Microbiol* **49**, 1363 (2011).

155. Hallez, R., Letesson, J. J., Vandenhaute, J. & De Bolle, X. Gateway-Based Destination Vectors for Functional Analyses of Bacterial ORFeomes: Application to the Min System in *Brucella abortus*. *Appl Environ Microbiol* **73**, 1375 (2007).

156. Tamarit, D., Neuvonen, M. M., Engel, P., Guy, L. & Andersson, S. G. E. Origin and Evolution of the *Bartonella* Gene Transfer Agent. *Mol Biol Evol* **35**, 451–464 (2018).

157. Québatte, M. & Dehio, C. *Bartonella* gene transfer agent: Evolution, function, and proposed role in host adaptation. *Cell Microbiol* **21**, (2019).

158. Guzzo, M., Castro, L. K., Reisch, C. R., Guo, M. S. & Laub, M. T. A CRISPR interference system for efficient and rapid gene knockdown in *Caulobacter crescentus*. *mBio* **11**, (2020).

159. Larson, M. H. *et al.* CRISPR interference (CRISPRi) for sequence-specific control of gene expression. *Nature Protocols 2013 8:11* **8**, 2180–2196 (2013).

160. Qi, L. S. *et al.* Repurposing CRISPR as an RNA-Guided Platform for Sequence-Specific Control of Gene Expression. *Cell* **152**, 1173 (2013).

8 Appendix

Appendix 1. Binding motif search result

Full motif: TTAANNNNNNNTTAAC

Identification via NCBI				classify genes using Uniprot			Alignment result	
Putative CtrA binding motif in promoter region	**Gene locus tag or name**	**Predicted gene product**	**Binding site distance from start site**	**protein**	**Organism**	**Identity**	**Orthologue in *C. crescentus***	**Amino acid identity**
TTAATACAGTTTTAAC TTAAGAGCGAATAAAC	**BQ_RS06180**	DNA translocase FtsK	61 bp & 139 bp	DNA translocase FtsK	Bartonella sp. JB15	76.1%	cell division protein FtsK	66.9%
TTAATACAGTTTTAAC/ TTAAGAGCGAATAAAC	BQ_RS06185	ubiquinone biosynthesis hydroxylase	81 bp & 23 bp	2-octaprenyl-6-methoxyphenyl hydroxylase	Bartonella bovis 91-4	75.8%	UbiH/UbiF/VisC/COQ6 family ubiquinone biosynthesis hydroxylase	39.0%
TTATGCTAGGGTTAAC	BQ_RS05910	DUF1465 family protein	135 bp	Regulator of CtrA degradation	Bartonella sp. JB15	71.3%	protease adaptor protein RcdA	38.5%
TTAACGATCTCTTCAC	BQ_RS04140	valine--tRNA ligase	182 bp	Valine--tRNA ligase	Bartonella henselae	86.7%	valine--tRNA ligase	57.2%
TTAAAAAGCGCTTATC	BQ_RS04595	glycosyltransferase family 4 protein	first 43 bp within the gene	Mannosyltransferase	Bartonella sp. JB15	77.9%	No significant similarity found	
TTAAGGGTATCTTTAC	BQ_RS03665	response regulator	52 bp	Histidine kinase	Bartonella sp. JB15	71.1%	hybrid sensor histidine kinase/response regulator	40.6%
TTAAGGGTATCTTTAC	BQ_RS03670	flagellar biosynthetic protein FliO	52 bp	Uncharacterized protein	Bartonella bacilliformis	47.2%	No significant similarity found	
TTAAGCCCACTTTAAA TTAAAGTGGGCTTAAT	***ftsH***	ATP-dependent zinc metalloprotease FtsH	0 bp and 1 bp (opposite strand)	ATP-dependent zinc metalloprotease FtsH	Bartonella bacilliformis	81.9%	ATP-dependent zinc metalloprotease FtsH	69.3%

Half motif (TTAACCAT)

Identification via NCBI			classify genes using Uniprot			Aligment result	
Gene locus tag or name	**Predicted gene product**	**Binding site distance from start site**	**protein**	**Organism**	**Identity**	**Orthologue in *C. crescentus***	**Amino acid identity**
BQ_RS06490	class I SAM-dependent methyltransferase	227 bp	Putative SAM-dependent methyltransferase protein	Bartonella bacilliformis	75.0%	methyltransferase type 11	38.9%
radA	DNA repair protein RadA	6 bp	DNA repair protein RadA	Bartonella bacilliformis	83.4%	DNA repair protein RadA	57.9%
BQ_RS02110	hemin-degrading factor	243 bp	Hemin transport protein HmuS	Bartonella bacilliformis	73.2%	No significant similarity found	
BQ_RS01700	ATP-binding protein	first 29 bp within the gene	Histidine kinase	Bartonella bacilliformis	78.2%	histidine kinase	41.0%
BQ_RS03815	SPOR domain-containing protein	39 bp	Sporulation related domain-containing protein	Bartonella sp. JB15	42.1%	No significant similarity found.	
ftsE	cell division ATP-binding protein FtsE	106 bp and 152 bp	Cell division ATP-binding protein FtsE	Bartonella bovis 91-4	90.9%	cell division ATP-binding protein FtsE	60.0%

Yellow highlight shows genes that this project worked on.

Appendix 2. CtrA induction on SDS-PAGE gel

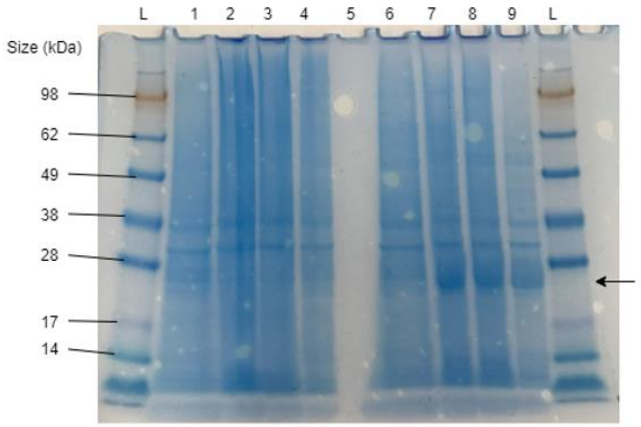

SDS-PAGE gel of the CtrA protein induction in BL21 *E. coli* harbouring pET28a(+)-*ctrA* plasmid.

Ladder: SeeBlue Plus2 Protein ladder(Thermo Fisher Scientific).

Lanes 1-4: BL21 pET28a(+)-*ctrA* plasmid, no IPTG at 0, 1.5, 2 and 3 hours, respectively.

Lanes 6-9: BL21 pET28a(+)-*ctrA* plasmid samples induced with IPTG at 0, 1.5, 2 and 3 hours, respectively.

Bands were observed just below the 28 kDa which is consistent with the predicted size of the CtrA protein

Appendix 3. Sequence of *ftsH* insertion in pACYC184-*lacZ*

Top line: sequenced result of pACYC184-*lacZ* with *ftsH* promoter region insertion

Bottom line: sequence of *ftsH* promoter region taken from *B. quintana* str. Toulouse genome (NCBI Reference sequence NC_005955.1).

```
             7105                                                                  7186
pACYC184_... acgccagggttttcccagtcacgacgttgtaaaacgacggccagtgaatccgtaatcatatgcatcatattaagcccacttt
FtsH prom... ------------------------------------------------------------TCATATTAAGCCCACTTT

             7187                                                                  7268
pACYC184_... aaaatacagattttaaacagtcgtccttaacatataaccttgtctgctccttgccaaggtgtgagaagatgtttattctctt
FtsH prom... AAAATACAGATTTTAAACAGTCGTCCTTAACATATAACCTTGTCTGCTCCTTGCCAAGGTGTGAGAAGATGTTTATTCTCTT

             7269                                                                  7350
pACYC184_... ttagagtgatttttctttatctttccaccttgatatcaaaaaaaggctcaagaacattcacaaaaggaacatcttcgcatga
FtsH prom... TTAGAGTGATTTTTCTTTATCTTTCCACCTTGATATCAAAAAAAGGCTCAAGAACATTCACAAAAGGAACATCTTCGCATGA

             7351                                                                  7432
pACYC184_... caaaagccaatcgaagggagccataatccgctttatggaagctttaatgcggtagtttatcacagttaaattgctaacgcag
FtsH prom... CAAAAGCCAATCGAAGGGAGCCATAATCCGCTTTATG-------------------------------------------

             7433   7443
pACYC184_... tcaggcaccgt
FtsH prom... -----------
```

Appendix 4. Sequence of *ftsK* insertion in pACYC184-*lacZ*

Top line: sequenced result of pACYC184-*lacZ* with *ftsK* promoter region insertion

Bottom line: sequence of *ftsK* promoter region taken from *B. quintana* str. Toulouse genome (NCBI Reference sequence NC_005955.1).

Two mismatches were identified, recurring consistently at the same locations across three attempts. I hypothesize that these mismatches represent minor differences between the genomes of *B. quintana* str. Toulouse and *B. quintana* JK-31.

```
            2932                                                                        3013
pACYC184_... gcttcataccttcattgagatcagaatacacaacacttccttctattgttcgcagtttattcgctcttaaacgaaaagggta
FtsK         -----ATACCTTCATTGAGATCAGAATACACAACACTTCCTTCTATTGTTCGCAGTTTATTCGCTCTTAAACGAAAAGGGTA

            3014                                                                        3095
pACYC184_... tttttcttcaatatcaccgttattataaggaaattgttatgattatgatagttaaaactgtattaatattttgcggtcataa
FtsK         TTTTTCTTCAATATCACCGTTATTATAAGAAAATTGTTATGATTATGATAGTTAAAACTGTATTAATATTTTGCGGTCATAA

            3096                                                                  3170
pACYC184_... ttttataactctttaatatgaaggttttgtatttggaattgatggatgctgcatatgattacggattcactggcc
FtsK         TTTTATAACTCTTTAATACGAAGGTTTTGTATTTGGAATTGATGGATGC-------------------------
```

Appendix 5. Sequence of *ctrA* insertion in pSRK

Top line: sequenced result of pSRK with *ctrA* gene insertion

Bottom line: sequence of *ctrA* gene taken from *B. quintana* str. Toulouse genome (NCBI Reference sequence NC_005955.1).

```
            3760                                                                        3841
KW_pSRKKm... caggaaacagcatatgcgcgtattattaattgaagatgataaagcaaccactcagagtattgagttaatgctaaagtcggca
CtrA         ------------atgcgcgtattattaattgaagatgataaagcaaccactcagagtattgagttaatgctaaagtcggca

            3842                                                                        3923
KW_pSRKKm... aattttaatgtctatatcactgatctaggtgaagaaggtgccgatttaggtaagctttatgattacgatatcattttgcttg
CtrA         aattttaatgtctatatcactgatctaggtgaagaaggtgccgatttaggtaagctttatgattacgatatcattttgcttg

            3924                                                                        4005
KW_pSRKKm... atctgaatctaccggatatgtcaggctacgatgtcctgcggaccttaagattggcaaaaataaaaaccccctgttctcattct
CtrA         atctgaatctaccggatatgtcaggctacgatgtcctgcggaccttaagattggcaaaaataaaaaccccctgttctcattct

            4006                                                                        4087
KW_pSRKKm... ttccggcatgaatgccattgaagataaagtccgggggtttggctttggtgcggatgattatatgactaagccattccataag
CtrA         ttccggcatgaatgccattgaagataaagtccgggggtttggctttggtgcggatgattatatgactaagccattccataag

            4088                                                                        4169
KW_pSRKKm... gatgagctcattgcacgtatccatgcggttgttcgtcgctctaaaggccatgcacaatcaatcattgtcactggcgatctca
CtrA         gatgagctcattgcacgtatccatgcggttgttcgtcgctctaaaggccatgcacaatcaatcattgtcactggcgatctca

            4170                                                                        4251
KW_pSRKKm... ccgtcaatcttgatgcaaaaacagtggaagttgctggacgtcccgttcatttaactagtaaagaataccagatgctagaact
CtrA         ccgtcaatcttgatgcaaaaacagtggaagttgctggacgtcccgttcatttaactagtaaagaataccagatgctagaact

            4252                                                                        4333
KW_pSRKKm... tctctctctacgcaaaggcaccacactcaccaaagaaatgtttctcaatcatctctacggtggaatggatgaaccagaactg
CtrA         tctctctctacgcaaaggcaccacactcaccaaagaaatgtttctcaatcatctctacggtggaatggatgaaccagaactg

            4334                                                                        4415
KW_pSRKKm... aaaattattgatgtttttatatgtaaactgcggaagaaattagaagaagtatcttctagcgcaaactacattgatacagttt
CtrA         aaaattattgatgtttttatatgtaaactgcggaagaaattagaagaagtatcttctagcgcaaactacattgatacagttt

            4416                                                                4489
KW_pSRKKm... ggggacggggctatgtgttacgtgatccagttgaagaaaacgtacgtaaaaccgcttaaccccgggctgcagga
CtrA         ggggacggggctatgtgttacgtgatccagttgaagaaaacgtacgtaaaaccgct------------------
```